



Origin of marginal basins of the NW Pacific and their plate tectonic reconstructions



Junyuan Xu ^{a,*}, Zvi Ben-Avraham ^b, Tom Kelty ^c, Ho-Shing Yu ^d

^a Department of Petroleum Geology, China University of Geosciences, Wuhan, 430074, China.

^b Department of Geophysics and Planetary Sciences, Tel Aviv University, Ramat Aviv 69978, Israel

^c Department of Geological Sciences, California State University, Long Beach, CA 90840, USA

^d Institute of Oceanography, National Taiwan University, Taipei, Taiwan

ARTICLE INFO

Article history:

Received 4 March 2013

Accepted 3 October 2013

Available online 16 October 2013

Keywords:

Marginal basins of the NW Pacific

Dextral pull-apart

Sinistral transpressional pop-up

Uplift of Tibetan Plateau

Back-arc basin

Diffuse plate reconstruction

ABSTRACT

Geometry of basins can indicate their tectonic origin whether they are small or large. The basins of Bohai Gulf, South China Sea, East China Sea, Japan Sea, Andaman Sea, Okhotsk Sea and Bering Sea have typical geometry of dextral pull-apart. The Java, Makassar, Celebes and Sulu Seas basins together with grabens in Borneo also comprise a local dextral, transform-margin type basin system similar to the central and southern parts of the Shanxi Basin in geometry. The overall configuration of the Philippine Sea resembles a typical sinistral transpressional “pop-up” structure. These marginal basins except the Philippine Sea basin generally have similar (or compatible) rift history in the Cenozoic, but there do be some differences in the rifting history between major basins or their sub-basins due to local differences in tectonic settings. Rifting kinematics of each of these marginal basins can be explained by dextral pull-apart or transtension. These marginal basins except the Philippine Sea basin constitute a gigantic linked, dextral pull-apart basin system.

Formation of the gigantic linked dextral pull-apart basin system in the NW Pacific is due to NNE- to ENE-ward motion of east Eurasia. This mainly was a response to the Indo–Asia collision which started about 50 Ma ago. The displacement of east Eurasia can be estimated using three aspects: (1) the magnitude of pull-apart of the dextral pull-apart basin system, (2) paleomagnetic data from eastern Eurasia and the region around the Arctic, and (3) the shortening deficits in the Large Tibetan Plateau. All the three aspects indicate that there was a large amount (1000 to 1200 km) of northward motion of the South China block and compatible movements of other blocks in eastern Eurasia during the rifting period of the basin system. Such a large amount of motion of the eastern Eurasia region contradicts any traditional rigid plate tectonic reconstruction, but agrees with the more recent concepts of non-rigidity of both continental and oceanic lithosphere over geological times. Based on these three estimates, the method developed for restoration of diffuse deformation of the Eurasian plate and the region around the Arctic, and the related kinematics of the marginal basins, we present plate tectonic reconstructions of these marginal basins in global plate tectonic settings at the four key times: 50, 35, 15 and 5 Ma. The plate tectonic reconstructions show that the first-order rift stage and post-rift stage of the marginal basins are correlated with the first-order slow uplift stage and the rapid uplift stage of the Tibetan Plateau, respectively. The proto-Philippine Sea basin was trapped as a sinistral transpressional pop-up structure at a position that was 20° south of its present position at about 50 Ma ago (or earlier). While the Japan arc migrated eastward during the rifting period of the Japan Sea basin, the Shikoku Basin opened and the Parece Vela Basin widened.

© 2013 Elsevier B.V. All rights reserved.

Contents

1.	Introduction	155
2.	Models of transtensional and transpressional basins	157
3.	Origin of major marginal basins of the NW Pacific	158
3.1.	Typical dextral transtensional basins on the east Asia land	158
3.1.1.	The Bohai Gulf basin	158
3.1.2.	The Shanxi Basin	158

* Corresponding author.

E-mail address: jyxu@cug.edu.cn (J. Xu).

3.2.	The South China Sea basin	158
3.2.1.	Geometry	158
3.2.2.	Rifting history	159
3.2.3.	Kinematics	160
3.3.	The Java, Makassar, Sulu and Celebes Seas basin system	164
3.3.1.	Geometry	164
3.3.2.	Rifting history	164
3.3.3.	Kinematics	165
3.4.	The Andaman Sea basin	165
3.4.1.	Geometry	165
3.4.2.	Rifting history	166
3.4.3.	Kinematics	166
3.5.	The East China Sea basin	166
3.5.1.	Geometry	166
3.5.2.	Rifting history	166
3.5.3.	Kinematics	166
3.6.	The Japan Sea basin	167
3.6.1.	Geometry	167
3.6.2.	Rifting history	168
3.6.3.	Kinematics	169
3.7.	The Okhotsk Sea basin	169
3.7.1.	Geometry	169
3.7.2.	Rifting history	170
3.7.3.	Kinematics	170
3.8.	The Bering Sea basin	171
3.8.1.	Geometry	171
3.8.2.	Rifting history	172
3.8.3.	Kinematics	172
3.9.	The Philippine Sea basin	172
3.9.1.	Geometry	172
3.9.2.	Rifting history	172
3.9.3.	Kinematics	174
3.10.	Summary of origin of the marginal basins	175
4.	Plate tectonic reconstructions of major marginal basins of the NW Pacific	175
4.1.	Estimation of movement of eastern Eurasia in the Cenozoic	175
4.1.1.	Amount of extension of the marginal basin system	175
4.1.2.	Paleomagnetic evidence	175
4.1.3.	Shortening history and deficits around the Tibetan Plateau	177
4.2.	Method of reconstruction of non-rigid deformation of the EUAR	181
4.2.1.	Non-rigid deformation of plates	181
4.2.2.	Method of reconstruction of non-rigid deformation of the EUAR	182
4.3.	Plate tectonic reconstructions of the marginal basins	182
4.3.1.	Plate reconstruction at 50 Ma	182
4.3.2.	Plate reconstruction at 35 Ma	186
4.3.3.	Plate reconstruction at 15 Ma	187
4.3.4.	Plate reconstruction at 5 Ma	188
5.	Discussion	189
6.	Conclusions	190
	Acknowledgments	191
	References	191

1. Introduction

A great deal of research has been devoted to studying the origin of Cenozoic basins along the NW Pacific margin since Wegener (1929) speculated that the basins had formed by extensional process that rifted the east Asian margin. Within the classical plate tectonics, there are numerous hypotheses proposed to explain the origin of these basins that include:

- (1) Active back-arc spreading that is the result of mantle diapirism caused by either heat generation along the subducting slab (e.g., Karig, 1971), secondary convection induced by the downgoing slab (Sleep and Toksöz, 1971), or asthenospheric injection (e.g., Miyashiro, 1986; Tatsumi et al., 1989).
- (2) Passive back-arc spreading related to “absolute” motions of major plates that includes the anchored-slab model (e.g., Uyeda and Kanamori, 1979), the slab-pull model invoking the seaward retreat or rollback of the downgoing slab (e.g., Dewey, 1980) or

by the downgoing asthenospheric flow below the subducted slab (e.g., Glatzmaier et al., 1990).

- (3) The collision–extrusion model in which the formation of the South China Sea and the extensional basins in North China are related to SE or eastward ejection of crustal blocks along NW and EW striking, sinistral fault systems, resulting from the collision of the Indian and Eurasian plates (e.g., Tapponnier et al., 1982; Jolivet et al., 1989, 1990; Worrall et al., 1996; Replumaz and Tapponnier, 2003; Royden et al., 2008; Yin, 2009).
- (4) Local dextral pull-apart basin development that includes the Andaman Sea, the Japan Sea, Kuril and the Bohai Gulf basins. The formation of the Andaman Sea is the result of the northward drift of India (e.g., Tapponnier et al., 1982; Maung, 1987). The Japan Sea basin was formed due to northward movement of the Amuria plate and the Kuril Basin from CW rotation of the Okhotsk plate (Lallemand and Jolivet, 1985; Kimura and Tamaki, 1986). Jolivet et al. (1994) suggest that the Japan Sea

and Kuril basins resulted from CW rotation of the American plate relative to the Eurasian plate. The Bohai Gulf basin rifted as a dextral pull-apart basin because of the dextral strike-slip offset along the Tanlu and East Taihanshan faults responding to the collision of India with Asia (e.g., Hu, 1982; Dewey et al., 1989).

- (5) Mixed models from the above for a single basin or most of those major basins. The formation of the South China Sea is mainly due to active (or slab-pull) spreading plus small SE ejection of the Indochina block resulting from the collision of India with Asia (e.g., Lee and Lawver, 1995; Hall, 2002, 2012; Morley, 2012); it is caused mainly by active back-arc spreading (or mantle plume swelling) mixed with small dextral transtension (Li et al., 1988, 1997a,b; Zhou et al., 2002). Some of the basins (e.g., South China Sea) are related to the collision–extrusion tectonics and others (e.g., Japan Sea and Kuril Basin) formed due to dextral pull-apart basins related to the CW rotation of the North

American plate relative to the Eurasian plate (e.g., Jolivet et al., 1990).

- (6) Entrapment of marginal basins including the West Philippine Basin (e.g., Ben-Avraham et al., 1972; Uyeda and Ben-Avraham, 1972; Hilde et al., 1977), Aleutian Basin (e.g., Cooper et al., 1976a; Ben-Avraham and Cooper, 1981) and Banda Sea basin (e.g., Hilde et al., 1977).

Geometry or tectonic style of a basin is usually a direct indication of its origin – a principle that has been repeatedly proved by numerous experiments (e.g., Schreurs and Colletta, 1998; Basile and Brun, 1999; McClay et al., 2002; Corti et al., 2003) and observations on small-scale basins (Burchfiel and Steward, 1966; Mann et al., 1983; Ben-Avraham and Zoback, 1992). On the basis of their geometry, it has been preliminarily proposed that the marginal basins of the NW Pacific constitute a gigantic, linked dextral pull-apart basin system and the Philippine Sea



Fig. 1. Tectonic sketch of Cenozoic basins in NW Pacific margin and its environ and their conceptual origin models. Yellow, white, ice blue, sky blue and purple areas denote land, shelf-slope (or transitional crusts), marginal basins' oceanic crust, open oceanic crust and rises in oceanic crusts, respectively. Red lines represent faults and faults barbed with solid triangles indicate boundaries between plates. Y, R and R' denote principal, synthetic Riedel and antithetic Riedel faults in dextral pull-apart rifting period, respectively. Dashed line with arrow shows direction of the eastern Eurasia displacement that resulted in dextral pull-apart rifting of marginal basins. Abbreviations (alphabetically): (1) basin (-B) or sea (-S): ADS = Andaman, BDS = Banda, BHB = Bohai Gulf, BKB = Baikal, CLS = Celebes, JVS = Java, MKS = Makassar, MRB = Mariana, PVB = Parece Vela, SKB = Shikoku, SUS = Sulu, SXB = Shanxi, TRB = Tarim; WWPB = West Philippine Sea, YSB = Yishu; (2) blocks (-K): BUK = Burma, ISK = Indochina-Sumatra, MGK = Mongolia; NCK = North China, SBK = Siberia, SCK = South China; (3) fault (-F): EOF = East Okhotsk, EVF = East Vietnam, MKF = Manila-E. Korea, NBF = NW Bering, SGF = Sagaing, RRF = Red River, SMF = Sumatra, STF = Stanovoy, TLF = Tanlu, TTF = Tartar-Tanakura, WOF = W. Okhotsk; (4) ridge or rise (-R): CAR = Caroline, IBMR = Izu-Bonin-Mariana, KR = Konipovich, KPR = Kyushu-Palau, LMR = Lomonosov, NGR = Narsen-Garkel, PLR = Palau, YPR = Yapu; (5) trench (-T): ALT = Aleutian, JPT = Japan, JVT = Java, KRT = Kuril, MAT = Mariana, SMT = Sumatra; (6) Others: CCO = Central China Orogen, EATZ = transitional zone between the Eurasian and American plates. Insets are used to explain basins' origin: lower-left inset shows the dextral pull-apart system model for the marginal basin system rifting, and lower-right inset indicates the experimental sinistral transpressional pop-up for Philippine Sea trapping. Arrows show relative block motion directions in the rifting and the trapping.

basin is originally trapped by sinistral transpression (e.g., Xu, 1996, 1997; Xu and Zhang, 1999, 2000a,b; Xu et al., 2010). This paper first reviews and improves the existing explanations about geometry, rifting history and kinematics of these marginal basins (Fig. 1), and then presents their plate tectonic reconstructions that help explain their tectonic evolutions through improving the traditional views on motions of the Eurasian and North American plates.

2. Models of transtensional and transpressional basins

Transtensional basins in a general sense include the pull-apart basin, the extensional transform-margin basin and the oblique extensional basin and only the former two are described here. Since Burchfiel and Steward (1966) introduce the term “pull-apart” to describe the origin of the Dead Sea rift, many recent and ancient pull-apart basins, have been identified. Many experimental, field and theoretical studies have added to the understanding of the geometry and kinematics of pull-apart basins (e.g., Mann et al., 1983; Ben-Avraham and Zoback, 1992; Xu, 1994; Basile and Brun, 1999). A principal strike-slip fault (Y-fault) is often accompanied by subsidiary faults that include synthetic Riedel faults (R-faults), the antithetic Riedel faults (R'-faults), as well as P faults and X faults (Bartlett et al., 1981) (Fig. 2 (left-upper)). A pull-apart basin mainly develops at the stepover between two offset Y-faults, and its boundary and internal faulting results from the development of Y-, R-, R'-, X- and P-faults (e.g., Swanson, 1990) (Fig. 2 (left-lower)). According to stages of development, initial geometry and boundary conditions,

pull-apart basins are divided into many sub-models. Fig. 2 illustrates the dextral pull-apart basin sub-models in plan view. Logically, due to mechanical heterogeneity of crust, various mixed pull-apart basin models could form.

Similar to transtensional basins, transpressional basins in general include basins that could form at the restraining stepover of strike-slip faults, the compressional transform-margin basin and the oblique compressional basin, and only the former one is described here. Usually, basins could hardly form at the restraining stepovers instead of transpressional pop-up structures. However, a transpressional pop-up structure can become a sub-basin if it develops within a large basin (e.g., a major ocean). Transpressional pop-up structures are much less studied compared with pull-apart basins and only a few authors have discussed these structures. Fig. 3 shows various tectonic styles of transpressional pop-up structures that are formed under different conditions in analog modeling (e.g., Mandl, 1988; McClay and Bonora, 2001). Overall geometry of all the sinistral pop-up structures have round rhombic or Lazy-Z shape that are similar to geometry of dextral pull-apart basins in plan-view. Within them there are two groups of conjugate faults that strike NW, NS, and most of these faults strike NW in Fig. 3(a) where plate motion is asymmetrical and in Fig. 3 c and d where the plate boundary connecting the two master faults also strikes NW. In addition, there are only a few larger-offset faults that strike NE to nearly NS. Also, a pair of major thrusts develops on the SE boundary of the pop-up in Fig. 3(c). These geometrical features help understand origin of the Philippine Sea basin (see Section 3.9 of this paper).

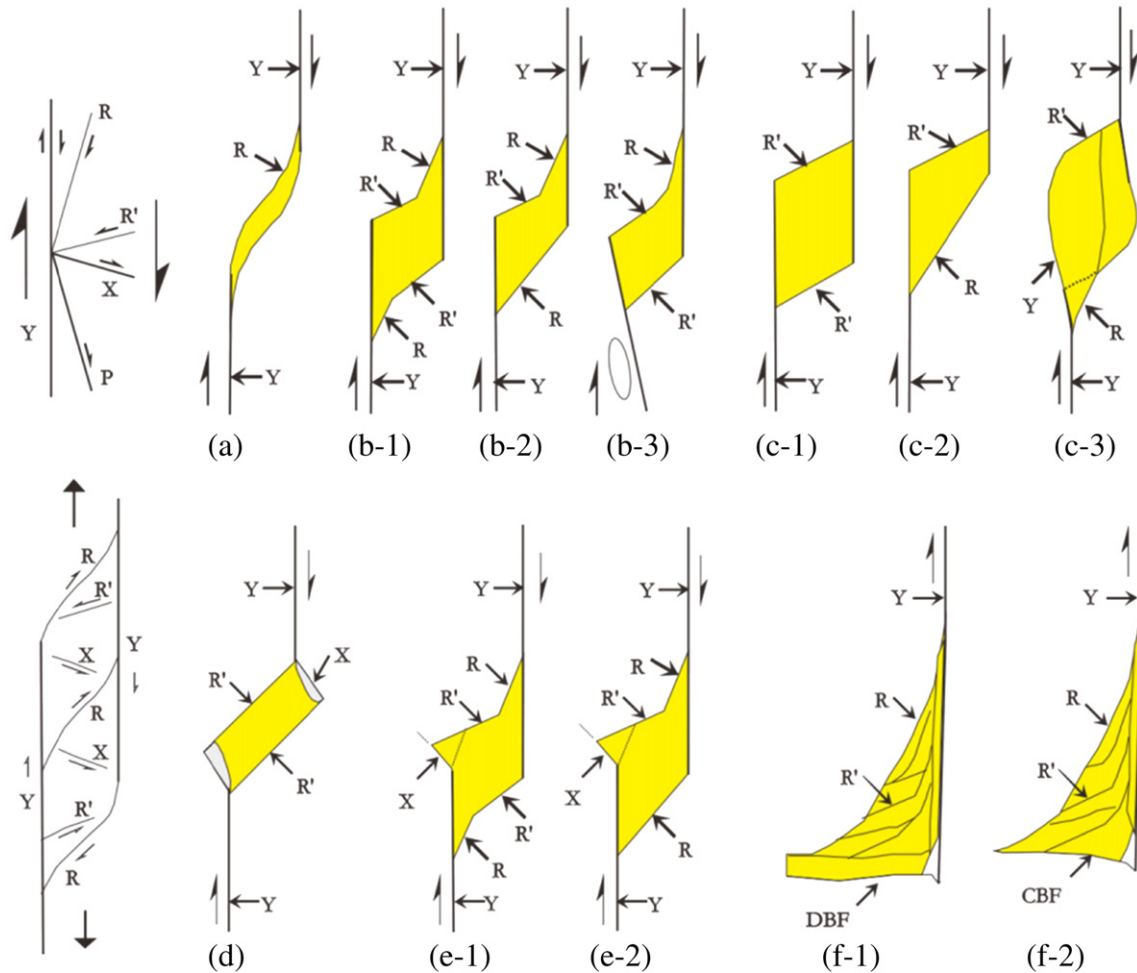


Fig. 2. Left panel: Orientations of and slip directions of R-, R'-, P-, X- and Y-shears relative to the overall right lateral sense of shear (upper: simplified from Bartlett et al. (1981) and geometry of a dextral extensional duplex (lower: after Swanson (1990), but omitting X'-shear). Right panel: models of the dextral pull-apart basin (a, b-1 to b-3, c-1 to c-3, d, e-1 and e-2), and the transform-margin basin (f-1 and f-2) (summary from Mann et al. (1983), Harding (1985), Xu et al., 1993; Dooley and McClay (1997), Basile and Brun (1999), Robert (2000), and Xu and Zhang (2000a)). The ellipse in (b-3) denotes local transpressional bulge. CBF = convergent boundary fault, DBF = divergent boundary fault.

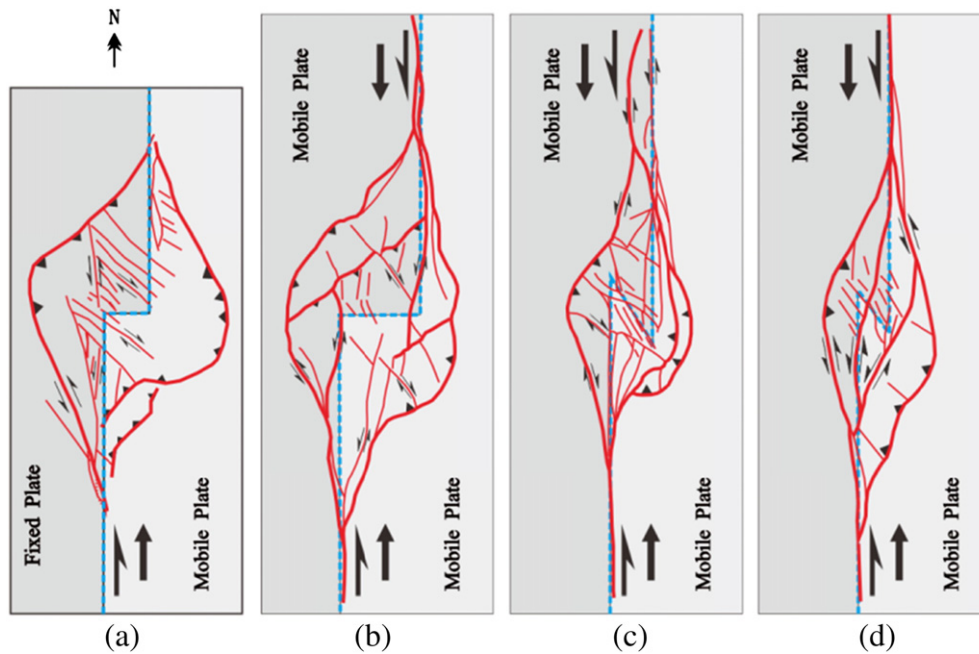


Fig. 3. Geometry of sinistral transpressional pop-up structures under different formation conditions in physical analog modeling. Red lines are faults and red lines barbed with black triangles are thrusts. Gray plates represent the plates in the analog models. Blue dashed lines are boundaries between the two plates and show the geometry of the restraining stepovers. (a) Neutral–90° restraining stepover where one plate is mobile and other is fixed. The tectonic pattern is mirrored from that of the dextral transpressional pop-up analog model of Mandl (1988). (b) Neutral–90° restraining stepover and 10 cm stepover width. (c) Overlapping–150° restraining stepover and 5 cm stepover width. (d) Overlapping–150° restraining stepover and 2.5 cm stepover width. Either of two plates is mobile and displacement on the master faults is 10 cm in (b), (c) and (d). The three tectonic patterns (b, c and d) are selected from Fig. 17 of McClay and Bonora (2001). N denotes North for convenience of discussion in the text. See the text for details.

3. Origin of major marginal basins of the NW Pacific

3.1. Typical dextral transtensional basins on the east Asia land

3.1.1. The Bohai Gulf basin

The Bohai Gulf basin generally exhibits a Lazy-Z shape in plan view (Fig. 4) and its boundary faults are analogs to shears in a typical dextral pull-apart model (Fig. 2).

Rifting in the basin began in the Mesozoic and episodically continued to Quaternary (e.g., Li, 1980; Li et al., 1997b; Hou and Qian, 1998; Ren, 1999; Xu and Zhang, 1999, 2000a) (Fig. 4 (lower-left)). The Eocene and Oligocene sediments comprise most of its rift sequences. A regional unconformity developed between the Paleogene and Neogene sediments, and the early Miocene strata were often eroded away or were not deposited (e.g., Xu and Zhang, 2000a). This basin then went into a post-rifting stage with sinistral–transpressional inversion (Li et al., 1997b). Rather weak rifting and faster subsidence resumed during Pliocene and Quaternary (Xu and Zhang, 2000b). Within the basin, igneous activity was episodic, and basalt layers of different ages were interbedded with the sediments (Yu et al., 1999) (Fig. 4 (right)), which helps in understanding why a first drilled basaltic layer may not represent the oldest oceanic basement at a place in oceanic crust of a marginal sea basin that has undergone episodic tectono-magmatic events.

Different kinematical models for its rifting have been proposed (e.g., Li, 1980; Hu, 1982; Tapponnier et al., 1982; Dewey et al., 1989; Li et al., 1997a,b; Allen et al., 1998). There are two models among them that seem more widely accepted: dextral pull-apart due to the northward motion of its west block relative to its east block (Hu, 1982; Dewey et al., 1989), and WNW–ESE directed extension due to sinistral strike slip along the Qinling fault (Tapponnier et al., 1982). Considering its geometry, we favor the former model.

3.1.2. The Shanxi Basin

The Shanxi Basin can be divided into three parts: the Datong graben system in the north; the Jinzhong graben in the center; and the Weihe graben system in the south (Fig. 5). There are NNE- to NS- trending

subsidiary grabens between the three parts. The northern and southern boundary faults that strike ENE are interpreted as R'-faults. The NNE-striking faults of the basins are R-faults. The Y-fault doesn't occur. The northern and southern parts of the basin are attributed to the model f-2 (Fig. 2) and the Jinzhong graben to the model d (Fig. 2). It rifted mainly during Pliocene and Quaternary, but the weak rifting in its some parts began in the Paleogene and its initial fault pattern might form in Paleogene (e.g., Liu, 1982; Xu et al., 1993).

The Shanxi Basin resulted from right-lateral transtension along a NNE- or NS-striking fault (e.g., Liu, 1982; Xu et al., 1993). Xu et al. (1993) believe that the right-lateral, strike slip along the NNE striking faults is only a by-product of large left-lateral, strike-slip along the Altyn–Qinling fault, as originally proposed by Tapponnier et al. (1982). However, its overall geometry that is similar to the composite models f-2 and d (Fig. 2) just indicates that its fault pattern mainly resulted from right-lateral strike-slip shear along the potential NS striking Y-fault (the Y-fault has not formed because a Y-fault can develop later than Riedel-faults and P-faults) (e.g., Basile and Brun, 1999). Of course, mechanically sinistral strike-slip displacements along the Qinling and Jincheng faults could intensify the basin's rifting. Therefore, the Shanxi Basin originated from a combination of both the dextral strike-slip shear along the potential NS-striking Y-fault and the sinistral strike-slip shear along the Qinling and Jincheng faults.

3.2. The South China Sea basin

The South China Sea basin (SCS) is a key member among the marginal basins in the NW Pacific. Its origin is related to many important conundrums regarding the tectonic evolution of this region.

3.2.1. Geometry

SCS generally resembles a dextral, pull-apart basin in plan view (Fig. 6). Its western boundary fault, the East Vietnam fault approximately strikes NS, and to the south it possibly plays into many faults that are concave to the NE (Kulinich and Obzhairov, 1985; Huchon et al., 1998; Liu, 1999; Fyhn et al., 2009; NGDC, <http://www.ngdc.noaa.gov/mgg>).

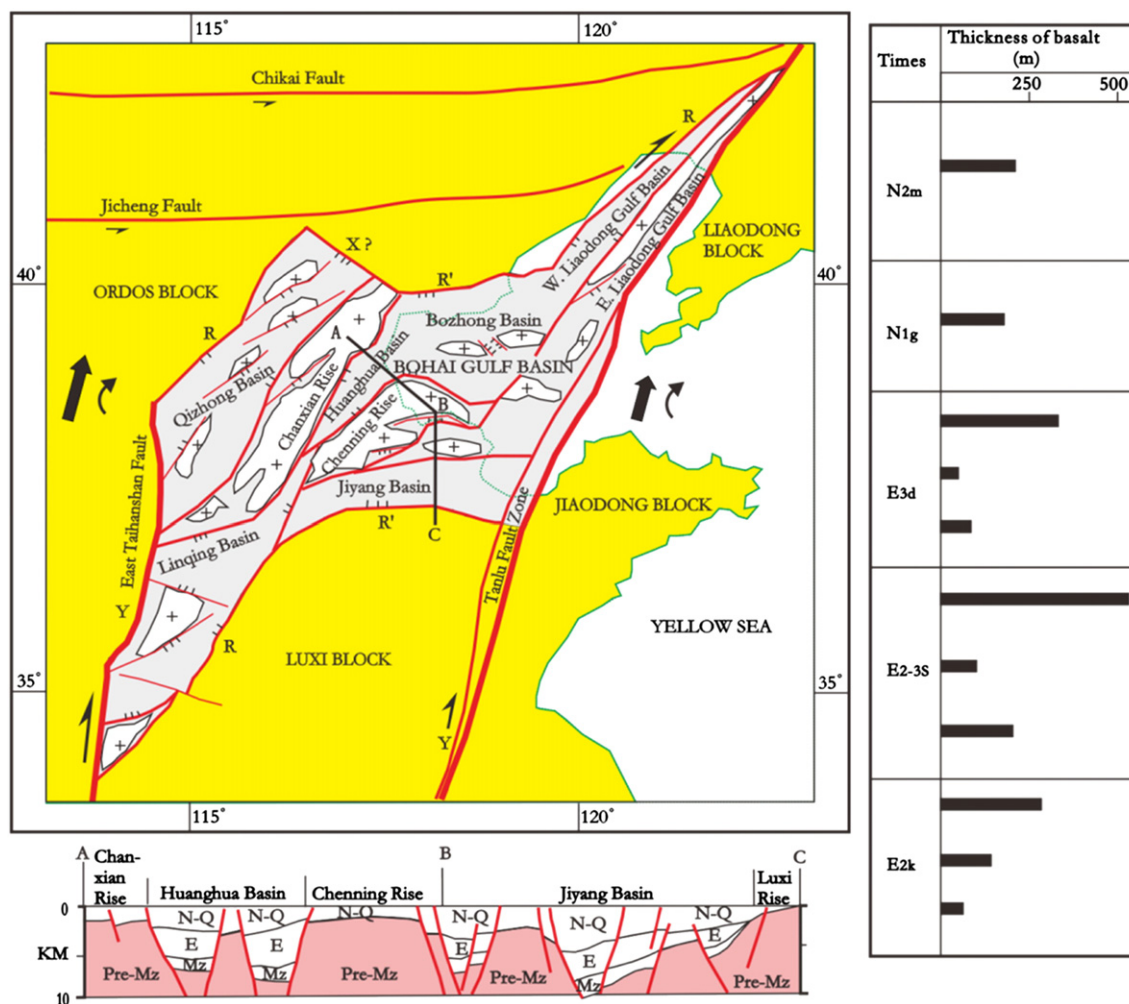


Fig. 4. Upper-left panel: Tectonic sketch of the Bohai Gulf basin showing its geometry and rifting kinematics. Closed curves with crosses in them represent rises covered with much thinner (or without) strata of the rifting-period. Faults with two short line bars represent normal faults with dextral strike-slip. Faults with three short line bars represent normal faults. Open arrows represent the translation vectors (not to scale) of the bilateral blocks of the basin and arc solid arrows do small-angle rotation direction of the blocks during the rifting period. Y, R, R' and X have the same meanings as in Fig. 2. Lower-left panel: simplified profile along the A–B–C line in the upper-left panel showing timing of its rifting sequence formation. N = Neogene, Q = Quaternary, E = Paleogene (and early Miocene), Mz = Mesozoic, Pre-Mz = Pre-Mesozoic. Right panel: Age and thickness of basalt and sills interlayered with sediments in the Huanghua sub-basin (after Yu et al. (1999)). E_{2k} = the early Eocene Kongdian Group, E_{2-3s} = the middle Eocene to early Oligocene Shahejie Group, E_{3d} = the late Oligocene Dongyin Group, N_{1g} = the Miocene Guantao Group, N_{2m} = the Pliocene Minghuazhen Group.

The East Vietnam fault does not extend toward the south as a large brittle fault cutting through the Natuna arch of Sunda Shelf during the Cenozoic, although some authors hypothesize it did during the early Tertiary (Hilde et al., 1977; Hutchison, 1989; Longley, 1997). Logically its southern extension could be presumed to be a large ductile shear zone (see Section 3.2.3 for details). The East Vietnam fault together with its presumed southern ductile extension is the Y-fault of this basin.

The northern segment of the West Philippine fault (WPF), generally striking NS, is the eastern boundary of SCS. The northern WPF, the Lishan fault in Taiwan, the west boundary fault of the Okinawa Trough, and the East Korea fault (west boundary fault of the Japan Sea basin), possibly were segments of a mega-fault according to geophysical and geological data (e.g., Kong et al., 2000; Hsu et al., 2001; NGDC, <http://www.ngdc.noaa.gov/mgg>) and speculations (Xu, 1997; Xu et al., 2004). The mega-fault is named the Manila–East Korea fault system (MKF) (e.g., Xu et al., 2004). MKF, which is curved at present, was possibly straighter before the northern WPF (proto-Manila trench fault) and the Lishan fault were compressed in NW during the post-rifting period of SCS, and could be a dextral strike-slip fault as a Y-fault during the main rifting period of SCS (e.g., Xu et al., 2004; see Section 4 for more details). Identification of MKF is a key to understand kinematic correlation between the South China Sea and Japan Sea basins.

The northern boundary fault of SCS is the northern boundary faults of the Pearl River Mouth and Qiongdongnan basins, which are interpreted as a R'- and R-faults respectively. The east southern boundary fault of SCS generally strikes NE along the Palawan Trough (also known as NW Borneo Trough (Hutchison, 2004, 2010); or called NW Borneo–Palawan Trough (Morley, 2012), or North Borneo Trough (Hall, 2012)) and can be interpreted as a Riedel shear. As the southern boundary fault approaches the East Vietnam fault, its SW segment progressively changes in strike from EW to NNW. This could be explained as the result from CW rotation of original NE striking R-fault (see Section 3.2.3 for explanation).

The four boundary faults of SCS delimit an asymmetric pull-apart basin, generally resembling the scaled analog model c-2 (Fig. 2) if the Red River fault as a rotated X-fault is considered.

3.2.2. Rifting history

Rifting in sub-basins on continental crust of SCS generally began in the late Mesozoic and episodically continued into the Quaternary (e.g., Li et al., 1999; Clift and Lin, 2001; Morley, 2002; Ren et al., 2002; Xu et al., 2004). Rifting in most of the sub-basins developed during Eocene and Oligocene (e.g., Morley, 2002). In the early Miocene, rifting of different intensity appeared in the continental margins: (1) the northern margin (Gong et al., 1997; Li et al., 1999; Clift and

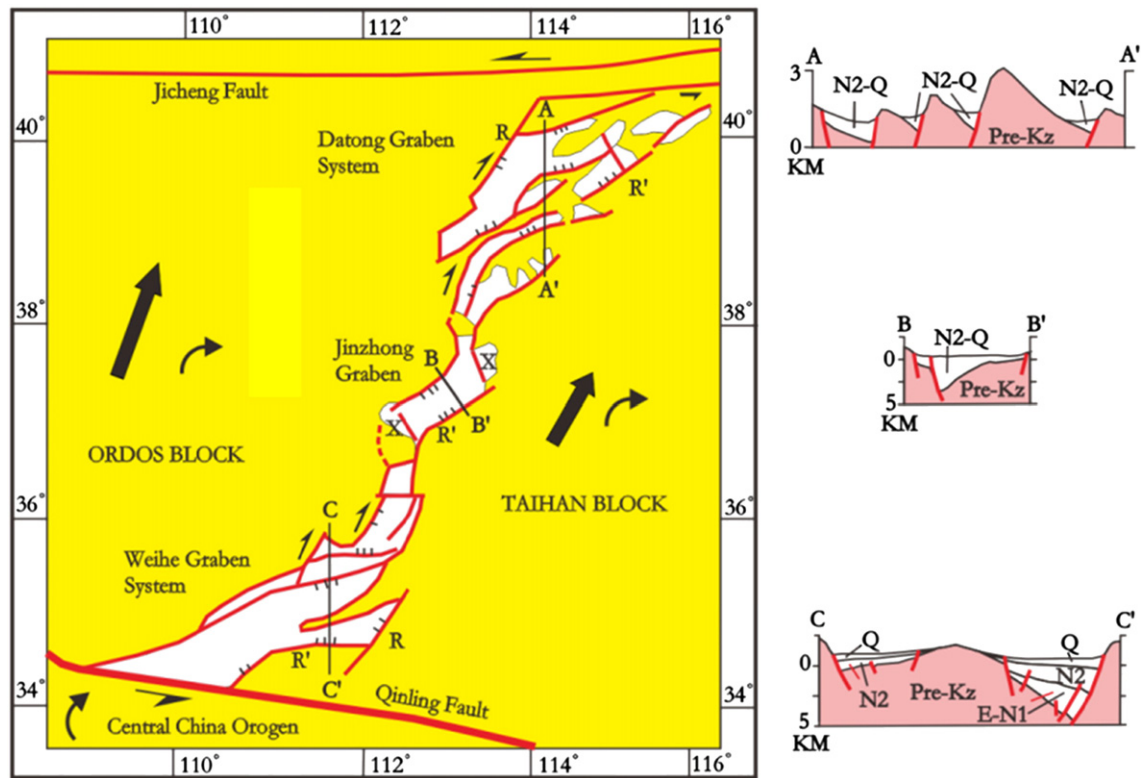


Fig. 5. Left panel: Tectonic sketch of the Shanxi Basin showing its geometry and rifting kinematics (modified from Xu et al. (1993)). Right panel: Three profiles along A–A', B–B' and C–C' lines, respectively (see locations in the left panel) showing development of rifting sequences. N2 = Pliocene, N1 = Miocene, Pre-Kz = Pre-Cenozoic. Other symbols and legends are the same as in Fig. 4.

Lin, 2001), (2) the western margin (e.g., Morley, 2002), and (3) the southern margin (e.g., Mat-Zin and Swarbrick, 1997; Hutchison, 2004; Xu et al., 2004; Qiu, 2005).

Taylor and Hayes (1980, 1983) interpret that the oceanic crust of SCS formed during Anomaly 11 to 5 day (32–17 Ma) and Briais et al. (1993) reinforced this interpretation, suggesting it formed during 32–15.5 Ma according to their updated magnetic reversal time scale. These isochrones are more widely accepted (e.g., Ben-Avraham, 1989; Gong et al., 1997; Clift et al., 2008; Hall, 2012; Morley, 2012) although the different ages are suggested (e.g., Yao et al., 1994; Barckhausen and Roeser, 2004; Hsu et al., 2004; Li et al., 2007).

Many authors believe that rifting in SCS resulted from active (and/or slab-pull) spreading (e.g., Taylor and Hayes, 1983; Li and Yang, 1997; Morley, 2002) or from the sinistral pull-apart (e.g., Tapponnier et al., 1982; Briais et al., 1993), but we don't favor the two models (see Section 5. Discussion for details). We suggest that SCS originated from dextral pull-apart, and was episodically reworked by dextral pull-apart rifting as well as other tectonic activities, based on the following lines of evidence.

- (1) Normal faults in the continental margins have NE to EW strikes (e.g., Taylor and Hayes, 1983; Yao et al., 1994) and the maximum principal axes of strain ellipses are oriented NW to NNW, suggesting the rifting was due to dextral pull-apart with principal faults (e.g., the East Vietnam fault) striking NS, as is a basic fault-mechanics theory (e.g., Mandl, 1988; Waldron, 2005).
- (2) Similar to normal faults in the continental margins, magnetic lineations (as extensional structures) in the oceanic crust trend NE to EW. The general trend of magnetic lineations appears to be Z-shaped from the central part of the Central Basin to the SW Basin (e.g., Okubo et al., 1997; Fang and Zhou, 1998; Chen et al., 2010a). Such geometry of magnetic anomalies of the SCS resembles that of R- and R'-faults of a dextral pull-apart.

- (3) Widely-distributed volcanic seamounts, some of which are dated as the Early Miocene and the Paleogene (e.g., Li et al., 1991), trend parallel to the R- and R'-faults.
- (4) Multiple volcanic episodes in the continental margins during both rifting and post-rifting periods are recorded (e.g., Li et al., 1999). Reflection seismic data from the oceanic crust (e.g., Zeng, 1991) show there are some dykes within the Layer 2 and the Layer 1, indicating the earlier oceanic crust was reworked by the later tectono-magmatic activities. Basaltic magmas can come from the upper mantle along extensional faults (rather than from deep mantle plumes) and modify continental and oceanic crusts (e.g., Anderson, 2004; Foulger, 2007; see Foulger and Jurdy (2007) for further discussion), as helps understand basaltic rock distributions and magnetic anomaly patterns in marginal seas of the NW Pacific where tectonic activities often happened due to interactions between the major plates.

3.2.3. Kinematics

The total pull-apart amount of SCS on average can be estimated to be approximately equal to the width of the Central Oceanic Basin plus extension of the northern and southern continental margins at longitude E116°. The width of the oceanic crust is about 700 km. The average extension coefficient of the thinned continental margin is about 1.4 (1.25 to 1.47) (Zeng, 1991) or slightly different (e.g., Hayes et al., 1995; Clift and Lin, 2001) and the length of the margin along the long. E116° is about 400 km. This leads to extension of the margin by about 115 km. The amount of the thinned southern continental margin (the Dangerous Grounds–Reed Bank block and Palawan Trough) is hypothesized to be about equal to that of the northern margin. Therefore, the total magnitude of pull-apart is estimated to be around 930 km (700 + 2 × 115 = 930 km). Further to the east, the amount of pull-apart of SCS is about the same or a little larger.

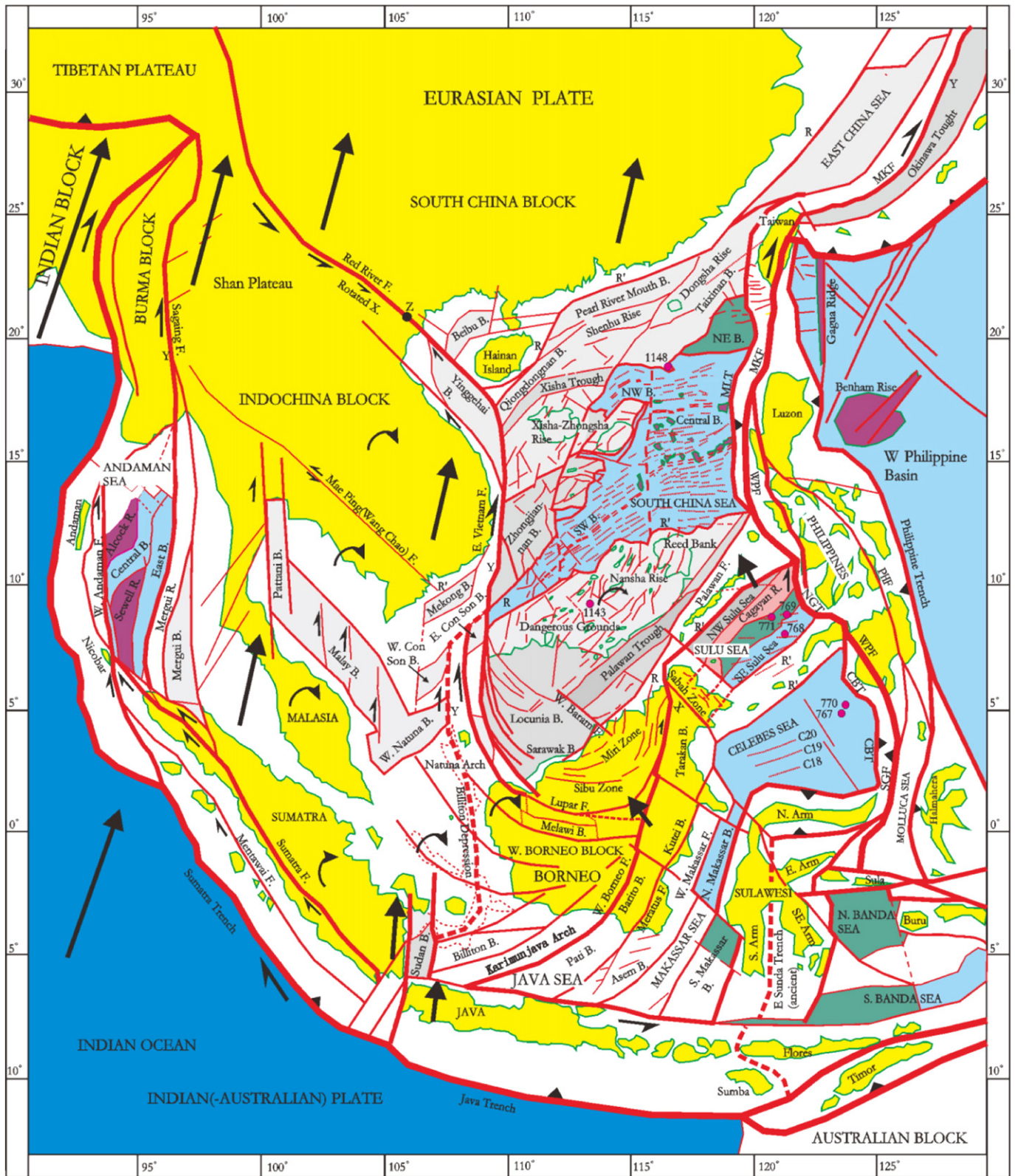


Fig. 6. Tectonic sketch map of the South China Sea basin and its environ, showing its geometry and rifting kinematics (modified from Xu et al. (2004)). Light and dark gray areas denote basins on generally heavily and weakly thinning continental crusts, respectively, but some basins on shelf and land are not painted gray for neatness. Purple and pink areas are oceanic and continental rises, respectively. Light green and ice blue areas represent the transitional and oceanic crusts in marginal seas, respectively. Red solid and dashed lines are faults and postulated faults, respectively. The red dotted lines and the red double dashed lines in the oceanic crust are magnetic anomaly lineations and the extinct spreading axes, respectively. Point Z is the point where the strike-slip offset of the Red River fault presumably is zero. Red-filled small circles and their labeled numbers are Sites of ODP and the Sites' numbers, respectively. Abbreviations: B. = Basin, F. = Fault, R. = Rise; CBT = Cotabato Trench, MKF = Manila-E. Korea Fault, MLT = Manila Trench, NGT = Negros Trench, SG F = Sangihe Fault, PHF = Philippine Fault, WPF = West Philippine Fault. Other legends are the same as in Figs. 1 and 4.

An important kinematic problem is how the East Vietnam fault (EVF), and its southern region (Malay Shelf–Sumatra and the west Borneo–Java Shelf) where there is no a large magnitude offset, accommodated the 930 km of pull-apart. We suggest that it could be accommodated in two ways: overall CW rotation of the Indochina–Sumatra region and overall CW rotation of the Borneo–Java Arc region. Detailed descriptions of these two ways are as follows:

- (1) The region west of the South China Sea and Borneo–Java Arc region, including the Indochina (Shan Plateau, Khorat Plateau), Malaysia and Sumatra sub-blocks, is delimited by four major faults—the East Vietnam, Sagaing, Red River and Sumatra (or Sumatra Trench) faults. Its geometry is similar to that of a dextral, strike-slip duplex, with many NW-striking faults similar with the Red River fault (RRF). The duplex is termed the Indochina–Sumatra block (ISK) (Xu et al., 2004). England and Molnar (1990) propose that the Red River fault and similar faults in eastern Tibet are by-products of a dextral NS-striking mega-shear (domino-style). Their model is also important to understanding accommodation of large-magnitude block rotation during pull-apart of SCS. We further refine England and Molnar (1990)'s model for ISK in following four aspects (Fig. 7):
 - (a) ISK is modeled as a rhomb which consists of small sub-blocks of different size that are delimited by NW-striking faults with small offsets.
 - (b) Different deformation styles and local rotational differences of sub-blocks (including CCW rotations of some sub-blocks) in ISK occur, as shown by some paleomagnetic declinations (e.g., Richer et al., 1999).
 - (c) Differential rotation between the Indochina–Sumatra block and the west South China block results in a small NS extension component (ΔT in Fig. 7b) in the Beibu Gulf and Yinggehai sub-basins, which lie north and south of the SW segment of the Red River fault respectively. Similar differential rotation

- between the Malaysia Peninsular sub-block and the Indochina sub-block results in extension of the Malaysia Gulf sub-basin (this differential rotation is not shown in Fig. 7 for simplicity).
- (d) Small right-lateral displacements might have taken place on some NW-striking faults within the block when right-lateral shear components occurred along the Sumatra Trench fault (SMF) due to oblique subduction of the India plate and when NW-striking faults rotated CW to an enough oblique orientation. The block finally forms a dextral transpressional duplex. Deformation of this duplex in this way can greatly increase its length (ΔL) or provide pull-apart motion (ΔE_n in Fig. 7b and c) of SCS. The simple relation between ΔE_n and other parameters in such a rhombic duplex is expressed in Fig. 7d.
- (2) The Borneo–Java arc region (BJK) east of ISK, modeled as a distorted rhomb (Fig. 7), also undergoes CW rotation because of diffuse dextral NS striking mega-shear. The CW rotation is similar to that of the Indochina–Sumatra block, but inhomogeneous. Dextral, diffuse inhomogeneous rotation is supported by the following tectonic features: gravity anomalies (e.g., Sandwell and Smith, 1997) show that strikes of the Lupar fault and similar faults change from ENE (or EW) progressively to NW or NNW across the Natuna arch (Fig. 6). Many small discrete faults developed on the Sunda Shelf, especially along the Billiton Depression (Ben-Avraham and Emery, 1973). The nearly NS-striking west boundary fault of the Sunda Basin was a dextral strike-slip fault (Simandjuntak and Barber, 1996) that formed during the dextral rifting period of the Sunda Basin and is currently active (Fujita, 1987). Deformation in this manner could provide extra dextral displacement (E_d in Fig. 7b and c).

In order to calculate the resulting total pull-apart ΔE_t (ΔE_n and ΔE_d in Fig. 7b and c) and to describe motions of any point in both ISK and BJK from time 0 (at the present) to t , a coordinate system is set up

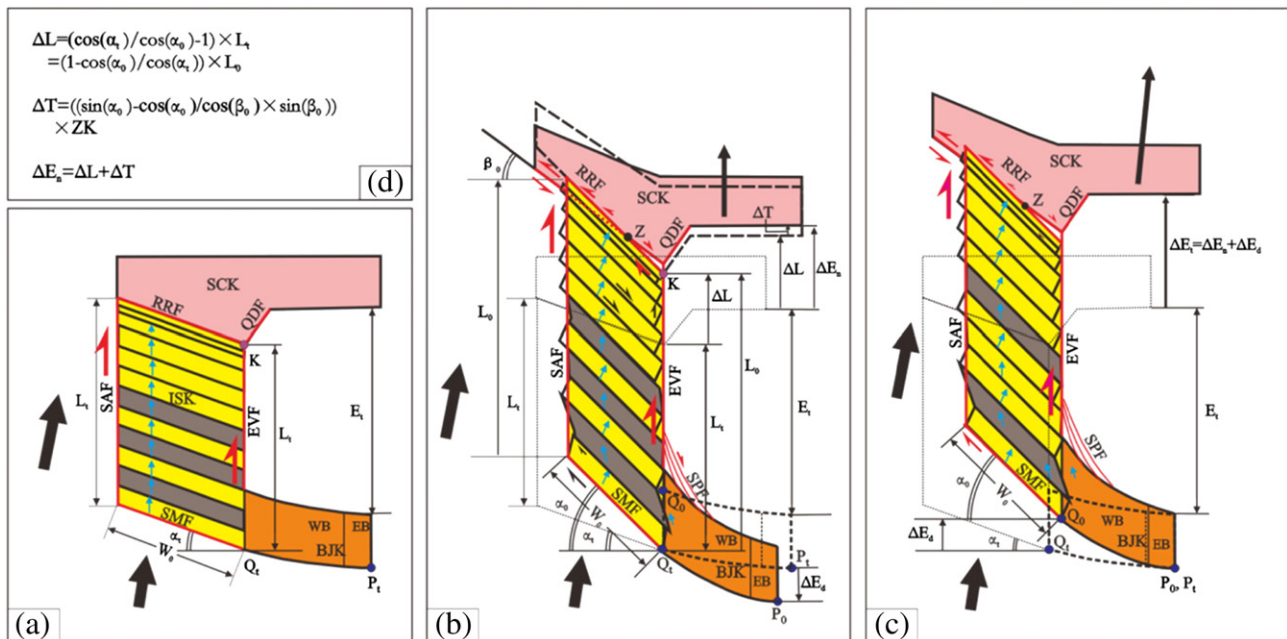


Fig. 7. Sketch model showing kinematics of the Indochina–Sumatra block (ISK) and the Borneo–Java arc region (BJK, WB = West BJK, EB = East BJK) to accommodate the pull-apart amount of the South China Sea. Shapes of ISK, BJK and SCK (South China Block) are highly simplified. Abbreviations: EVF = East Vietnam fault, QDF = Qiongdongnan fault, RRF = Red River fault, SAF = Sagaing fault, SMF = Sumatra fault (or Trench), SPF = splays of southern East Vietnam fault zone; SCK = South China block. Thick and middle thick arrows denote the Indian plate and SCK motion directions, respectively. The small blue arrows within small blocks in ISK represent local paleomagnetic declinations (shaded small blocks are non-rigid). See the text for symbols' meanings. (a) Pre-CW rotation of ISK at time t ; (b) after CW rotation of ISK with reference point Q_0 fixed; (c) After CW rotation of ISK with reference point P_1 fixed. (d) Formulae between the parameters. See the text for more details.

(Fig. 8a) where the spherical surface curvature of Earth is approximately treated as a planar surface and differences in deformation style between the small blocks shown in Fig. 7 are neglected.

For the present-day ISK strike-slip duplex, the modeled rhomb is more properly delimited by a rhomb of NNE-striking principal strike-slip faults (dotted black line rhomb in Fig. 8b). However, for simplicity, a NS-striking modeled rhomb is chosen (dashed blue line rhomb in Fig. 8b). The coordinate origin is hypothesized to be located at (long. 110°E, lat. -10°) and the X-axis passes through Samba Island (Fig. 8b). If the position of any point at present is (x_0, y_0) , its previous position (x_t, y_t) at time t can be calculated using the following formula:

$$\begin{cases} x_t = x_0 \frac{\cos(\alpha_t)}{\cos(\alpha_0)} & (x_0 \leq 0) \\ y_t = (y_0 + x_0 \operatorname{tg}(\alpha_0)) \frac{\cos(\alpha_0)}{\cos(\alpha_t)} - \frac{\sin(\alpha_t)}{\cos(\alpha_0)} x_0 - \Delta E_d \end{cases} \quad (1)$$

Where ΔE_d is defined as in Fig. 8a.

In order to calculate ΔE_d , we assume (again for simplicity) that, the non-rigid deformation of BJK is similar to that of ISK in that its area and length of curve P_tQ_t are kept constant from t to 0. However, the rotation angles eastward linearly decreased with distance to longitude 110° E ($x = 0$, the east boundary of ISK), with the maximum angle equal to that of ISK along longitude 110° E. The minimum angle is equal to zero along longitude 120° E at about the eastern border of West Sulawesi Arm–Samba Island. Such a coordinate system means that point P_t is located at (long. 120° E, lat. -10°) in Samba Island, or that there is no latitudinal shift between P_t and P_0 (compare Fig. 8b with Fig. 8a) and Samba Island can basically act as a latitude-fixed location. Under this simple assumption, the position of any point (x_t, y_t) in both ISK and BJK at any given rotational angle can easily be calculated

from the position of its correspondent point (x_0, y_0) according to the following analysis.

It is assumed that the x-coordinate projections of the microelement length dl_t along the curve P_tQ_t at t and dl_0 along the curve P_0Q_0 at 0 are dx_t and dx_0 , respectively (Fig. 8a). Since dl_t is equal to dl_0 , then:

$$\begin{cases} \frac{dx_0}{\cos(\alpha_0 - k_0 x_0)} = \frac{dx_t}{\cos(\alpha_t - k_t x_t)} & (x_0 \geq 0) \\ k_0 = \frac{\alpha_0}{x_{0\max}} \\ k_t = \frac{\alpha_t}{x_{t\max}} \end{cases} \quad (2)$$

where angles α_t and α_0 are the maximum rotation angles at t and at 0 respectively as shown in Fig. 7a, and $x_{t\max}$ and $x_{0\max}$ are x coordinates of points that have no rotation at time = t and at time = 0, respectively. Because differences between $X_{t\max}$ and $X_{0\max}$ are so small (less than 1.5°) and if differences in rotation angles are less than 30°, then $x_{t\max} \approx x_{0\max} = 10^\circ$ ($120^\circ - 110^\circ$). The above formula (2) can be written:

$$\frac{1}{k_0} \int_0^{x_0} \frac{1}{\cos(\alpha_0 - k_0 x_0)} d(k_0 x_0) = \frac{1}{k_t} \int_0^{x_t} \frac{1}{\cos(\alpha_t - k_t x_t)} d(k_t x_t) \quad (3)$$

Integrating the above formula, it then becomes

$$\begin{aligned} & -\frac{1}{k_0} (\operatorname{Ln}(\operatorname{tg}(\pi/4 + \alpha_0/2 - k_0 x_0/2))) - \operatorname{Ln}(\operatorname{tg}(\pi/4 + \alpha_{0\max}/2)) \\ & = -\frac{1}{k_t} (\operatorname{Ln}(\operatorname{tg}(\pi/4 + \alpha_t/2 - k_t x_t/2))) - \operatorname{Ln}(\operatorname{tg}(\pi/4 + \alpha_t/2)) \end{aligned} \quad (4)$$

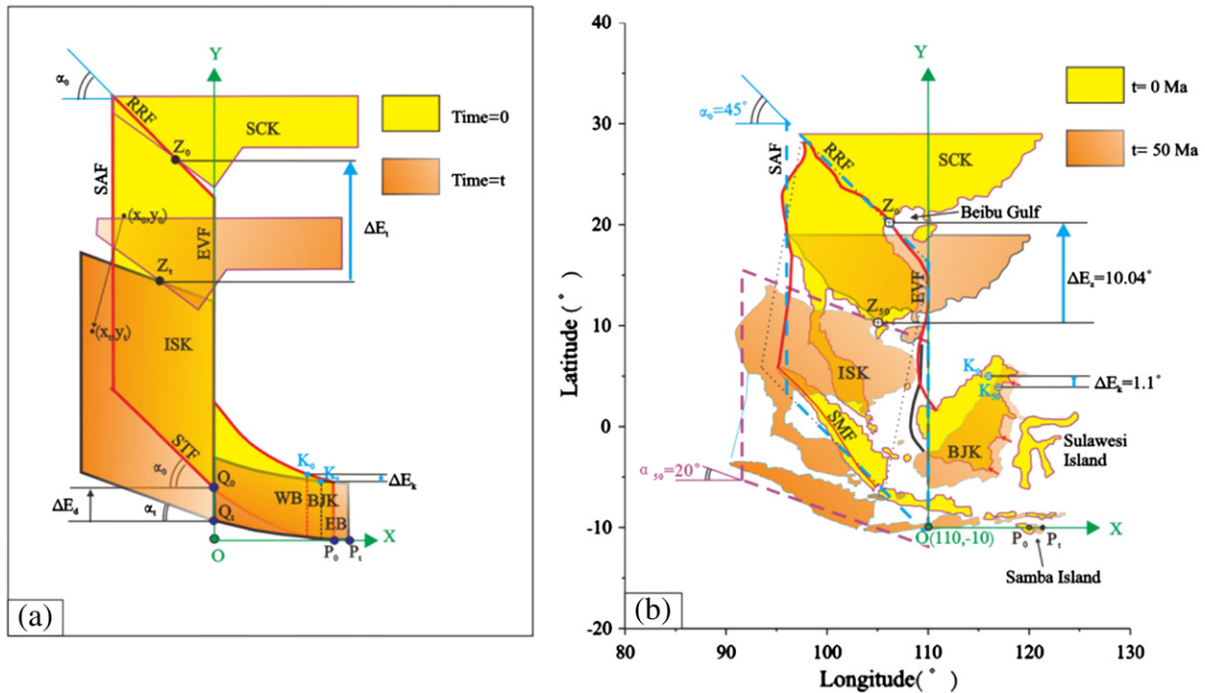


Fig. 8. Motions of points in the Indochina–Sumatra block (ISK) and the Borneo–Java Arc region (BJK, WB = West BJK, EB = East BJK) in a given coordinate system. Abbreviations and symbols' meanings are same as in Fig. 7. (a) Explanatory diagram for the point motions, which is simplified from Fig. 7 (b, c); (b) Reconstruction of shorelines of ISK and BJK based on the model shown in (a) if $\alpha_0 = 45^\circ$ and $\alpha_{50} = 20^\circ$. The dotted-line rhomb delimits actual ISK, and the dashed-line rhomb delimits apparent ISK that is used to calculate the point motions in ISK. ΔE_2 is the total north displacement of the present point Z_0 located at the intersection between the Beibu Gulf shoreline and the Red River fault (RRF), and ΔE_1 is the total north displacement of a present point K_0 in NE Borneo. Red arrows represent extensional vectors between Borneo and West Arm of Sulawesi Island if this arm is fixed. See the text for more details.

So:

$$x_t = \frac{2}{k_t} [\pi/4 + \alpha_t/2 - \arctg \left(\left\{ \frac{\tg(\pi/4 + \alpha_0/2 - k_0 x_0/2)}{\tg(\pi/4 + \alpha_0/2)} \right\}^{\frac{k_t}{k_0}} \times \tg(\pi/4 + \alpha_t/2) \right)] \quad (5)$$

If the area from t to 0 keeps constant, then

$$\left(y_0 - \int_{x_0}^{x_{0max}} \tg(\alpha_0 - k_0 x_0) dx_0 \right) dx_0 = \left(y_t - \int_{x_t}^{x_{tmax}} \tg(\alpha_t - k_t x_t) dx_t \right) dx_t \quad (6)$$

Integrating the above formula, it then becomes

$$\left[y_0 - \frac{1}{k_0} (\ln(\cos(0)) - \ln(\cos(\alpha_0 - k_0 x_0))) \right] \frac{dx_0}{dx_t} \quad (7)$$

$$= y_t - \frac{1}{k_t} [\ln(\cos(0)) - \ln(\cos(\alpha_t - k_t x_t))]$$

So:

$$y_t = \left[y_0 + \frac{1}{k_0} (\ln(\cos(\alpha_0 - k_0 x_0))) \right] \frac{\cos(\alpha_0 - k_0 x_0)}{\cos(\alpha_t - k_t x_t)} - \frac{1}{k_t} [\ln(\cos(\alpha_t - k_t x_t))] \quad (8)$$

By use of formulae (1) and (5) and (8), the position of any point both in ISK and BJK can be reconstructed at given rotational angles α_0 and α_t .

Present strikes of RRF and SMF are on average about N45° W and N50° W, respectively. This means that α_0 could be between 45° and 50°, the average of which, α_{0m} , is simply 47.5°.

If $\alpha_0 = 45^\circ$ at 0 Ma and $\alpha_{50} = 20^\circ$ at 50 Ma, then shorelines of ISK and BJK are reconstructed from their present location (Fig. 8b) using formulae (1), (5) and (8). The present position of reference point Z_t (long. 106.16° E, lat. 20.19°), which is hypothesized to be at intersection between the Beibu Gulf shoreline and the Red River fault, is reconstructed to (long. 105.06° E, lat. 10.21°) at 50 Ma. That is to say, the reference point's total latitude shift ΔE_t amounts to about 10.04° relative to (long. 120°, lat. -10°) at Samba Island, and to about 8.94° ($\Delta E_t - \Delta E_k$) relative to point K₀ (long. 116° E, lat. 5°) at the northernmost end of the eastern boundary of West Borneo (Fig. 8b). If $\alpha_0 = \alpha_{0m} = 47.5^\circ$ at 0 Ma and $\alpha_{50} = 20^\circ$ at 50 Ma, then ΔE_t is equal to about 11.17° relative to Samba Island and ($\Delta E_t - \Delta E_k$) is up to about 9.94°. If $\alpha_0 = \alpha_{0m} = 50^\circ$ at 0 Ma and $\alpha_{50} = 20^\circ$ at 50 Ma, ΔE_t is equal to about 12.25° relative to Samba Island and ($\Delta E_t - \Delta E_k$) is up to about 11.25°. To summarize, the generally diffuse CW rotations of ISK and BJK amply provided the 1000 km, or 9° latitude, of pull-apart to SCS along longitude 116° E.

Furthermore, if the Samba and Sulawesi islands are fixed to the coordinate system, Borneo generally moves NW-ward relative to the two islands. Motion on average is about 120 km if $\alpha_0 = 45^\circ$ at 0 Ma and $\alpha_{50} = 20^\circ$. This motion can accommodate partial transtension of the Java–Makassar–Celebes–Sulu seas transtensional system (Fig. 8b). This motion is not enough to provide full transtension of this local basin system and Borneo must have additionally moved NW-ward relative to the two islands during the rifting period (see Section 3.3.3 in this context for more).

3.3. The Java, Makassar, Sulu and Celebes Seas basin system

3.3.1. Geometry

Geometry of the Java, Makassar, Sulu and Celebes Seas basins together with rift basins in Borneo is similar to that of the southern and central parts of the Shanxi Basin in North China (Figs. 6 and 5). The NW and SE

boundary faults of the Sulu Sea and Celebes Sea basins, striking NE, are R'-faults. Their SW boundary faults, striking NW, may be rotated X-faults. The NE boundary faults of the two basins, the northern segment of the West Philippine fault which includes the Negros and Cotabato trench faults, seems parallel with X-faults. The NW part of Celebes Sea basin has a similar geometry to the Sulu Sea basin like the Jinzhong Graben of the Shanxi Basin, but is fan-shaped in its southern part. The Java Sea and Makassar Sea basins together with grabens in Borneo are similar to the southern part of the Shanxi Basin. Also the pattern of faults bounding sub-basins in the Java Sea and Makassar Sea basins (Weerd and Armin, 1992; Simandjuntak and Barber, 1996; Morley, 2002) is similar to that of the Shanxi Basin and consists of R- and R'-faults. Basins of the four seas together with the onshore basins possibly comprise a local dextral transform-margin basin system (here abbreviated as the JMCS basin system).

3.3.2. Rifting history

Rifting history of sub-basins on the present continental crust in the JMCS basin system is controversial because post-rift inversion modified the basins significantly. Satyana et al. (1999) attribute the 50 to 15 Ma and Middle Miocene to the present strata in the Barito, Kutei and Tarakan basins to transgressive and regressive sequences, respectively. The transgressive and regressive sequences probably are rifting and post-rifting (inversion) sequences, respectively. Morley (2002) suggests that mainly rifting in the three sub-basins occurred during Eocene and Oligocene and the inversion began in the early Miocene, which is different from the inversion time of the early Middle Miocene as suggested by Weerd and Armin (1992). The Crocker and Central basins in the Sabah zone (also in the southernmost margin of the South China Sea basin) received the Eocene to the earliest Neogene sediments, and were inverted in the middle Miocene (Rangin, 1989; Rangin et al., 1990; Hutchison, 1996). Again, the Crocker turbidite fan of north Borneo that was derived from local sources from the Eocene to the Early Miocene (Hall et al., 2008) could deposit in a narrow deep-marine rift trough on the southernmost margin of the South China Sea basin and its compressional deformation could form after the early Miocene. Some authors (e.g., Rangin and Sliver, 1991; Hall, 2002) believe that sediments within the NW and SE Sulu Sea basins are underlain by continental crust and oceanic crust, respectively. From the seismic profiles reported by Rangin (1989), the NW Sulu Sea basin rifted during Paleogene (to early Miocene?), and the inversion began at approximately 15 Ma, which is indicated by regional unconformity below the middle Miocene sediments (Rangin and Sliver, 1991). Therefore, the sub-basins on the continental crust generally rifted during the Paleogene (Eocene) to the early Miocene, and then entered the post-rifting period with inversion.

Based on data from Holes 768, 769 and 771 of ODP Leg 124, Rangin and Sliver (1991) suggest that the SE Sulu Sea basin opened as a back-arc basin during the early Miocene, while Roeser (1991) reinterprets magnetic anomalies and suggests it started to open during 35–30 Ma. We propose an alternative interpretation: it began to open during Paleogene and closed around 15 Ma. The basements of the NW and SE parts of the SE Sulu Sea basin are transitional and oceanic crusts, respectively, and the early Miocene oceanic crust occupies only a fraction of the SE part. This interpretation is mainly based on the two reasons: (1) The Cagayan Ridge may be composed of continental basement (Silver and Rangin, 1991a). The NW part of the SE Sulu Sea basin possibly has the same type of basement as this ridge, or just is the southeastern flank of this ridge (e.g., Hsu et al., 1991; Rangin and Sliver, 1991). This means that the crust composition of this part possibly is transitional crust that consists of continental fragments and basaltic rocks. (2) K–Ar age dates of the dredged volcanic rock capping the Cagayan Ridge at different sites range from 36 to 10 Ma (Kudrass et al., 1990). These volcanic rock ages indicate that the rifting in the NW part of the SE Sulu Sea basin probably started in the Eocene, and the multiple episodic tectono-magmatic activities occurred during the rifting and post-rifting periods.

Weissel (1980) identified three anomalies of the SW Celebes Sea as C20–C18, which get younger toward the south (Fig. 6). This is basically supported by data from the Holes 767 and 770 of the ODP Leg 124 (Lewis, 1991). In the model of Gaina and Müller (2007), the seafloor spreading began shortly before C21 (49 Ma) and ceased C17y (36.6 Ma) or C16o (36.3 Ma). However, its origin remains uncertain. Three alternative origins for this basin are: a fragment of an older ocean basin, a back-arc basin, or a basin rifted from the SE Asian continental margin (Silver and Rangin, 1991b). Silver and Rangin (1991a,b) suggest that this seafloor formed in Mid-Eocene under open-ocean conditions, and favor an origin for the Celebes Sea as either a basin rifted from the east Asian margin or one trapped from a once much larger Molucca Sea plate. We agree with this suggestion of Silver and Rangin (1991a,b).

3.3.3. Kinematics

Formation of the JMCS basin system is related to NW-ward motion of the Borneo block relative to the west arm of Sulawesi and Samba Island of the east Java arc. However, in NW direction, extension across the Celebes and Sulu seas is obviously much larger than the extension of the southern half of this basin system. This kinematic imbalance means that this dextral transtensional system is not a “pure” passive, dextral-transtensional-rift system and the active rifting associated with magmatic activity assisted its rifting, if the Celebes Sea basin rifted from the east Asian margin. From view of kinematic balance, it is more possible that it originated from entrapment of an older ocean. However, the magnetic lineations are oriented in same orientation as the strike of the R'-shears and may indicate that its seafloor spreading was triggered by the dextral transtension. Or the magnetic lineations resulted from intrusion and extrusion of basaltic magma along the R'-faults. Here the first hypothesis is used.

It is difficult to distinguish between the passive and active extensional magnitudes. However, we can make an approximate estimate

of the passive amount to a first order. As is shown in Fig. 8b, the west Borneo generally moved toward the NW relative to the west Sulawesi Arm and the dextral transtension happened across the JMCS basin system. We hypothesize that the dextral transtension shown in Fig. 8b represents its passive transtension and its residual extensional amount is attributed to the magmatic activity. Based on this hypothesis, the reconstruction at beginning of rifting is made (Fig. 9). Almost all the sea-floor spreading of the Celebes Sea basin and a small fraction of the sea-floor spreading of the Sulu and Makassar Seas basins are attributed to the active spreading. The motion vectors vary with the points, and the most northeastern Borneo moved about 150 km, which is responsible for the spreading of the Sulu Sea basin and extension of the Sabah sub-basin.

3.4. The Andaman Sea basin

The Andaman Sea basin (often referred to the central Andaman Sea basin) together with the Mergui Basin is not geography included in NW Pacific marginal basin system, but is closely related to the basin system in origin.

3.4.1. Geometry

The eastern boundary fault of the Andaman Sea basin is the Sagaing fault, which possibly extends southward to connect the Sumatra fault system. The western boundary fault is the West Andaman fault and links with the Sumatra Trench and Mentawai faults toward the SE (Fig. 6). The south boundary fault of the Andaman Sea basin is the Sumatra fault system, and the northern boundary fault is not clear (Curry, 2005) and may strike NE (Polachan and Racey, 1994) or NNE (e.g., Khan and Chakraborty, 2005). The overall geometry of the basin resembles that of b-3 in Fig. 2 in which the principal faults are not parallel.

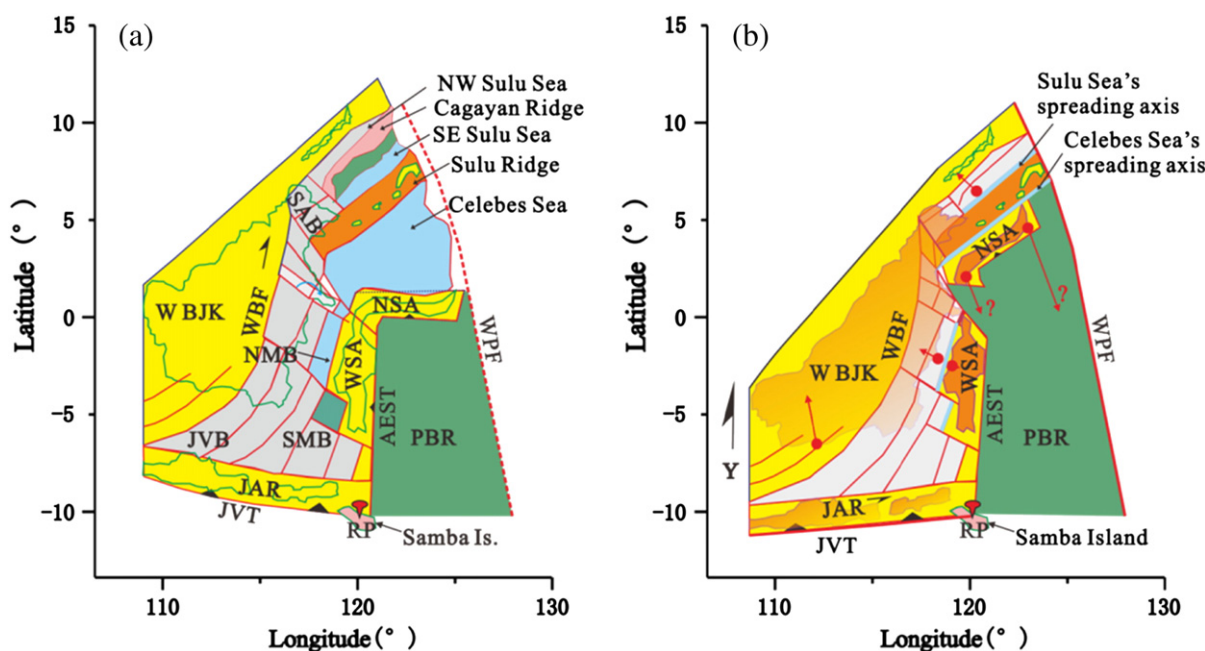


Fig. 9. Sketch of kinematic model for formation of the local transtensional basin system of the Java, Makassar, Celebes and Sulu Seas. (a) Tectonic model of this basin system. Dark gray area is the modeled basin on continental crust. Spring green area is a mosaic of oceanic and continental crusts. The stud marked by RP is the relatively fixed point that serves a reference point for reconstruction. It is emphasized that the faults within the system are not necessary continuous mega-faults but can be small discrete faults that make this tectonic pattern. Abbreviations (alphabetically): AEST = ancient East Sunda Trench, JVB = Java Sea, NMB = North Makassar Sea, SAB = Sabah Basin, SMB = South Makassar Sea, JAR = Java Arc, JVT = Java Trench, NSA = North Sulawesi Arm, PBR = Paleo-Banda Region, SUR = Sulu Ridge, WSA = West Sulawesi Arm, WBJK = West Borneo–Java block, WPF = West Philippine plate boundary fault. Other legends are the same as in Fig. 6. (b) Reconstruction of this system at beginning of rifting of this basin system. It is hypothesized that the North Sulawesi Arm rifted away from Asia, but this remains uncertain. The light gray area is the reconstructed area of the modeled basin on continental crust. Ice green bars are spreading axes of the Sulu, Celebes and Makassar seas. Red arrows are motion vectors of their starting points (red dots). Note that the Sabah region is reconstructed to the much smaller region than its present region. Other legends are the same as in (a).

The Andaman Sea basin consists of several secondary elements including the Central Andaman Basin, the Alcock and Sewell rises and the East Basin. The Central Andaman Basin consists of oceanic crust and displays rhombic geometry with a spreading axis trending toward the NE. The Alcock and Sewell rises also contain faults similar with those in the other nearby sub-basins. The East Basin trends nearly NS and stretches long and narrow, and its geometry is different from that of a typical sub-basin of a pull-apart basin.

The Mergui Basin is to the east of the Andaman Sea basin and generally trends NS to NNE and becomes wider toward the south. NS- to NNE-striking normal faults and NW-striking transform faults develop within the basin (Polachan and Racey, 1994; Curray, 2005), but its southern boundary fault (a northwestern branch fault of the Sumatra fault system) displays thrust geometry (Curray, 2005). The Mergui Basin together with North Sumatra Basin geometrically resembles a dextral, transform-margin basin (Fig. 2 (f)) with the principal fault being the Sumatra fault system.

3.4.2. Rifting history

Tapponnier et al. (1982) propose that dextral, pull-apart rifting in the Andaman Sea basin that started at the same time as the collision between the Indian and Eurasian plates. Rifting in the Mergui Basin began in Oligocene and propagated northward (e.g., Molnar and Tapponnier, 1975; Curray, 2005). Curray (2005) revises earlier anomaly interpretations of the anomalies of oceanic crust of the Central Andaman Basin (13 to 11 Ma) (Curray et al., 1979), and concludes that the anomalies could be identified back to only 4 Ma for the central Andaman Basin in agreement with Raju et al. (2004).

Nature of the Alcock and Sewell rises is still problematic. On basis of plate tectonic setting and two basaltic rocks dredged from one location on top of the Alcock Rise with an age of about 20 Ma, Curray (2005) believes that the two rises are oceanic and formed by normal seafloor spreading during 23 to 15 Ma. However, if the two rises are oceanic, they should be oceanic plateaus, because water depths of their basements are shallower than that of the younger central Andaman Basin. Only two dredged basaltic rocks cannot be used to determine how long it took for the two plateaus to form. Based on the available data, we suggest that the central Andaman Sea is floored by oceanic crust and its northern shelf is probably composed of thinned continental crust, and the normal seafloor spreading in the central Andaman Sea basin began in Eocene or early Oligocene after the collision between India and Asia. The Alcock and Sewell plateaus are younger than the formation of normal oceanic crust formed by the seafloor spreading and may have formed through multiple magmatic events, including the important magmatic events during 23 to 15 Ma (Curray, 2005). Rifting history of the East Basin might be the same as the central Andaman Basin because basement depths of the two basins are not distinct and even the latter is deeper (Curray, 2005).

3.4.3. Kinematics

The geometry of the Andaman Sea basin and its secondary elements basically supports that this basin originated from dextral pull-apart (e.g., Tapponnier et al., 1982; Maung, 1987; Lee and Lawver, 1995). We further propose that the Mergui Basin together with the East Basin formed as a transform margin-type of basin when the Indochina–Sumatra block rotated CW and the obliquity of subduction of the Indian plate motion along the Sumatra Trench was enough to trigger the dextral displacement along the NW segments of the Sumatra fault system and the Mottawi fault (see Section 4 for the reconstructions of this basin).

3.5. The East China Sea basin

3.5.1. Geometry

The East China Sea basin is composed of two sub-basins: the Shelf Basin in west and the Okinawa Trough in east, between which is the Taiwan–Sinzi Rise that is cut by NW-striking faults (Fig. 10). The Shelf

Basin, displays a rhombic shape in plan-view and contains a number of rhombic half-grabens that can be interpreted as the northeastern part of a Lazy-Z shaped, proto-South China Sea basin. There are left-stepping array normal faults close to the Taiwan–Sinzi Rise (Huang et al., 1992; Liang et al., 1997).

Geographically the Okinawa Trough is divided into three segments: the northern, central and southern troughs. The Trough displays arcuate rhombic shape with large ratio of length to width. The Okinawa Trough contains many grabens exhibiting a left-stepping array (e.g., Kimura, 1985; Kirillova, 1993).

3.5.2. Rifting history

The Shelf Basin seems to have rifted from late Cretaceous through to the early Miocene on basis of interpretation of the original data reported by some workers (e.g., Huang et al., 1992; Yu and Chow, 1997; Kong et al., 2000; Song et al., 2010; Cukur et al., 2011). Its rifting was interrupted by episodic tectonic events, among which the earliest Oligocene and earliest Miocene events were the most remarkable. It should be pointed out that many workers insist that the northern part (e.g., the Xihu sub-basin) or even the whole Shelf Basin went into a post-rifting period and was inverted in the Oligocene and Miocene (e.g., Kong et al., 2000; Zhao, 2004; Song et al., 2010). However, these seismic data show that the post-rifting and inversion might be misinterpreted by them, and that weak rifting did occur in Oligocene and early Miocene, when the east boundary fault often accommodated the extension instead of many small faults within this basin. The post-rifting subsidence occurred after the early Miocene and the strongest inversion happened around the earliest Pliocene. Most recently, Cukur et al. (2011) suggest that rifting in the northern part is divided into two stages: major extension during Paleocene to Eocene and mild extension during Oligocene and early Miocene. The inversion in the northern part is of greater magnitude than that in the southern part during the post-rifting period.

Different starting times of rifting of Okinawa Trough are suggested: the late Miocene (e.g., Kimura, 1985; Shinjo, 1999), Pliocene (e.g., Yamaji, 2003) and early Pleistocene (e.g., Park et al., 1998). Strata in the trough mainly consist of Pliocene and Quaternary sediments (Kimura, 1985; Kirillova, 1993), but the age of the deepest strata of great thickness (the central and northern troughs) and the earliest rifting remain unknown (e.g., Letouzey and Kimura, 1986). It is difficult to explain how it rifted in middle and late Miocene while nearby Shelf Basin was inverted. We suggest that the Okinawa Trough region rifted in Paleogene and early Miocene when sediments deposited in some left-stepping en-echelon grabens beside the Manila–E. Korean fault. It might enter the post-rifting period during Middle and Late Miocene and its most intensive rifting happened in Pliocene–Quaternary.

3.5.3. Kinematics

The geometry of the East China Sea basin indicates dextral transtension played a role in its tectonic evolution. The long half grabens are approximately parallel with its eastern principal fault and seem exceptional for transtensional basins, but the geometry of the grabens resembles that of some transtensional basins in profile-view (e.g., profile-view geometry of the transtensional Queen Charlotte Basin in western North America (Irving et al., 2000)). The rifting intensity difference between Eocene and Oligocene to early Miocene indicates some kinematic change of this region. We postulate that this change is related to either of seafloor spreading of the South China Sea basin or the small eastward extrusion component of the South China block during Oligocene to early Miocene.

Different rift kinematics of the Okinawa Trough are proposed and most of authors suggest it had an active back-arc origin (e.g., Letouzey and Kimura, 1986; Viallon et al., 1986; Park et al., 1998; Sibuet et al., 1998; Shinjo, 1999). However, the geometry of the trough can hardly be explained by the NW-ward subduction of the oceanic plate. What is more, if the rifting was only related to subduction of the Philippine

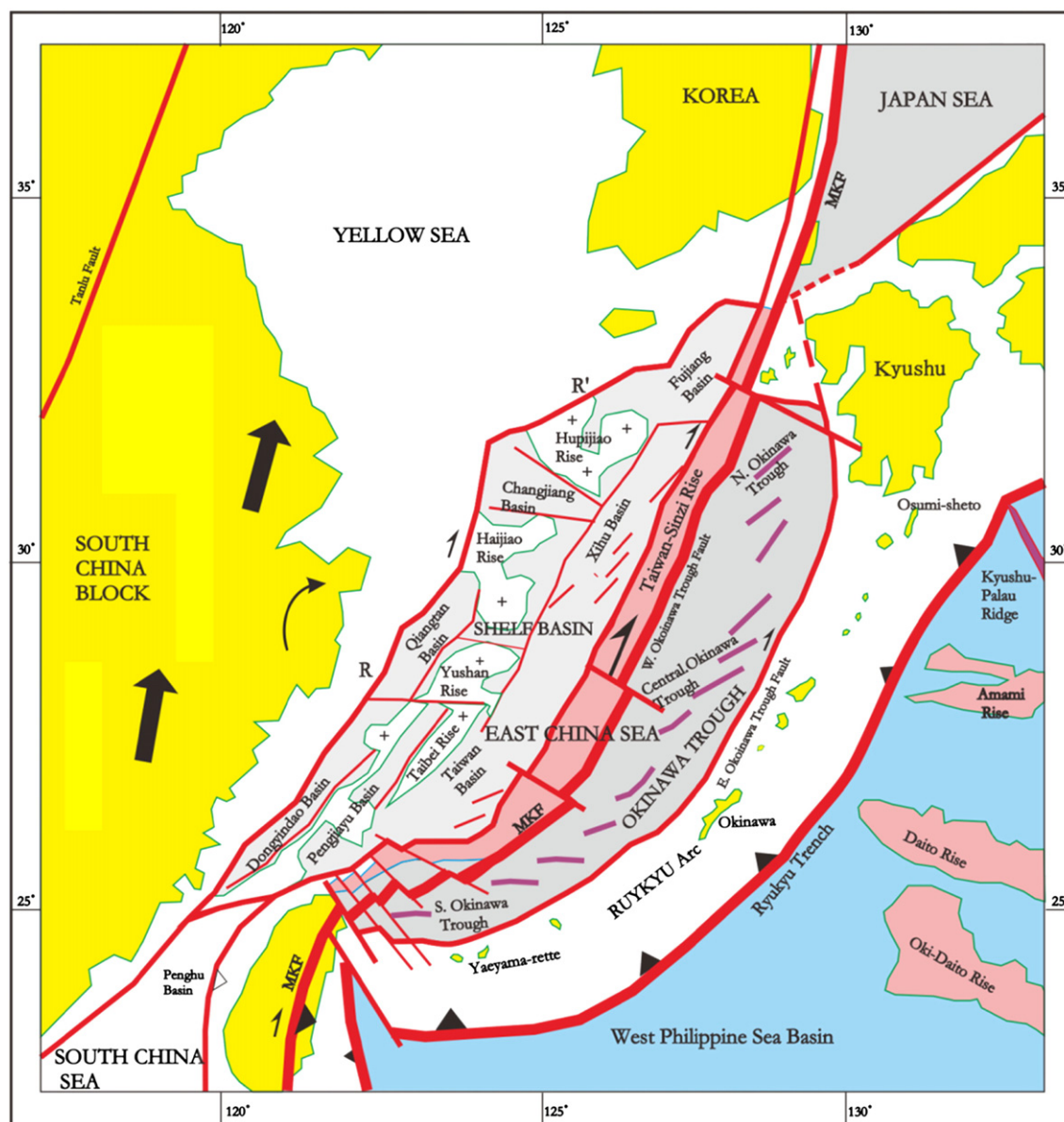


Fig. 10. Tectonic sketch of the East China Sea basin showing geometry and rifting kinematics. Purple bars in left-stepping array in the Okinawa Trough represent axes of grabens. The legends are the same as in Figs. 1, 4 and 6.

Sea plate, it should be explained why the trough did not continue to rift when the oceanic plate subducted. Origin of the trough is indeed difficult to understand. Based on the geometry and rifting history, we try to explain its kinematics as follows: (1) during Paleogene and Early Miocene, the Okinawa Trough region might be a dextral transtensional deformation belt where boundary faults of the left-stepping en-echelon grabens formed as R-shears beside the right-lateral Manila-E. Korea fault, and embryonic Okinawa Trough began to form, (2) during Middle and Late Miocene, it subsided without rifting and/or inverted, and some rifting sequences were eroded away and, and (3) during Pliocene and Quaternary, dextral transtension resumed because the south China block moved northward to north-northeast relative to the Ryukyu Arc, and because the back-arc magma could easily intrude in such a narrow faulted belt and could significantly assist its rifting. The collision of the northern Luzon Arc sliver with the South China block could intensify extension of the southern Okinawa Trough. At present, faster southward motion of south Ryukyu Arc, as shown by GPS (e.g., Heflin et al., 2004), might result from active spreading in the southern trough.

3.6. The Japan Sea basin

3.6.1. Geometry

The Japan Sea basin, which is another key member of Cenozoic basin system in the NW Pacific, contains some rises and three main sub-basins that include the Japan, Yamato and Tsushima basins (Fig. 11). The Japan Sea basin generally has a Lazy-Z shape in plan view though it was deformed during the post-rifting period. Its western boundary fault is the northern segment of the Manila-E. Korea fault, consisting of the Tsubima, Yangsan, Hupo faults and their northern extensions. Its eastern boundary fault, the Tartar-Tanakura fault, extends from the east of the Tartary Strait southwards, linking to the wide fault zone between the Tanakura and Itoigawa-Shizuoka tectonic lines, and further south it is probably linked to the Izu-Bonin-Mariana arc. The two mega-faults can be interpreted as Y-faults. The northern and southern boundary faults of the Japan Sea basin strike NE and ENE to EW and can be interpreted as R- and R'-faults, respectively.

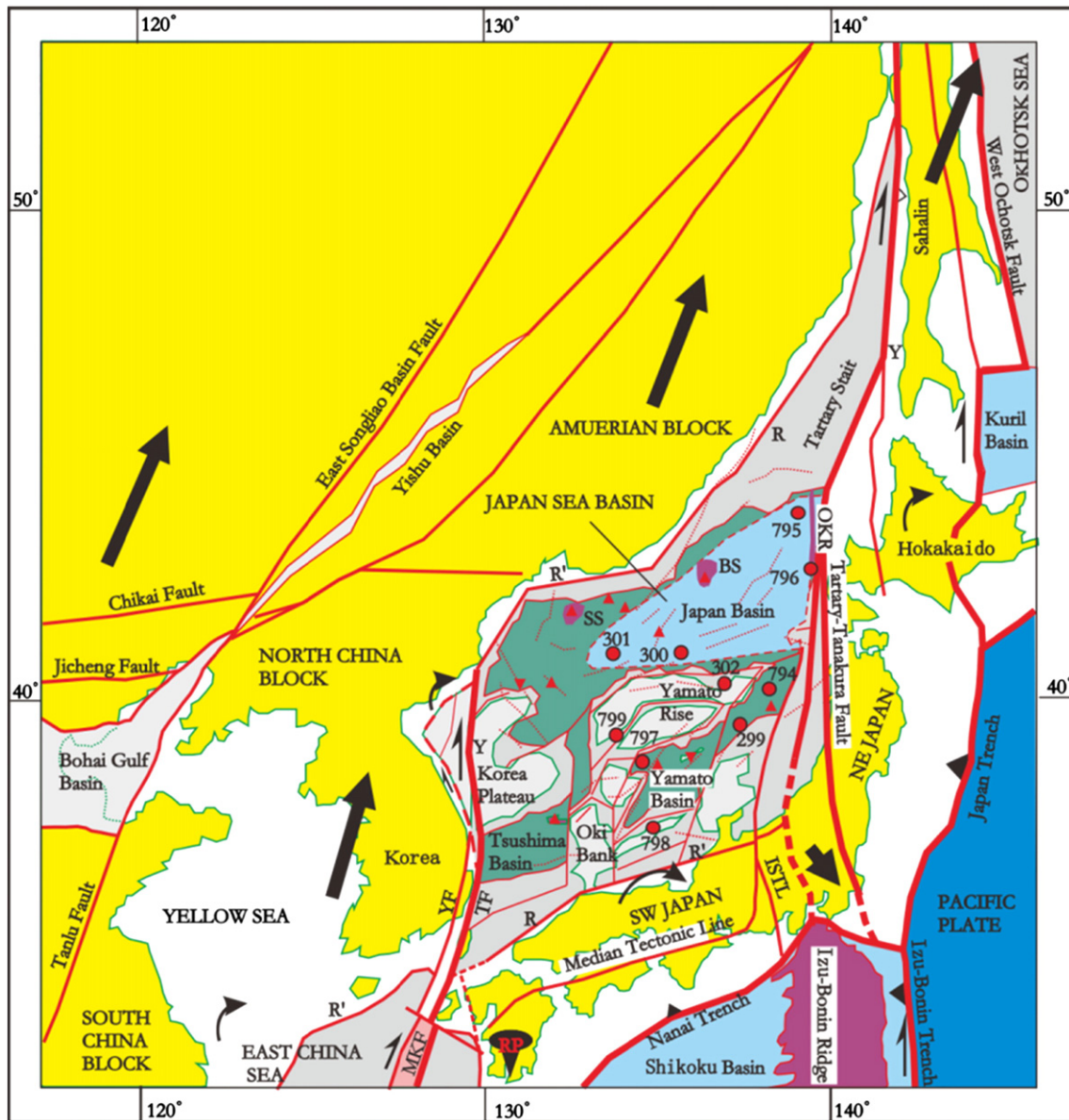


Fig. 11. Tectonic sketch of the Japan Sea basin showing its geometry and rifting kinematics. Thick black line arrows show the vectors (not to scale) of motion of points relative to the point RP (stud). Red triangles and upside-down triangles denote sites of the sampled volcanic rocks Paleogene–Neogene and Mesozoic ages, respectively. Red-filled small circles labeled by numbers are Sites of DSDP and ODP and their numbers. Abbreviations: TF = Tsushima fault, YF = Yangsan fault, ISTL = Itoigawa-Shizuoka Tectonic Line, BS = Bogrov Seamount, SS = Siberia Seamount, OKR = Okushiri Ridge. Other legends are the same as in Figs. 1, 4 and 6.

3.6.2. Rifting history

Some workers believe that that rifting of the Japan Sea basin started in Eocene (e.g., [Lallemand and Jolivet, 1985](#); [Filatova, 2004](#)). It is widely accepted that its intensive rifting began in the Oligocene (30 Ma or 35 Ma) and lasted to the earliest Middle Miocene (around 15 Ma) (e.g., [Kimura and Tamaki, 1986](#); [Jolivet et al., 1991, 1994](#)). It then generally went into a post-rifting period and was inverted by tectonic events including sinistral transpressional deformation (e.g., [Yamamoto, 1993](#); [Fabri et al., 1996](#)). Weak dextral transtensional rifting might have resumed since about 5 Ma on basis of the reported data from around the Japan Sea (e.g., [Yoon and Chough, 1995](#)).

Distribution, age and origin of the oceanic crust are still enigmatic. The oceanic crust generally is believed to occupy the eastern deep-sea area of the Japan Basin (e.g., [Jolivet et al., 1994](#)) though probably including the whole deep-sea areas of the sea ([Karp et al., 1996](#); [Taira, 2001](#)). Radiometric ages of volcanic rocks from seamounts in the Japan Basin are Neogene, Paleogene and even Mesozoic ([Bersenev et al., 1988](#)) (Fig. 11). ODP drilling at sites 794, 795 and 797 (Fig. 11) reached hard

basaltic rock with an age of 25 Ma (or 21.2 to 17.7 Ma), which would provide the minimum age since it was not certain whether the rock reached was the real basement or not ([Leg 127 and Leg 128 shipboard scientific parties, 1990](#); [Uyeda, 1991](#); [Nohda, 2009](#)). The ^{40}Ar – ^{39}Ar ages of the basement rocks are 24–17 Ma at Site 795 and fossil age of the oldest sedimentary cover at this site is 14 Ma ([Kaneoka et al., 1992](#); [Tamaki et al., 1992](#)), indicating that there are sedimentary hiatuses between the basement and the cover. Some drilled Miocene igneous basements perhaps represent local intrusive and extrusive rocks rather than real oceanic basement (cf. the right panel of Fig. 4). [Kaneoka et al. \(1994\)](#) date the basalt dredged from the northern part of the oceanic Okushiri Ridge at 34 Ma (^{40}Ar – ^{39}Ar age), which might be age of the oldest oceanic crust (?). Heat-flow and basement–depth data suggest an age of 30–15 Ma based on the standard plate-cooling mode, whereas the paleomagnetic study claims that “double-door-type” rotation of the northeast and southwest Honshu arcs took place at about 21–14 Ma and 15 Ma, respectively (within almost a 1-m.y. period) (e.g., [Otofuji et al, 1985](#); [Uyeda, 1991](#)). Clearly, it was impossible

that the oceanic crust formed within such a short period and the paleomagnetic declinations possibly reflected the local rotation (e.g., strike-slip shearing). Up to now, any convincing seafloor spreading axes and convincingly dated magnetic lineation patterns have not been determined (e.g. Isezaki, 1986; Uyeda, 1991). Three main sub-basins are approximately fan- or rhombic-shaped, resembling the overall configuration of the sea. Sparse magnetic anomaly lineations in the deep-sea areas that trend NE to ENE (Isezaki et al., 1996; Okubo et al., 1997) are parallel with the strikes of R- and R'-faults respectively, indicating that the oceanic crust (or dikes) possibly formed by the dextral pull-apart. The NW-trending magnetic anomalies perhaps resulted from magnetic dikes that intruded along X-faults that could be extensional during sinistral transpression episodes of the post-rifting period.

3.6.3. Kinematics

The Japan Sea basin has been considered as a dextral pull-apart basin but with various opinions in detailed kinematics (e.g., Lallemand and Jolivet, 1985; Kimura and Tamaki, 1986; Jolivet et al., 1994; Mashima, 2008). Considering geometry and rifting history of the Japan Sea, we

partly accept suggestions of the previous authors, that is, the rifting of all its sub-basins was due to dextral pull-apart and this was caused by the northward retreat of the Amurian block relative to the SW Japan arc, which underwent CW rotation about the relative fixed point "RP" (Fig. 11). The detailed kinematics of the Japan Sea is correlated to the opening of the Okhotsk Sea, and will be described and discussed together with kinematics of the Okhotsk Sea basin in Section 3.7.3.

3.7. The Okhotsk Sea basin

3.7.1. Geometry

The Okhotsk Sea basin has an asymmetric Lazy-Z shape, mainly includes the Kuril Basin, the central Okhotsk Basin, the Okhotsk arch and the Zeliz Gulf basin (Fig. 12). Its western boundary, a roughly NS-striking fault (the West Okhotsk fault, equivalent to the Shakalin–Hokkaido deformation zone) can be interpreted as a Y-fault. Its eastern boundary can be interpreted as a Y- or P-shear (cf. Fig. 2 (b-3)). Its southern boundary fault may be a Riedel fault. This northern boundary fault can be a CW-rotated R'-fault, which links to the NE-striking

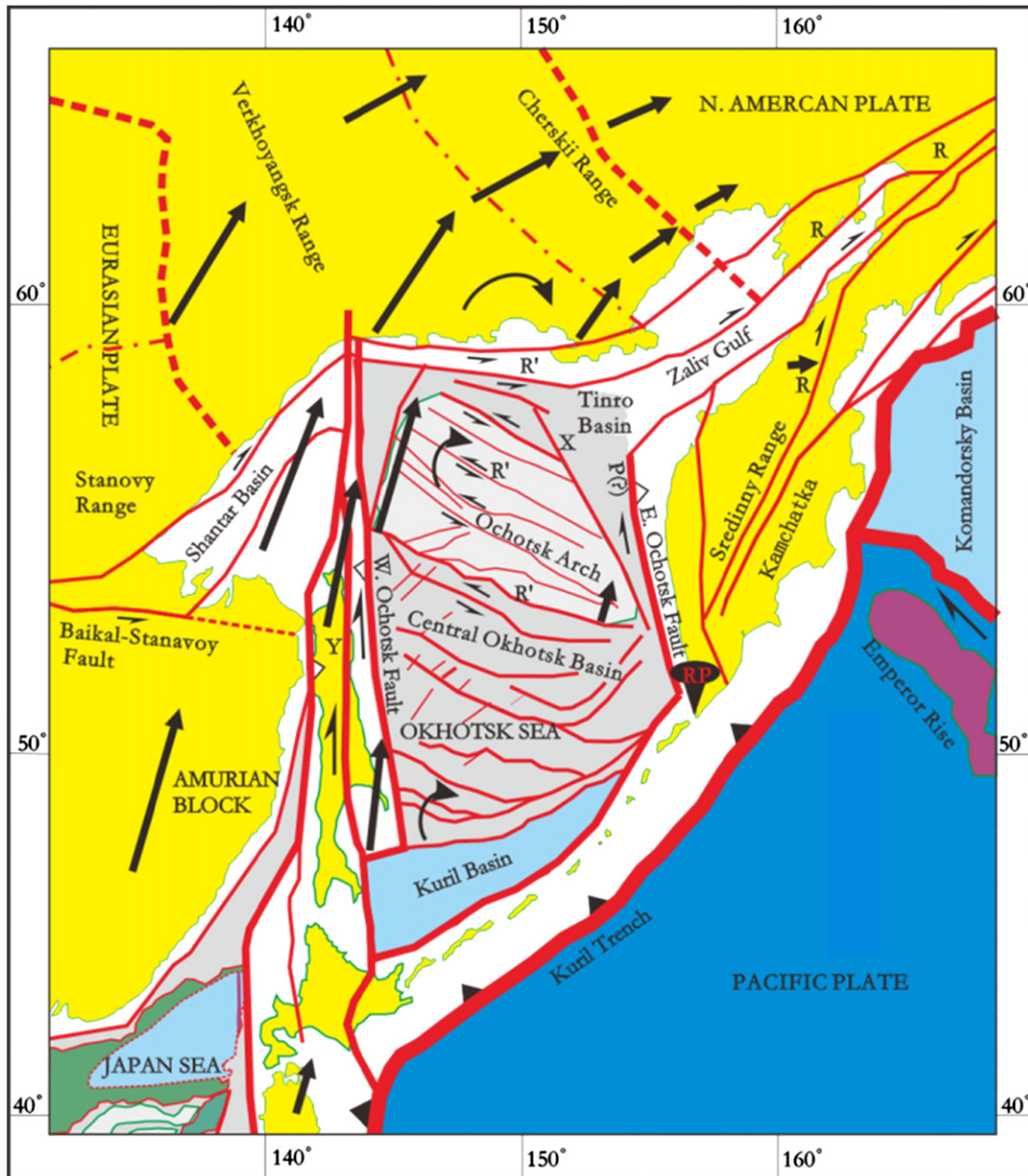


Fig. 12. Tectonic sketch of the Okhotsk Sea basin showing its geometry and rifting kinematics. Thick black line arrows show the vectors (not to scale) of motion of points relative to the point RP (stud). The legends are the same as in Figs. 1 and 6. See the text for details.

boundary faults (R-faults) in the Zeliv Gulf basin. There are WNW- to EW-striking faults within the sea, which can be CW-rotated R'-faults. There are also NE to ENE striking faults that often cut the R' faults perhaps are rotated R faults that developed earlier. Geometry of some sub-basins around the sea (e.g., Shantar and Pustorets basins (Worrall et al., 1996)) resembles that of the Shanxi Basin.

3.7.2. Rifting history

Sedimentary rocks of Paleocene and Eocene ages have been recorded in the northern part of the Okhotsk Sea basin (Kosygin et al., 1985) and the Eocene strata may fill in the grabens in its western part and some sub-basins in other locations in the Okhotsk Sea (e.g., Worrall et al., 1996). The Oligocene-early Miocene rifting history of the Okhotsk Sea may have a similar history as that of the Japan Sea (Kimura and Tamaki, 1986; Jolivet et al., 1994). Paleomagnetic data support that dextral, strike-slip deformation along the West Okhotsk fault may have occurred in the mid-Eocene (or earlier) and continued to the Early Miocene (e.g., Weaver et al., 2004). This basin then generally went into a post-rifting period.

The crust beneath the Kuril Basin is oceanic, but its northeastern part might be stretched continental crust (e.g., Baranov et al., 2002). Up to now, any deep sea drilling has not been made in the Kuril basin, and so its spreading time remains more uncertain than that of the Japan Sea basin. Kimura and Tamaki (1986) propose that the Kuril Basin formed during the same time as the Japan Basin. Gribidenko et al. (1995) conclude that it opened during a short period of time between the Late Cretaceous and the Miocene. Baranov et al. (2002) suggest that its spreading began during the early Late Oligocene and continued into the early Late Miocene because the back-arc-spreading affinity of basalts erupted in eastern Hokkaido. However, young rifting episodes might have occurred as in other marginal basins, but couldn't

necessarily represent the main rifting period. We basically agree with Kimura and Tamaki (1986) in the oceanic rifting history of the Okhotsk Sea basin.

3.7.3. Kinematics

As mentioned above (Section 3.6.3), we partly agree with the previous authors about rifting kinematics of the Japan Sea and Okhotsk Sea basins. However, some aspects of their models should be improved. Kinematics of the Okhotsk Sea basin has been schematically shown in Fig. 12 where the regions north of the Okhotsk Sea accommodate their pull-apart in complex motion circuits. To understand kinematics of the Japan and Okhotsk seas and their correlations more easily, simplified kinematic analysis is shown in Fig. 13 and explained as follows.

- (1) The pull-apart amount of the Japan Sea is evidently much larger than 200 km suggested by Kimura and Tamaki (1986), because the maximum width of the oceanic crust of the Japan Basin (the northern half of the Japan Sea) in NS direction is about 250 km. The pull-apart amount of the southern half of the sea is about 150 km, if the thickness of continental crust of the southern half before rifting is hypothesized to be about 30 km that is equal to the crustal thickness under the present coastline of Japan Sea, and if the thickness of thinned continental crust of the southern half after rifting is hypothesized to be on average about 20 km (e.g., Xu and Zhang, 2000a). In other words, the total pull-apart amount is about 400 (250 + 150) km.
- (2) Northward movement of the eastern Amurian block is the same amount as that of the westernmost side of the northernmost Okhotsk block because both the Tartar–Tanakura and the Western Okhotsk faults, which get closer to each other toward their northern ends, did not offset the northern Okhotsk Sea region.

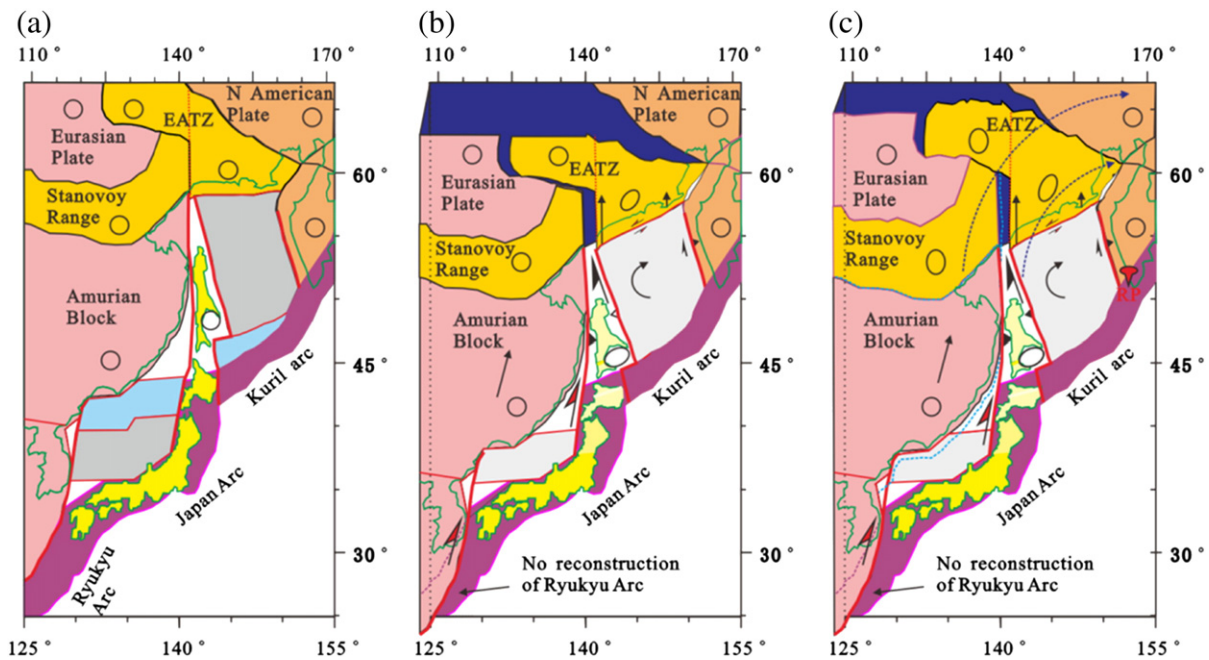


Fig. 13. Simplified kinematic models for the Okhotsk Sea and Japan Sea basins, focused to show how to form geometry of the two basins and kinematic correlation between them. (a) Tectonic model map around the Japan and Okhotsk seas. Ice blue areas are modeled as oceanic crust and dark gray areas as dextral transtensional continental crusts in the two basins. Red dotted line is dividing line of the east and west halves of EATZ (the transitional zone between the Eurasian and American plates). Open circles are strain unit circles. (b) Simplified reconstruction model for the two basins before their rifting, provided that regions in the Eurasian and N. American plates are all rigid except the east half of EATZ that is diffusely simple-sheared along NS-striking vertical planes by 25°. The Kuril and Japan arcs and the N. American plate are fixed. Two light gray areas are modeled as the two regions to be lost (shortened) during the rifting period. Ellipses are reconstructed from the unit circles in (a). The small white slot at the northeastern corner of the Okhotsk block is an overlapped area. Other colored areas represent the same regions as in (a). (c) Simplified reconstruction model for the two basins before their rifting, provided that EATZ and regions in the Eurasian plate are non-rigid except the Amurian block and that the N. American plate is rigid. The Stanovoy Range and the west half of EATZ are extended 1.33 times in NS direction; the region to the north of the Stanovoy Range are extended 1.05 times in NS direction; the east half of EATZ are extended compatible with the west half of EATZ plus the same simple-shear as in (b). Blue dashed line is the Amurian block boundary if it is extended 1.05 times, in the case of which the amount of pull-apart of the Japan Sea is a little larger than that of the west side of the Okhotsk Sea. Two dark blue, dotted arc lines with arrows represent the “actual” circuits of motion of the points relative to the point RP (schematically shown in Fig. 12) if the N. American plate is non-rigid as well. Other legends are the same as in (b). See the text for details.

Through the dextral transpressional deformation (lengthening) along the NE Japan arc and Sakhalin Islands (see the average strain ellipse marked in this region), the dextral strike-slip deformation of the Tartar–Tanakura fault was transitioned to the west Okhotsk fault. Accordingly, the pull-apart amount of the Japan Sea basin is the same as that of the maximum extension along the western side of the Okhotsk block, if the Kuril and SW-Japan arcs are relatively fixed.

- (3) The Okhotsk Sea block is not as rigid as Kimura and Tamaki (1986) suggest because there are a lot of EW- to NW-striking normal faults and several sub-basins within this block. Furthermore, there would have been a large convergent zone along the north margin of the sea if the Okhotsk Sea block had rotated CW in rigid way and if the Verkhoyangsky and Cherskii ranges (the transitional zone between the Eurasia and N. America plates in Fig. 13 (a)) had been rigid and fixed. Generally deformation of this block can be treated as dextral distributed transtension along about NS-striking boundary faults of this block. The transtension intensity changed from maximum along the western boundary of this block to minimum (little extensional deformation) along its eastern boundary.
- (4) The wide regions north of the two seas accommodated their pull-apart deformation in non-rigid way. The “non-rigid” Stanovoy Range could absorb northward motion of the “rigid” Amurian block including shortening and subduction (about 200 km) (Kimura and Tamaki, 1986). In the similar way the Verkhoyangsky and Cherskii ranges could also absorb the partial motion of the

Okhotsk Sea block in addition to the NS-striking simple shear (Fig. 13 (b) and (c)). The residual northward motion of the Amurian and Okhotsk Sea blocks could be accommodated by non-rigid strain in the very wide regions north of the Stanovoy, Verkhoyangsky and Cherskii ranges. Actually, the regions north of the two basins accommodated their pull-apart in more complex circular motion circuits approximately like dark blue dashed lines with arrows in Fig. 13 (c) if the N. American plate is non-rigid as well, as schematically shown in Fig. 12

3.8. The Bering Sea basin

3.8.1. Geometry

The Bering Sea basin comprises the oceanic Aleutian, Komandorsky and Bowers basins and many continental sub-basins (e.g., Navarin, St. George-Bristol and Anadyr sub-basins) (Fig. 14). It in general has an asymmetric rhomboid shape in plan view. Its NW and SE boundary faults, the NW Bering fault and the SE Bering fault respectively, are interpreted as Y-faults. The orientations of the Y-faults are different from the main faults of the other pull-apart basins described above due to geometric effects relating to the Earth's sphericity. The SW boundary fault (Bering fault) may have resulted from R'-shear. There is no one clear NE boundary fault delimiting the sea, but there are many NW-striking faults on the Bering Shelf, which are oriented along about the R'-faults. The arcuate shape of the Aleutian Arc possibly resulted from linkage of the SE Bering Fault and SW boundary fault, similar to the Japan Arc.

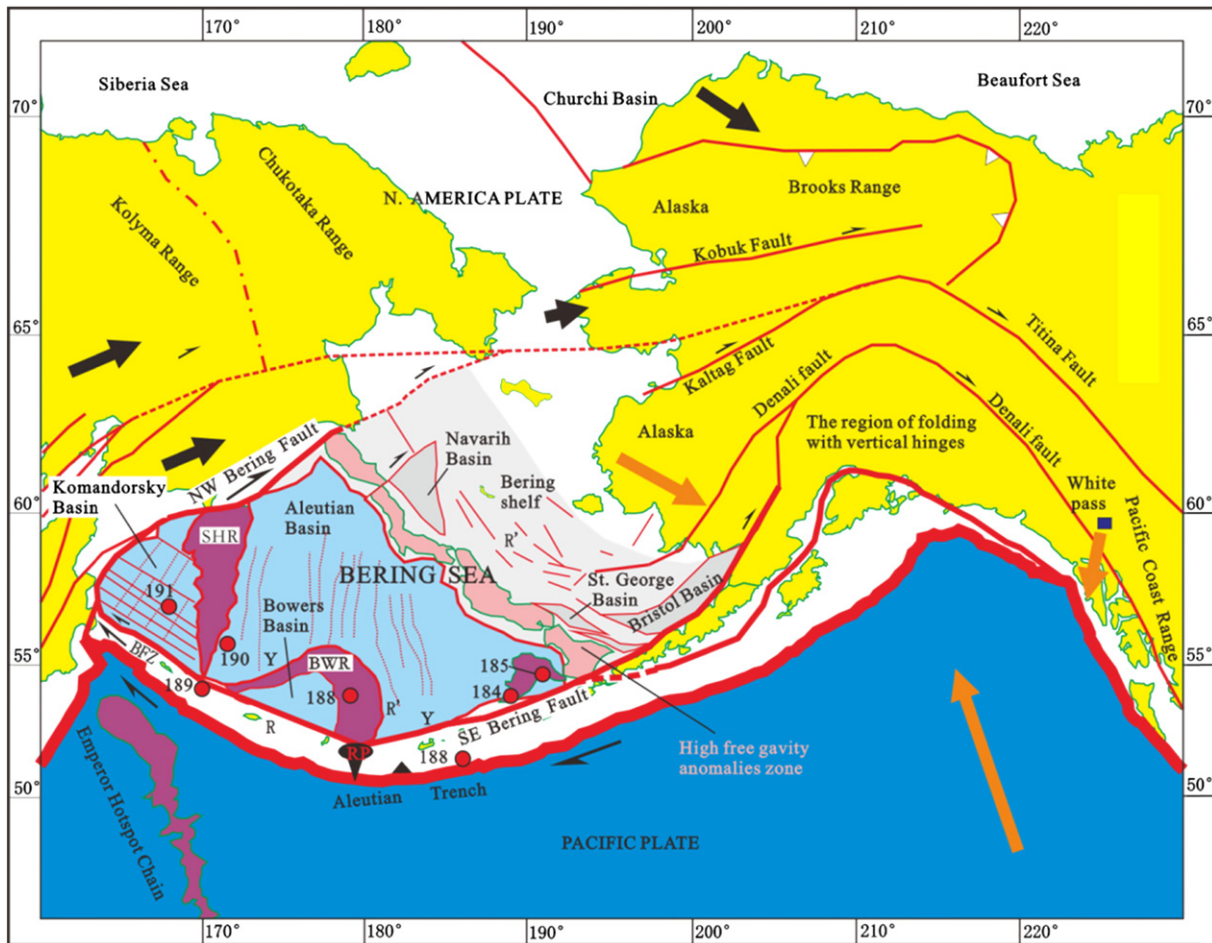


Fig. 14. Tectonic sketch map of the Bering Sea basin showing its geometry and rifting kinematics. Thick black line arrows show the vectors (not to scale) of motion of points relative to the point RP (stud). Orange arrows shows the translate vectors (not to scale) of points relative to the central North American craton. Red-filled small circles and their labeled numbers are Sites of DSDP and their Site numbers, respectively. BFZ = Bering fault zone, BWR = Bowers Ridge, SHR = Shirshov Ridge. Other legends are the same as in Figs. 1 and 6.

3.8.2. Rifting history

Rifting of the sub-basins on the outer Bering Shelf (e.g., the St. George, Navarin and Anadyr sub-basins) began in the Eocene and ended in the Miocene (e.g., Bour, 1994; Worrall et al., 1996). The Norton sub-basin on the Bering Shelf has subsided since the Paleocene at a fairly constant rate (Fisher et al., 1982).

The age of the oceanic crust of the Bering Sea basin seems uncertain although there are some data from Leg 19 holes drilled at some sites around the sea (Creager et al., 1973). The oceanic Shirshov and Bowers ridges were covered with Upper Miocene strata. The radiometric age of basalts from Site 191 in the Komandorsky (Kamchatka) basin was 9.3 ± 0.8 Ma. Age of the dredged andesites from the Shirshov ridge is 27.8 ± 1.1 Ma.

Magnetic lineations have been interpreted as M1 to M13 (Cooper et al., 1976b). Scholl et al. (1975), Cooper et al. (1976a) and Ben-Avraham and Cooper (1981) suggest that the Bering Sea is an example of an entrapped marginal sea, cut off from the northern Pacific (Kula) by the Aleutian Ridge formation, which probably occurred during late Cretaceous or early Tertiary time. Langseth et al. (1980) argue that if the Aleutian Basin was formed by the sea floor spreading process, then the heat flow suggests an age of about 44 Ma. From plate tectonic settings, corrected heat flow and drilling data, Baranov et al. (1991) postulate that the Komandorsky Basin has several stages of evolution or several times of magmatic activities due to changes in the relative motion between Pacific and North America plates: it started 40 Ma ago; all magmatic processes terminated 32–25 Ma in its NE part and are continuing at present in its SW part.

By synthesis of the above data, we believe that the Aleutian basin including the Komandorsky sub-basin was trapped in the Pacific (or Kula) plate in the early Tertiary (e.g., Eocene), and then was intensively reworked by tectonic and magmatic processes in various periods. The Cenozoic rifting history of the Bering Sea Shelf is probably similar to that of the Okhotsk Sea.

3.8.3. Kinematics

The Bering Sea basin was possibly formed by dextral pull-apart deformation in the early Tertiary with the Aleutian, Bowers and proto-Komandorsky basins entrapped in the major ocean because of EW motion of the NE Asia–Alaska region and dextral, strike-slip offset along the Y-faults (Fig. 14). This means the North American plate is non-rigid around the arctic region. The Arctic region of the North America plate possibly was generally non-rigid and the NE Asia region rotated CCW relative to the North America craton during the rifting period of the Bering Sea shelf. This rotation led to the Alaska region being folded with vertical fold hinges. The angles between the trends of the eastern Aleutian Arc and the Pacific Coast Range in Canada became smaller and smaller (Fig. 14). For example, the Denali fault had been more straight before the dextral pull-apart activity began within the Bering Sea. This folding could have also caused NE-striking faults to exhibit local “domino-style faulting” in west Alaska and some dextral, strike-slip displacements took place along them. On the other hand, the Titina fault and similar faults in the western North America developed dextral strike-slip offset during the NNW motion of Pacific plate. The Cenozoic EW compression that resulted in thrusting in north Alaska as reported by Lane (1998) can also be interpreted as eastward motion of NE Asia with respect to North America craton. The non-rigidity of the Arctic region of North America plate is supported by paleomagnetic data (e.g., Symons et al., 2000).

Because the Pacific plate moved NW-ward after entrapping of the Bering Sea basin, seafloor spreading (or reworking) in the Komandorsky sub-basin might be triggered by dextral pull-apart behind the NW-trending dextral transform plate boundary (the SW basin boundary). Under this dynamic condition, the R'-faults in the Aleutian sub-basin could be oriented approximately NS. The Shirshov Ridge and east segment of the Bowers Ridge (and even magnetic anomalies in the Aleutian

Basin?) might result from intrusion and extrusion of magma along the R'-faults.

3.9. The Philippine Sea basin

3.9.1. Geometry

The Philippine Sea basin (PHS) comprises four sub-basins: the West Philippine (Sea) basin (WPB), the Parece Vela Basin (PVB), the Shikoku Basin (SKB) and the Mariana Basin (MRB) (Fig. 15). Between PVB and SKB is a NE-striking major fault (the Sofugan tectonic line, Uyeda (1982)). The overall configuration of the Philippine Sea plate resembles that of a typical sinistral, transpressional “pop-up” structure of analog model (e.g., Fig. 3 (a) and Fig. 15 (inset)). The inner NW- and NNW- to NS-trending structural fabrics in WPB (Okino et al., 1998; Deschamps and Lallemand, 2002) and possibly in proto-PVB also are similar to the fault pattern within the sinistral pop-up structures (e.g., Fig. 3(a, c and d)), but different from that of Fig. 3(b). Furthermore, the Mariana and West Mariana ridges could be compared to the pair of SE thrusts shown in Fig. 3(c). However, it is different from a sinistral “pop-up” in some aspects: (1) there is a ridge, the Palau-Kyushu Ridge (KPR), within PHS; (2) there are NNW to NS magnetic lineations dominant in SKB and the western part of PVB; (3) there are extensional basins (e.g., Mariana Basin, Bonin Trough, Suimu Rift) along the overthrust boundary zone (the Izu-Bonin-Mariana arc (IBM)); and (4) the sub-basins partly have different ages. All of those aspects mean that PHS was not a product of a single, sinistral-transpressional event and had a more complex history.

3.9.2. Rifting history

Since the NW-trending magnetic lineations and the extinct spreading center, Central Basin fault (CBF), were discovered (Ben-Avraham et al., 1972), different spreading directions and ages have been proposed for WPB (Lewis and Hayes, 1980; Shih, 1980; Hilde and Lee, 1984; Shiki et al., 1985; Tokuyama, 1985; Kirillova, 1988; Fujioka et al., 1999; Okino et al., 1999; Deschamps and Lallemand, 2002; Deschamps et al., 2002; Lewis et al., 2002; Gaina and Müller, 2007; Müller and Sdrolias, 2008). PVB and SKB were generally considered to have formed later than WPB, and several slightly different opening directions and ages have been proposed for PVB and SKB (e.g., Mrozowski and Hayes, 1979; Lewis and Hayes, 1980; Uyeda, 1982; Taylor, 1992; Okino et al., 1998, 1999; Deschamps and Lallemand, 2002; Sdrolias et al., 2004). The Mariana Basin (Trough) is suggested to have possibly formed from around 5 Ma to present due to interarc seafloor spreading (Scott et al., 1980).

However, any of the different seafloor spreading histories previously proposed for WPB, PVB and SKB can hardly explain the geometry of PHS because there is little possibility that the different time seafloor spreading in WPB, PVB and SKB coincidentally made a sinistral, transpressional “pop-up” structure just in front of a north-ward moving block (the Australia block). We believe that there are alternative interpretations of the resulting dataset, and suggest that WPB and most of PVB possibly was originally entrapped in major ocean by sinistral transpression in the mid-Eocene (or some earlier) and constituted a sinistral transpressional pop-up structure, and then were reworked with widening of PVB (and WPB) and opening of SKB, based on the following reasons.

- (1) There are wide NW-trending magnetic lineations cut by the thin well-known NS-trending and NNW-magnetic lineations in both the western and the central PVB (Fig. 15). The wide NW-trending lineations in PVB are similar to NW-trending magnetic lineations in the east central WPB in trend and width (please carefully inspect Fig. 3 of Okino et al. (1999)). The wide NW-trending magnetic lineations linking to the NNW-trending lineations make Lazy-S shaped lineations in some places in the central PVB. Some thin NS-trending and short NNW-trending anomalies clearly cut the NW-trending wide magnetic anomaly lineations

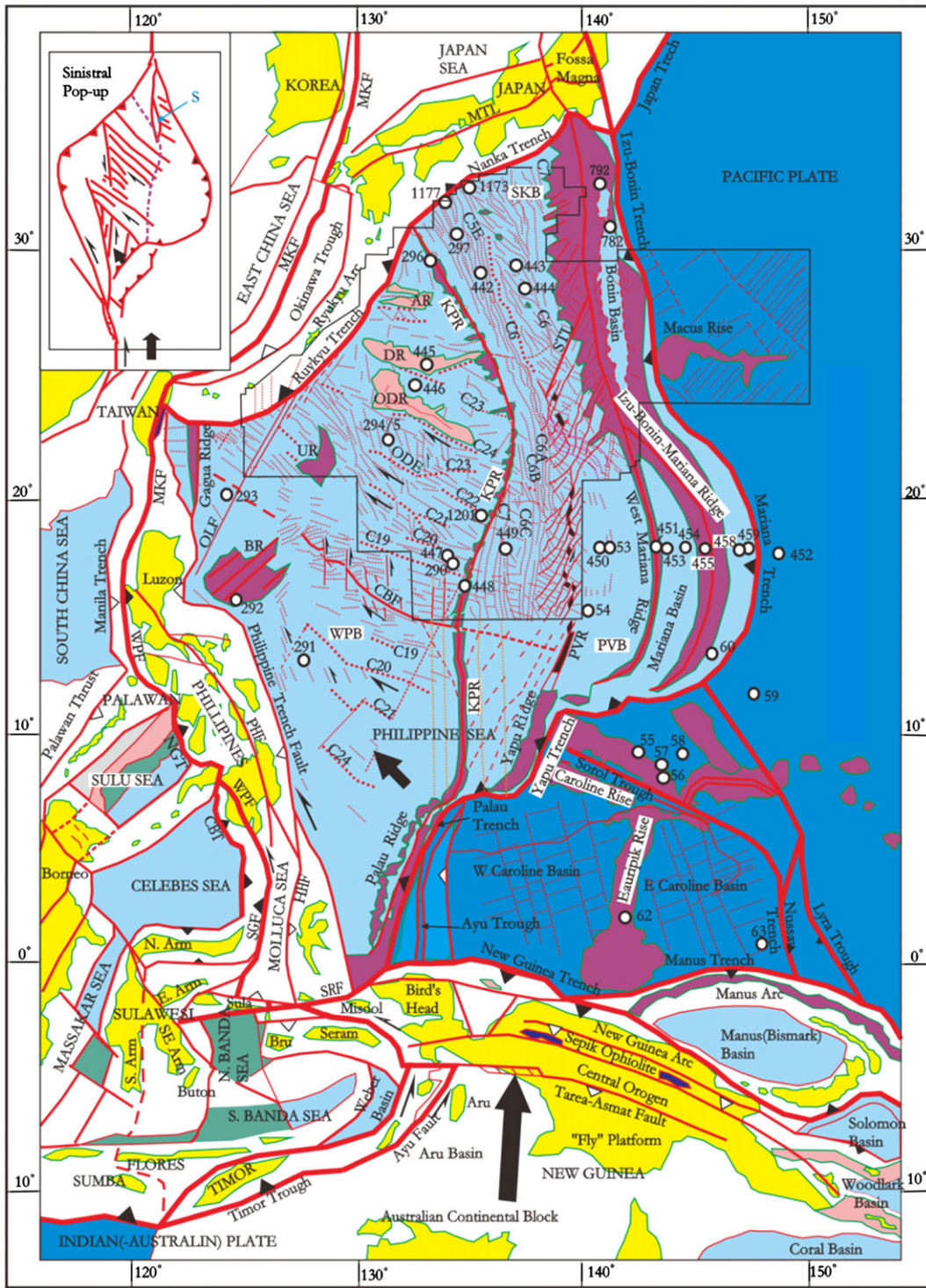


Fig. 15. Tectonic sketch of the Philippine Sea basin, showing its present geometry and kinematics of its formation as a sinistral transpressional pop-up structure in Mid-Eocene. Red dotted lines are magnetic anomalies and thick red dotted lines are the large anomalies. The magnetic anomalies within the polygon are positive ones drawn from Okino et al. (1999), the short NNW-trending magnetic anomalies in the south WPB and around the Central Basin fault (CBF) are after Deschamps and Lallemand (2002) and other anomalies labeled with chron numbers in WPB are after Hilde and Lee (1984) and the chron number in SKB and PVB are after Okino et al. (1999). The anomalies in the Caroline Basin are after Hall (2002). Four NS-trending deep-yellow dotted lines in SE WPB and SW PVB are “reduction-to-the-pole magnetic anomaly” lineations selected from Sdrolias et al. (2004). The white-filled circles and their labeled numbers are Sites of DSDP and the Sites’ numbers, respectively. The up-left inset is a sinistral transpressional pop-up structural analog model (except the purple dashed kinked line) in plan-view, which is simply the mirror image of the plan-view dextral pop-up structural analog model presented by Mandl (1988). In this inset, segments of faults barbed with triangles are thrusts, S is denoted as a small rhombic structure that is some like magnetic anomaly pattern in the central SKB and the purple dashed kinked line is added to show the “KPR” location. Abbreviations: PVB = Parece Vela Basin, SKB = Shikoku Basin, WPB = West Philippine Basin; HHF = Halmahera Fault, MTL = Median Tectonic Line, OLF = Okinawa–Luzon Fault, STL = Sofagan Tectonic Line, SRF = Sorong Fault; KPR = Kyushu–Palau Ridge, PVR = Parece Vela Rift; AR = Amami Rise, BR = Benham Rise, DR = Daito Rise, ODR = Oki–Daito Rise, UR = Urdaneta Rise. Black Arrows represent translate vectors (not to scale) at the time of formation of the pop-up structure. Dark blue areas represent ophiolites. Other legends and abbreviations are the same as in Figs. 1 and 6.

- in PVB and have to have formed later than the NW-trending ones. SKB has remarkable NS-trending anomalies in its east and west and the Lazy-S shaped anomalies in the central part as in the central PVB, but contains no wide NW-trending magnetic lineations. All these anomaly patterns indicate that WPB and proto-PVB formed first, and then EW spreading and NE spreading successively occurred in both SKB and PVB. It should be pointed out that, although there are no NW-trending “reduction-to-the-pole magnetic anomaly” lineations in PVB and SKB, the remarkable NS-trending “reduction-to-the-pole magnetic anomaly” lineations exist not only in bilateral PVB and SKB, but also in east WPB, the south central PVB and other regions (please inspect Fig. 3 of Sdrolias et al. (2004)) (four of the NS-trending “reduction-to-the-pole magnetic lineations” are selected as shown in Fig. 15).
- (2) Magnetic anomaly patterns in WPB (Fig. 15) indicate that its earlier formed crust was intensively reworked by the later tectono-magmatic activities. The magnetic anomaly pattern in WPB (Okino et al., 1999; Deschamps and Lallemand, 2002) evidently is neither symmetrical about any hypothesized spreading center and cannot be fitted with theoretical models of geomagnetic reversal time scales. The different trending anomalies can hardly be interpreted as “local” seafloor spreading or as different direction seafloor spreading as suggested by Okino et al. (1999) and Deschamps and Lallemand (2002). Origin of magnetic anomalies in a seafloor can be different (Wyllie, 1971). The NNW- to NS-trending magnetic lineations conjugate with NW-trending anomalies and this anomaly pattern resembles the fault pattern within a sinistral pop-up structure (Fig. 3). The NW-trending magnetic anomalies in WPB (and PVB) (Fig. 15) possibly were basic (background) magnetic anomalies and resulted from combination of NNE-directed seafloor spreading before the entrapment and tectono-magmatic reworking after the entrapment. It is noted that the “combination coincidence” that the NW-trending of seafloor-spreading axis is the same as the trending of the NW faults interestingly agrees with the physical modeling in Fig. 3(d). The NNW- to NS-trending magnetic lineations possibly resulted from the magnetic dykes, sills and flows that formed along the leaky NNW- to NS-trending faults and (or) faulting demagnetization, during the reworking after the entrapment. The EW-trending anomalies (Hilde and Lee, 1984) or more complex trending anomalies in the central WPB (Deschamps and Lallemand, 2002) possibly resulted from local CCW rotation by later sinistral shearing episodes along the NS-trending transform faults that cut CBF.
 - (3) Sedimentary hiatuses widely exist (e.g., Sites 447, 293, 294, 1201) and the igneous rocks of different ages (e.g., the CBF zone and Sites 294/295) appear around the same region (e.g., Karig et al., 1975; Kroenke et al., 1978; Kirillova, 1988; Fujioka et al., 1999; Salisbury et al., 2002). This indicates that the older oceanic crust could underlie the younger basalt overflows (cf. the right panel of Fig. 4), which could be mistaken as (oldest) basement if drilled. It can be predicted that the oceanic crust as old as Eocene will be found in PVB. But the opportunity to find Eocene basement could be less in PVB than in WPB because PVB was more intensively reworked during Oligocene to the early Miocene.
 - (4) The geometry of KPR and IBMR-Yap Ridge (YPR) suggests the two ridges couldn't unite as one arc before the opening of PVB-SKB. The Minimum Overlap Model and Minimum Space Model in the reconstruction of the East Philippine Sea (Haston and Fuller, 1991) clearly have overlaps and gaps between IBMR-YPR and KPR. If arcuate IBMR-YPR and zigzag KPR had been one arc before opening of PVB and SKB, it would have required “peculiar”, actually impossible, non-rigid deformation of IBMR-YPR and KPR.

Mechanically, the thin and long KPR, consisting of spotted volcanoes, was impossibly split apart from the united arc during extensional stress regime (unless a “knife-like” tectonic mechanism had peeled KPR apart from IBMR).

- (5) KPR possibly was a volcanic chain along mega-fault within the Philippine Sea plate. Volcanic rock chains in major oceans were considered as hotspot trails. Recently some workers have advocated an old suggestion that they possibly formed along extensional faults and even well-known hotspot trails did (e.g., Favela and Anderson, 1999; Davis et al., 2002; Foulger and Natland, 2003; for further discussion see www.MantlePlumes.org).
- (6) Paleomagnetic data don't support that there was a large-scale seafloor spreading in WPB after mid-Eocene. Paleomagnetic data show that there was about 10° systematic paleo-latitude difference between DSDP Sites 292 and 445 for last 40 Ma or 45 Ma according to their paleolatitude trends (Seno and Maruyama, 1984) (in fact, the Site 292 had a little more northward drift than the Site 445), and that the Benham and Daito rises had the same northward migration processes during the Cenozoic (Otsuki, 1990), contradicting any magnetic anomaly interpretation proposed for a younger opening. Of course, there is possibility that a small-scale seafloor spreading occurred in WPB after the entrapment.

3.9.3. Kinematics

Two end models for origin of the Philippine Sea basin have been proposed: the entrapment anchored-slab model and the rotational retreating-trench model (e.g., Summary of Seno and Maruyama (1984)). Recently, many publications have favored the rotational model on basis of paleomagnetic declinations (e.g., Jolivet et al., 1989; Deschamps and Lallemand, 2002; Hall, 2002; Müller and Sdrolias, 2008). But there can be alternative interpretations of the paleomagnetic data and new paleomagnetic data don't support the rotational model. We basically support the entrapment anchored slab model (Ben-Avraham et al., 1972; Uyeda and Ben-Avraham, 1972; Hilde et al., 1977), but in a new trapping way. As mentioned above, dynamic requirements for the formation of the Philippine Sea basin as a sinistral transpressional “pop-up” was just accommodated by the northward motion of the Australian continental block in the Cenozoic.

The CW paleomagnetic declinations along the eastern margin of PHS have two interpretations: local deformation of the arc and plate-wide rotation (e.g., Haston and Fuller, 1991). The CW declinations increasing systematically with increasing ages along the east margin of PHS as well as paleomagnetic declinations from Halmahera Island in the SW corner of PHS appear to support the rotational model (see summary of paleomagnetic data, Haston and Fuller, 1991; Koyama, 1991; Hall et al., 1995). Difficulties for the rotational model arise in two aspects: (1) the Izu Peninsula rotated 25°–30° CW since 11 Ma, but the floor of the Shikoku Basin has not rotated since 25.5 Ma (e.g., Otsuki, 1990; Koyama, 1991), indicating the rotation could be local. (2) Paleomagnetism of the seamounts and edifices of the West Philippine Sea is not consistent with a CW rotational model of the whole of the Philippine Sea plate (Ueda, 2004). (3) There is little possibility that the Izu–Bonin–Mariana trench retreated and coincidentally aligned with the Japan trench, forming a sinistral pop-up after the large plate-wide rotation. The trench retreating can hardly match the WNW- to W-ward motion direction of the Pacific plate as well. There also is no reason why the trench didn't continue to retreat after the cessation of spreading of SKB while the Pacific plate continued to subduct into the trench.

The systematic declination changes with ages along the east margin of PHS can be explained by continuous (or episodic) dextral shearing between the Pacific and Philippine Sea plates because the northward movement of PHS was quite larger than northward components of motion of the Pacific plate after PHS formed as a sinistral pop-up structure. The paleomagnetic declinations within PHS resulted from the complex

internal local deformation at different episodes. The CW declination of Halmahera Island is very special and might result from collision of the southernmost Palau arc and New Guinea arc with it. The CCW declinations of edifices of KPR possibly originated from sinistral shear along KPR. There probably exist unknown causes to produce some abnormal declinations and inclinations (e.g., local abnormal non-dipolar paleomagnetic fields). In addition, tomography data (e.g. Handiyani, 2004) support that the Izu–Bonin–Mariana trench was basically anchored rather than rotational.

Based on the above various data and plate tectonic setting, we suggest the following general kinematic model for the Philippine Sea plate: The proto-Philippine Sea plate, that included WPB and proto-PVB, was trapped across the Pacific and North New Guinea plates as an embryonic sinistral transpressional pop-up structure when the Australia continental block moved northward and collided with the New Guinea arc in the mid-Eocene. Between the Pacific and North New Guinea plates was a NW-trending spreading axis (proto-CBF). Proto-KPF was trapped within this pop-up structure. The proto-Philippine Sea plate was located about 20° south of its present position at its trapping time, and then episodically moved northward and was intensively reworked by tectono-magmatic activities. Volumetric basaltic magma intruded and extruded along KPF and KPR formed. At about 30 Ma, the Shikoku Basin (in its present range, not including the subducted part of the proto-Shikoku basin) began to form by the seafloor spreading in nearly EW direction, and this seafloor spreading propagated southward and PVB was widened. From 19 to 15 Ma, the seafloor spreading in SKB and PVB occurred in NE direction for sinistral transtension as indicated by Lazy-S shaped magnetic anomalies in their central parts. At about 5 (or 8) Ma, the seafloor spreading began in the Mariana basin (McCabe and Uyeda, 1983). See Section 4 for detailed plate tectonic evolution of PHS.

3.10. Summary of origin of the marginal basins

The above-stated marginal basins except the Philippine Sea basin each have geometry of dextral transtensional basins. Geometry of the Philippine Sea basin generally resembles a sinistral transpressional pop-up.

These marginal basins have similar (or compatible) rifting histories in the Cenozoic. Each of them started rifting in Paleocene or Eocene and episodically continued to present. Generally their most intensive rifting occurred during the mid-Eocene to the early Miocene though there did tend to be some differences in their rifting intensity and history due to local differences of tectonic settings and geometric and mechanic conditions. They generally went into the post-rifting period and inverted by sinistral transpression from the middle Miocene to present, but weak rifting in some of them resumed from Pliocene to Quaternary. We emphasize that it cannot be expected that all basins (or even all parts of one basin) in a wide region that undergoes a similar geodynamic process (especially in a wide strike-slip deformation region) have the exactly same tectonic history. In addition, oceanic crusts of the marginal basins are similar to, but different from those of major oceans because of being located in transitional tectonic domains from continental plates to major ocean plate. They possibly often are reworked and hiatuses may be more widely distributed due to frequent tectono-magmatic activities that result from the interactions between the major plates. Some drilled basalts (e.g., in the Philippine Sea basin) may not represent real oldest oceanic basement.

The marginal basins except the Philippine Sea basin originated from dextral transtensional rifting and together constituted a gigantic dextral pull-apart system from the mid-Eocene to the early Miocene, and then generally went into post-rifting period. The Philippine Sea basin originally formed as a sinistral transpressional pop-up structure in the mid-Eocene and then was reworked with widening and opening of its sub-basins.

4. Plate tectonic reconstructions of major marginal basins of the NW Pacific

Development of a gigantic dextral pull-apart rift system along the NW Pacific margin, as stated above, indicates that there was a large amount of northward movement of the South China block and compatible movements of other blocks in eastern Eurasia and region around the Arctic (EUAR) during its rifting period. We suggest that the northward movement of the EUAR was predominantly the product of the collision between the Indian and Eurasian plates during the rifting period of the basin system (Fig. 16). However, such a large displacement contradicts any traditional rigid-plate tectonic reconstruction. This section first estimates the displacement amount and then presents plate tectonic reconstructions of the basin system together with the Philippine Sea basin that challenge traditional views on the history of movement of the Eurasian and North American plates.

4.1. Estimation of movement of eastern Eurasia in the Cenozoic

4.1.1. Amount of extension of the marginal basin system

As shown in Fig. 8 (b), the South China block could move northward by 10.04° to 11.25° relative to Samba Island of the east Java arc, which was enough to produce the dextral transtension of the South China Sea basin and the Java–Makassar–Celebes–Sulu Seas basin system. If Samba Island is fixed in NS-direction to the hotspot reference frame or paleomagnetic reference frame for absolute plate motions (e.g., Müller et al., 1993; Torsvik et al., 2008), the amount of extension is equal to absolute northward motion of the South China block during the rifting period of these marginal basins.

However, the absolute motion of the South China block could have been larger (or even some less) than the amount of extension if Samba Island moved northward (or even southward) relative to these reference frames. As shown in non-rigid analog modeling of dextral transform deformation (e.g., Fournier et al., 2004), the southeastern part of the Indochina–Sumatra block and the east Java arc together with West Sulawesi could move southward in a small scale if the lithosphere of southeast Asia is non-rigid. In other words, the Java Trench could retreat southward in a small scale.

In order to better understand the displacement amount and history of eastern Eurasia, other significant evidence for these movements will be considered as follows.

4.1.2. Paleomagnetic evidence

Paleomagnetic data can be used to reconstruct the movement of plates or blocks. However, paleomagnetic data sets often contradict each other and have large errors and multiple solutions that are caused by many factors (e.g., local re-magnetization, shallowing of inclinations by overburden or steepening of inclinations by horizontal tectonic compression, abnormal declinations by local deformation rotation, non-dipolar geomagnetic field and even true polar wandering). Movements of blocks or plates that are predicted using these data should therefore be constrained with geological data. Generally paleomagnetic data support or don't contradict the large movements of east Asia since 50 Ma which is presumed to be the initial time of the collision of India with Asia (see Section 4.1.3 for detail).

The paleomagnetic data from the South China block suggest that it moved northward 10° to 12° since 50 (or 40) Ma and then shifted southward or remained stable (McElhinny and McFadden, 2000; Clyde et al., 2003). However, earlier workers report that the northward latitude shift was 8° between 50 to 15 Ma and then –4° (negative means “southward”, which will be the same in the following text) for the eastern South China block (Liu et al., 1990; similar results see Yuan et al., 1992) and 19.4° ± 6.3° since Paleocene to Eocene for the western South China block (Huang and Opdyke, 1992) (see summary of Cogne et al. (1999)).



Fig. 16. Tectonic sketch of the marginal basins of NW Pacific, tectonic division of the Large Tibetan Plateau (LTP) and general motion circuits of the east Eurasian plate and region around Arctic (EUAR) during the dextral pull-apart rifting of the marginal basins. Yellow, white, ice blue, sky blue and purple areas denote land, shelf-slope (or transitional crust), marginal basins' oceanic crust, open oceanic crust and rises in oceanic crust, respectively. Dotted and solid cyan curve lines with an arrow are the model background and possibly real maximum rotation lines (MRLb and MRLr), respectively. Straight thick dark-blue arrow denotes the largest motion vector of India. About zero strike-slip displacement on the RRF is at the point Z. Name abbreviations (alphabetically): (1) basin (-B) or sea (-S): ADS = Andaman, AYB = Ayu, BDS = Banda, BHB = Bohai Gulf, BKB = Baikal, CLS = Celebes, ECS = East China, JGB = Junggar, JVS = Java, MRB = Mariana, MKS = Makassar, PVB = Parece Vela, QDB = Qaidam, SKB = Shikoku, SUS = Sulu, SXB = Shanxi, TRB = Tarim, WPB = West Philippine, YSB = Yishu; (2) block (-K): BUK = Burma, HSK = Hoh xil-Sangpan-Ganze, ISK = Indochina-Sumatra, KLK = Kunlun, MGK = Mongolia; NCK = North China, QLK = Qilian, SCK = South China; (3) fault (-F): ATF = Altyn Tagh, EOF = East Okhotsk, EVF = East Vietnam, KAF = Karakoram, MKF = Manila-E. Korea, NBF = NW Bering, SGF = Sagaing, RRF = Red River, SMF = Sumatra, TTF = Tartar-Tanakura, WOF = W. Okhotsk, WPF = W. Philippine; (4) ridge or rise (-R): CAR = Caroline, IBMR = Izu-Bonin-Mariana, KR = Konipovich Ridge, KPR = Kyushu-Palau, LMR = Lomonosov Rise, NGR = Narsen-Garkel Ridge, PLR = Palau, YPR = Yapu; (5) trench (-T): ALT = Aleutian, IBMT = Izu-Bonin-Mariana, JPT = Japan, JVT = Java, KRT = Kuril, LYT = Lyra, MST = Mussau, SMT = Sumatra; (6) others: CCO = Central China orogen, EATZ = the transitional zone between the Eurasian and North American plates.

Jin et al. (2004) invert the magnetic anomalies of the seamounts in the South China Sea and show that the nine seamounts in the Central sub-basin moved northward 3.09° , 2.99° , 5.04° , 3.53° , 7.79° , 9.48° , 9.94° , 11.06° and 7.77° , respectively, from a spreading center (located at $N14.5^\circ$) progressively to about $N17.7^\circ$, and the seven, randomly located seamounts in the SW sub-basin moved southward 4.52° on average. The exact ages of the seamounts are uncertain, but clearly show the northern oceanic crust had large-scale, northward movement and probably later moved southward in a small scale.

Scant and contradictory Cenozoic paleomagnetic data from the Indochina-Sumatra block cannot fully describe its Cenozoic movements. According to paleomagnetic data from Mae Mho Basin (18.32°N , 99.74°E), Phetchaburi Basin (13.16°N , 99.67°E) and Krabi Basin (8°N , 99.05°E) in the west of the Indochina-Sumatra block (Richer et al., 1993), the three basins moved northward $11.84 \pm 9.91^\circ$, 8° and -7.5° respectively, since Oligocene-Miocene. The -7.5° contradicts the basic tectonic history of the block. The inclinations from this block, especially

its NW part close to the Red River fault, were probably steepened by transpressional deformation.

Fujita (1987) summarizes that southwest Japan drifted 4° (α_{95} not given) north since the early Paleogene, and Tosha and Hamano (1988) report Oga Island (40°N , 140°E) of NE Japan moved northward about $8.4 \pm 10^\circ$ since about 52 Ma. According to paleomagnetic inclinations reported by Otofujii (1995, 2002) from the Shihote-Alin region of the Mongolia block, north of the Japan Sea, moved northward about 6.7 to 14° since about 50 Ma.

Gilder et al. (1996) propose that there is the possibility of northward movement of the Siberia block relative to Europe along the Ural orogenic belt due to the India-Eurasia collision on the basis of paleomagnetic and geological data. Cogne et al. (1999) summarize that the Lhasa block (30°N 91°E), the Qiangtang block (32.8°N 96.6°E), the Tarim block (43°N 90.5°E or 37.7°N 79°E) and the Junggar block (44.2°N 86°E) south of the Altai orogen drifted northward by $16.6 \pm 6.4^\circ$, $15.3 \pm 6^\circ$, $22.2 \pm 16.7^\circ$ (or $10.3 \pm 12.7^\circ$) and $12.2 \pm 6.4^\circ$, respectively, since the Paleocene to Eocene. Cogne et al. (1999) further

conclude that predictions of positions of the Siberia block based on the Apparent Pole Wonder Path (APWP) of Eurasia (e.g., Besse and Courtillot, 1991) is erroneous, and suggest that the Eurasian plate might not be rigid and could be divided into three sub-plates between which there are the Urals and the Tomquist-Tesseyre Line, respectively. The possible northward drift of $12.2^\circ \pm 6.4^\circ$ of the Junggar block manifests that the southeast Siberia block and the western Mongolia block must have moved northward because the Altai orogen between the southeast Siberia and Junggar blocks could not accommodate large shortening of $12.2^\circ \pm 6.4^\circ$. This assumes that the western Siberia block had remained stable. It should be noted that a sinistral strike-slip mega-fault between the Junggar-Mongolia region and the Siberia block as hypothesized by Halim et al. (1998) doesn't exist. If the mega-fault had existed, the region of the Okhotsk Sea would have been intensively compressed. Besides, this great northward movement of NW China (the Junggar block) also suggest that north China would have to have moved northward in a large scale because there is no evidence that a major dextral fault (or ductile shear zone) existed between NW China and north China.

Hankard et al. (2007) report that Paleogene and Neogene paleomagnetic data from Siberia and Mongolia indicated that their paleomagnetic poles at 13 and 20 Ma are fairly consistent with those of the reference APWP for Eurasia (Besse and Courtillot, 2002). However, the 30 Ma pole appears far-sided with respect to the corresponding reference pole. They suggest that Siberia was located 1000 km south of the predicted position at 30 Ma and the Eurasian plate underwent non-rigid deformation. Most recently, Cogne et al. (2013) conclude that Tertiary “East Asia Plate” was located 10° farther south than expected from the current Europe APWP on the basis of the new Late Cretaceous to present APWP for Asia, reinforcing the conclusions of Cogne et al. (1999) and Hankard et al. (2007).

Dupont-Nivet et al. (2010) also provide new paleomagnetic results from volcanic rocks from Mongolia, and sedimentary data sets from China corrected for inclination shallowing, which together with compiled reliable Asian data sets confirm that Asian paleolatitudes are $5\text{--}10^\circ$ lower than predicted by the APWP in the 50–20 Ma period. Dupont-Nivet et al. (2010) investigate two explanations: (1) Asia was indeed >1000 km further south than predicted by the APWP (due to Eurasian non-rigidity, inaccurate plate circuit for Eurasia, or inaccurate global APWP) or (2) large and long-standing time dependent octupolar contributions (up to 16%) to the geomagnetic field. We favor the first explanation, which is basically consistent with conclusions of Hankard et al. (2007) and Cogne et al. (2013).

The paleomagnetic data from White Pass in the northern North American Cordillera indicate a paleolatitude discordance of $8 \pm 4^\circ$ south and a CW rotation of $40 \pm 9^\circ$ with respect to the North American craton since 50 Ma (Symons et al., 2000). The northernmost North American Cordillera possibly moved southwards relative to the North American craton, responding to the eastward movements of the region around the Arctic and the NNE- to ENE-ward movements of east Asia during formation of the gigantic pull-apart basin system.

In conclusion, the above paleomagnetic data show that the South China block possibly moved northward by about 10° and the other blocks of eastern Eurasia and the region around the Arctic had compatible motions since 50 Ma.

4.1.3. Shortening history and deficits around the Tibetan Plateau

4.1.3.1. Time of the initial collision. Age of the initial collision between India and Eurasia has been contentious for the past decades and its estimates range from the Late Cretaceous (>65 Ma) to the Late Eocene (<40 Ma) (see summary of Rowley (1996) and Henderson et al. (2011)). Most authors believe that the collision started about 55 to 50 Ma ago (e.g., Powell and Conaghan, 1973; Patrit and Achache, 1984; Searle et al., 1987; Clift et al., 2002; Hall, 2002; Leech et al., 2005; Royden et al., 2008; Chen et al., 2010b; Morley, 2012). Some

authors (e.g., Aitchison et al., 2007) reject the “around 55 Ma dogma of the initial collision time” and propose the “continent–continent collision is very young” (about 34 Ma ago) partly because the youngest marine facies in the Himalaya is very young (34 Ma) as originally proposed by Wang et al. (2002) and partly because India was too far from Asia at 55 Ma according to the classical plate reconstruction. However, with regard to Aitchison et al. (2007), Garzanti (2008) concludes that among the numerous unsolved chronic problems that afflict Himalayan geology, the date of arrival of the Indian continental margin at the Transhimalayan trench at 55 Ma stands as one of the few major events that are robustly constrained by multidisciplinary geological evidence. Zhu et al. (2005, 2006) use foraminifera to date the youngest marine facies at 50.6 Ma, coeval with the youngest marine facies >1000 km along strike (e.g., Green et al., 2008). Wang et al. (2008) agree that the initial continent–continent collision time is about 55 Ma, although they insist shallow marine formation survived to about 34 Ma (Wang et al., 2002). Najman et al. (2010) made a detailed discussion on ideas of Aitchison et al. (2007) and come to the same conclusion as Garzanti (2008), suggesting the initial time is about 50–52.8 Ma along the central segment of the India–Asia suture. Khan et al. (2009) and Morley (2012) support that the continent–continent collision began around 50 Ma in their plate reconstructions of the collision. Most recently, van Hinsbergena et al. (2012) propose that the initial continent–continent collision time is as young as around 25 Ma, but this new extraordinary idea still needs to be supported by more convincing geological and geophysical evidence in the future. Any young hard-collision idea to aim to solve the problem of too large size of Greater India or too large crust-shortening deficits around the Tibetan Plateau could be discarded (see following sections). Therefore, 55 to 50 Ma is more convincing as a time of the initial collision at the present knowledge's level.

However, the exact time of the initial collision and time of the “full” collision between India and Asia are very difficult to determine. Rates of the India–Asia convergence and rates of absolute motion of India vary with authors (e.g., Torsvik et al., 2008; Molnar and Stock, 2009; Copley et al., 2010). The time of the first drop in these rates could be 55, 50, or even 47.1 Ma (Fig. 17). The rate change alone cannot determine the exact initial collision time. The rate change of a plate not only depends on its interaction with other plates, but also on the state of convection of asthenosphere below related plates or even global plates and other factors (e.g., van Hinsbergen et al., 2011; White and Lister, 2012). For example, India moved at very different rates from its rifting away from Gondwana to its collision with Asia (e.g., Fig. 17(a)), but no other plate helped or resisted its motion during this period of time. Cessation of marine facies deposition, located between India and Asia, could be a good approximate indication of the collision time (e.g., Rowley, 1996; Najman et al., 2010). The conservation of crust matter between India and Asia could be another good indicator of the collision time (see Section 4.1.3.3 for further discussion). Taking the time of rate change in the India's motion, the cessation of the marine facies deposition and the conservation of crust matter between India and Asia, we agree with the diachronous collision along the suture and propose that India touched Asia along the central–eastern segment of the suture at about 50 Ma and the collision propagated westward with the full collision beginning at about 45 Ma or later (see Section 4.3 for further detail).

4.1.3.2. Shortening history. The Himalayas, the Tibetan Plateau and the high-altitude region (Tarim–Tianshan–Altai) north of the plateau are designated as the *Large Tibetan Plateau* (LTP) for simplicity (Fig. 16). Uplift of the Tibetan Plateau was formed by shortening and thickening of its crust (e.g., Dewey et al., 1988). Although the uplift of the plateau could have resulted from thermal convection or delamination of upper mantle (e.g., Molnar et al., 1993; Chung et al., 1998), the recent studies (e.g., McKenzie and Priestley, 2010) find that cold and thick (about 300 km) lithosphere is present everywhere beneath the Tibetan plateau, thus denying the thermal-related uplift mechanism. The uplift is therefore simply related to thickening of the crust or lithosphere and

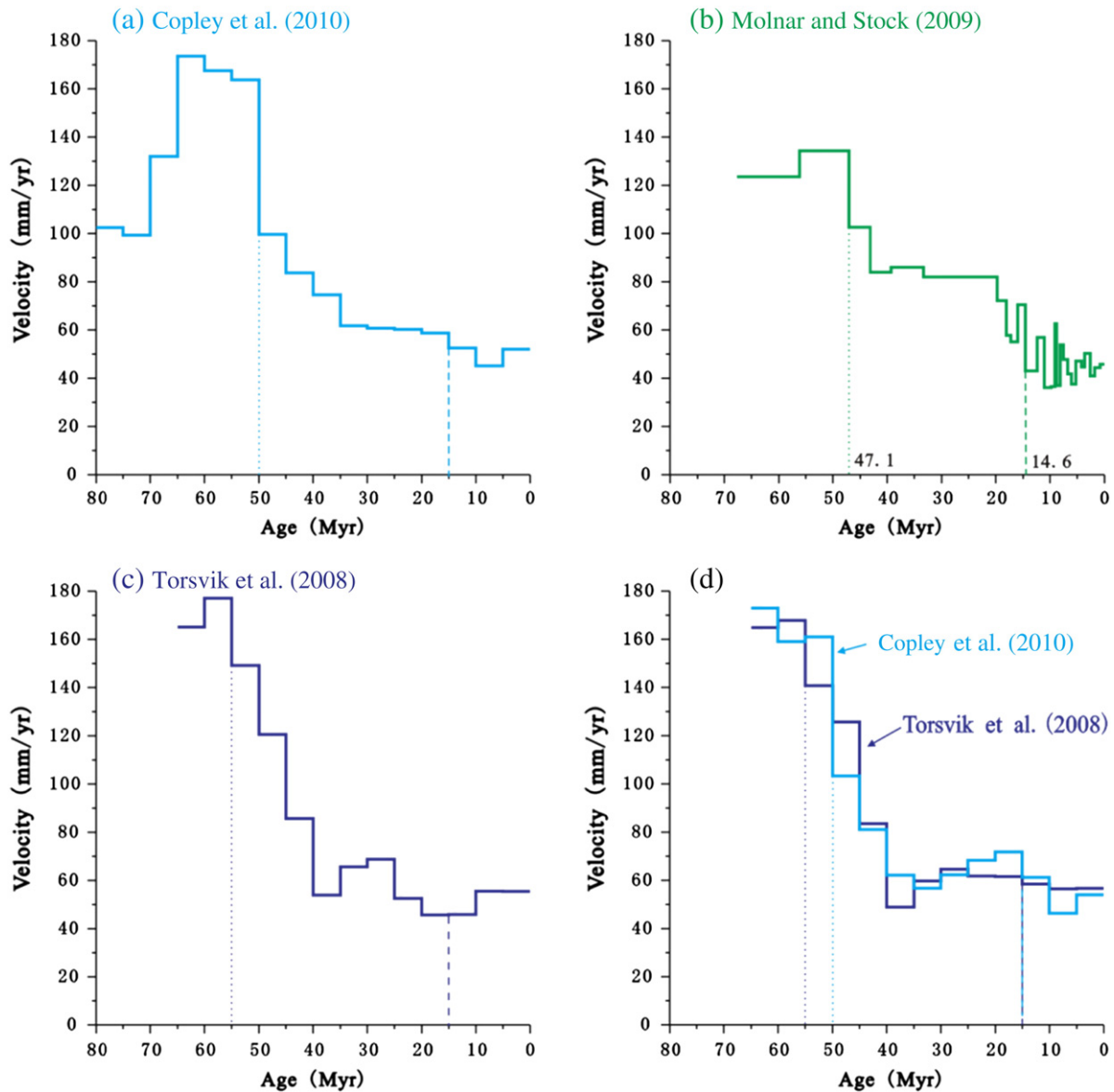


Fig. 17. (a)–(c) India–Asia convergence rates at the reference point (28°N, 90°E) calculated on basis of data provided by Copley et al. (2010), Molnar and Stock (2009) and Torsvik et al. (2008), hypothesizing that Eurasian plate is rigid and fixed. (d) Rates of India relative to the African Hotspot Fixed Frame according to data of Torsvik et al. (2008) and Copley et al. (2010). Dotted lines denote time of the first sharp drop of these rates, and dashed lines denote change in these rates around 15 Ma.

the shortening history of the LTP can be shown by its uplift history, if erosion is not considered.

However, the uplift history of the LTP has been very controversial and many different hypotheses have been proposed (e.g., Powell and Conaghan, 1973; Patrait and Achache, 1984; Mercier et al., 1987; Dewey et al., 1988; Molnar and England, 1990; Wang and Coward, 1990; Harrison et al., 1992; Coleman and Hodges, 1995; Li, 1995; Fielding, 1996; Le Pichon et al., 1997; Murphy et al., 1997; Yin and Harrison, 2000; Tapponnier et al., 2001; Spicer et al., 2003; Rowley and Currie, 2006; Zhou et al., 2006; Wang et al., 2008). It is difficult to know which of these hypotheses is most accurate. But there are some convincing facts as follows.

- (1) There were episodic uplifts in the LTP from the initial collision time throughout to the present. The episodic stages can be divided according to unconformities or sedimentary responses in the Cenozoic basins.
- (2) The southern, central and northern Tibetan Plateau achieved its elevations close to today's or underwent a significant uplift

before the Eocene–Oligocene transition (EOT) (about 35 Ma, maximum 38 Ma, minimum 32 Ma) (e.g., Yin and Harrison, 2000; Dai et al., 2005; Rowley and Currie, 2006; Dupont-Nivet et al., 2008; Wang et al., 2008; Yin, 2009). This means that there existed either more rapid uplift between time of the initial collision (50 Ma) and 35 Ma if its pre-collision elevation was low (e.g., the elevation is zero or less than 500 m) (e.g., Dewey et al., 1988), or slow uplift if its high elevation was created before 50 Ma (e.g., Murphy et al., 1997; Kapp et al., 2005).

- (3) The Tibetan Plateau had a relatively slow deformation episode either between about 35 to 15 Ma or between 50 to 15 Ma. According to Searle et al. (2003), the Everest Himalaya and south Tibet underwent crustal thickening from 50 to 32.2 Ma, remained constant in crust thickness between 32.2 Ma and 16.2 Ma, and collapsed from 16.2 Ma to the present. It is worth mentioning that around 25 Ma there was a tectonic event that caused a wide-distributed unconformity between Paleogene and Neogene both in the Tibetan Plateau and in the marginal basins of the NW Pacific. This short tectonic event possibly did not

cause evident uplift in the LTP. There could be some uplift in the northern Tibetan Plateau (around the Qaidam and Tarim basins) between 35 to 15 Ma, but the shortening rate was quite lower and the rapid uplift occurred after 15 (or 12) Ma (e.g., [Zhou et al., 2006](#)). There was more intensive tectono-magmatic activity in the Himalayas between 35 Ma and 15 Ma (e.g., [Dewey et al., 1988](#); [Yin and Harrison, 2000](#)).

- (4) Intensive tectonic activity in the LTP rejuvenated and started since 15 Ma (e.g., summary of [Molnar and Stock \(2009\)](#)). We emphasize that compression between the eastern Tibetan Plateau and the Sichuan basin initiated (e.g., [Kirby et al., 2002](#); [Wang and Meng, 2009](#)) and most of NS-trending grabens in the Tibetan Plateau formed after about 15 Ma (e.g., [Blisniuk et al., 2001](#); [Kapp and Gunn, 2004](#)).

Based on the above basic facts related to uplift of the LTP and the rifting history of the marginal basin system of the NW Pacific, we suggest two first-order stages for uplift of the LTP:

- (1) A slow uplift stage. This stage lasted from around 50 to 15 Ma when intensive rifting of the marginal basin system took place. During this stage, both the India–Asia convergence and the Tibetan Plateau uplift were generally slow. But the uplift and convergence could have been more rapid from 50 to 35 Ma than from 35 to 15 Ma.
- (2) A rapid uplift stage. This stage lasted from 15 Ma to the present when intense rifting of the major marginal basins generally ceased. During this stage, the rapid uplift of the plateau was simply due to the rapid convergence. Uplift and thickening of the Tibetan crust could have occurred in one of ways as suggested by some authors (e.g., [Zhao and Morgan, 1985](#); [England and Searle, 1986](#); [Powell, 1986](#)) or in a combination of these ways, which depends on the uplift stages and the places, and will be discussed in [Section 4.3](#).

4.1.3.3. Shortening deficits. Recent studies have found an important but puzzling phenomenon related to the shortening of the LTP: A large shortening deficit in the LTP, that is, the shortening amount of the LTP is much less than the India–Asia convergence that is predicted based on the plate reconstructions (e.g., [Le Pichon et al., 1992](#); [Johnson, 2002](#)). We suggest that the shortening deficits mainly result from the large northward motion of eastern Eurasia and can be used as an independent kinematical parameter to make new plate tectonic reconstructions of the marginal basins of the NW Pacific.

The shortening amount budgets of the LTP vary with authors (e.g., [Dewey et al., 1988](#); [Le Pichon et al., 1992](#); [Yin and Harrison, 2000](#); [Johnson, 2002](#)). Among the previous works, [Le Pichon et al. \(1992\)](#) most systematically estimate the shortening amounts and shortening deficits in a straight-forward way. Their basic dataset combined with the shortening history of the LTP (stated above) are used by us to further estimate the shortening amount. On the other hand, we use the rotational parameters of several recent Indian and Eurasian plate reconstructions ([Torsvik et al., 2008](#); [Molnar and Stock, 2009](#); [Copley et al., 2010](#)) together with the initial collision time (stated above) to predict the convergence between India and Asia.

Shortening deficits at the various hypothetical initial collision times are presented in [Figs. 18 and 19](#). Only if the initial collision time is 35 Ma and the preexisting topography level is zero, the deficits could be neglected according to [Torsvik et al. \(2008\)](#)'s reconstruction. However, such young initial collision time of 35 Ma has been denied by the reasoning stated above. It should be noted that, even if the initial collision time was really 35 Ma, but if elevation of the Tibetan Plateau before 35 Ma was the about the same as its present elevation (e.g., [Wang et al., 2008](#)), the shortening deficits in the LTP would also be very large (1000's km). If the initial collision time is 65 Ma, the large shortening deficits seem unrealistic, once again indicating such an early initial collision time is impossible. If the initial collision time is 45 Ma, the

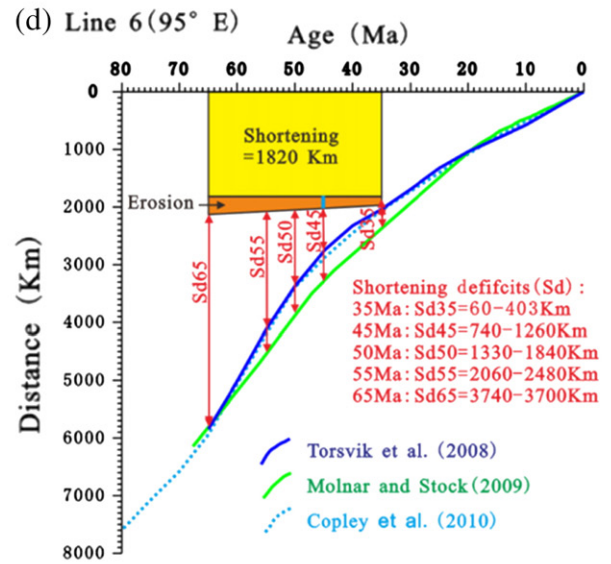
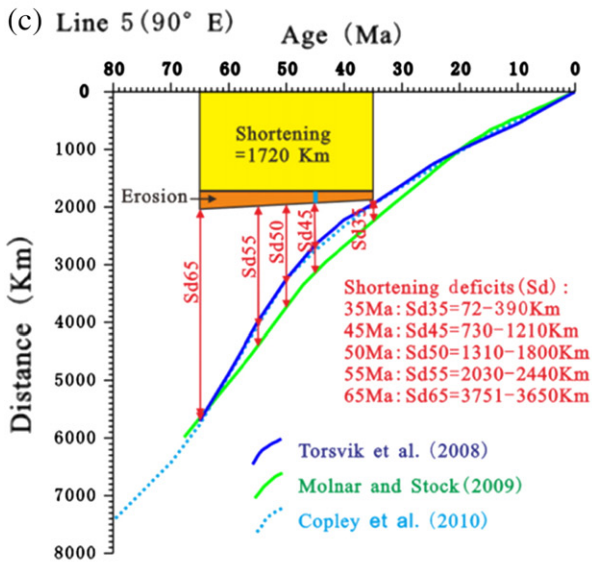
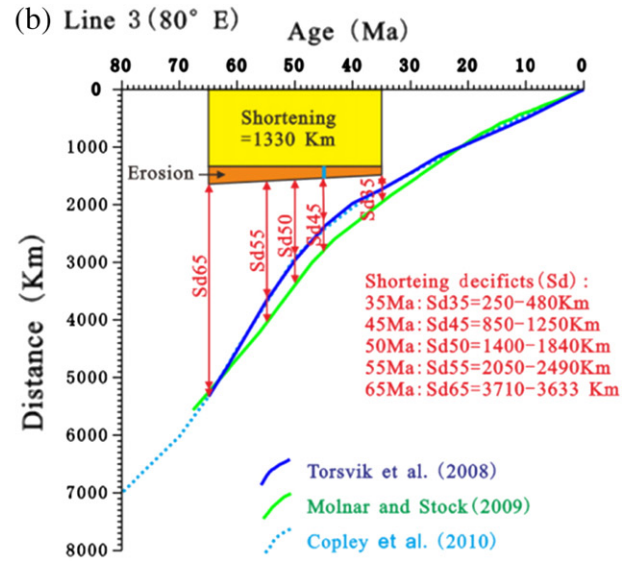
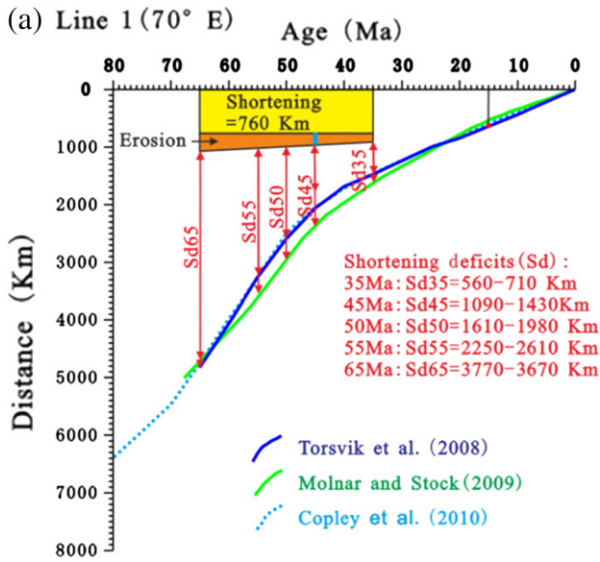
deficits are 730 to 1840 km ([Figs. 18 and 19](#)), being a little larger than 700 to 1200 km that [Le Pichon et al. \(1992\)](#) calculate ([Fig. 18](#), inset, lower right). However, 45 Ma is also somewhat too young for the initial collision time for the east and central collision zone (stated above). If the initial collision time is 50 Ma and the LTP's average elevation at 50 Ma is zero meters along every line, the shortening deficits along all the four lines are more than 1310 km, with the maximum reaching 1980 km ([Fig. 18](#)). If the LTP's average elevation is 500 m at 50 Ma, the deficits are more than 1820 km, reaching a maximum of 2410 km ([Fig. 19](#)). Much more than 500 m of the LTP's average elevation at 50 Ma will result in unrealistic shortening deficits, and the average elevation should be between 0 m and 500. But its real value remains unknown. In fact, it is impossible that the LTP's average elevation at 50 Ma is zero meters because the southern margin of Asia was an Andes-type margin and the wide Tibetan Plateau had been the Mesozoic orogenic belt which supplied sediments to basins around the plateau during the late Mesozoic and earliest Paleogene. If the crust thickness of the southern Tibetan Plateau could be about 55 km from 65 to 50 Ma ([Murphy et al., 1997](#)), its elevation was about 2850 m. In this case, the LTP's average elevation at 50 Ma could not be less than 500 m. So the deficits in the easternmost part of the LTP could range from 1840 to 2330 km ([Fig. 19d](#)).

Where is the missing crust? [Le Pichon et al. \(1992\)](#) propose that a combination of transfer of the lower crust to the mantle through eclogitization and the lateral extrusion could account for a minimum of one third and maximum of one half of the total amount of the shortening between India and Asia (since 45 Ma). They also believe that the excess mass west of the eastern syntaxis that resulted from the lateral extrusion does not account for one third to one half of the deficits west of the eastern syntaxis. Some other authors also postulate that the deficits mainly resulted from the lateral extrusion, supporting the collision-extrusion tectonics proposed by [Tapponnier et al. \(1982\)](#) (e.g., [Jaeger et al., 1989](#); [Tapponnier et al., 2001](#); [Royden et al., 2008](#)). However, [Dewey et al. \(1988\)](#) and [England and Molnar \(1990\)](#) and others (e.g., [Clift et al., 2008](#); [Hall et al., 2008](#)) reject any great magnitude of lateral extrusion after thorough analysis of tectonic history of the region around the Tibetan Plateau (also see [Section 3.2.2](#)). [Dewey et al. \(1988\)](#) estimate that, if any, the lateral extrusion is less than 15% of total east-west width of the Tibetan Plateau. After re-examination of the recently published data from the plateau, we basically support [Dewey et al. \(1988\)](#) and [England and Molnar \(1990\)](#), and further emphasize that the uplift and crustal thickening of the region east of the eastern syntaxis was mainly caused by the northward motion of the western Indochina–Sumatra block rather than the lateral extrusion.

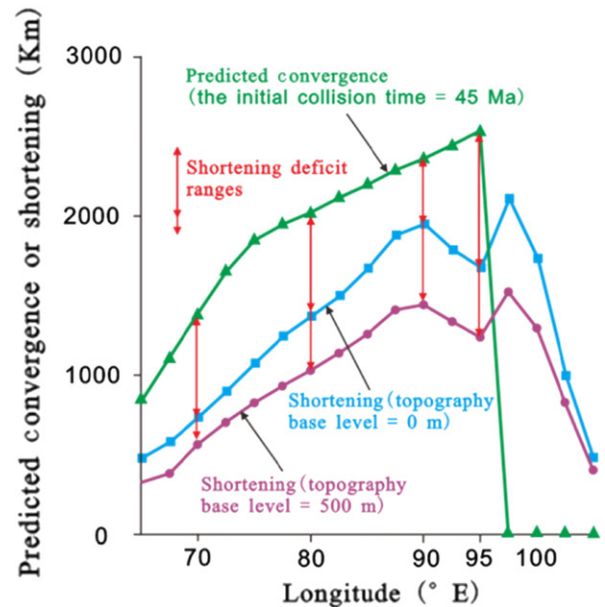
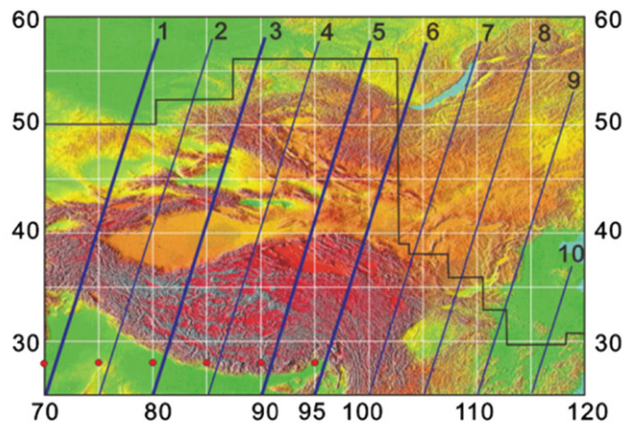
Eclogitization could account for a part of the shortening deficits. [Le Pichon et al. \(1992\)](#) conclude that if a significant part of the lower crust has been eclogitized, the amount of "lateral extrusion" could be reduced to as little as 10%, the minimum amount compatible with the eastward transfer of the Tibetan crust. But in contrast [Le Pichon et al. \(1997\)](#) propose the eclogite in the lower crust changed into granulites and caused the Neogene uplift of the Tibetan Plateau. Although some part (e.g., 30%) of the lower crust in the LTP may have been eclogitized (e.g., [Schulte-Pelkum et al., 2005](#); [Hetényi et al., 2007](#)), it can only account for a very small fraction of such large deficits as shown in [Figs. 18 and 19](#) if the initial collision time is 50 Ma or earlier.

It is noted that if the time of the initial collision along the whole suture is the same (50 Ma), the shortening deficits in the westernmost part of the LTP (e.g., [Figs. 18\(a\) and 19\(a\)](#)) are a little larger than in the easternmost part (e.g., [Figs. 18\(d\) and 19\(d\)](#)), but both the real and predicted shortenings in the westernmost part are much smaller. It is more reasonable that more predicted convergence has more shortening deficits. The initial collision may be diachronous and could be 45 Ma or later in the westernmost part if the shortening deficits are considered.

It is conclusive that at least 1200 km (only 65% of the 1840 km or about half of the 2330 km of the deficits stated above) of the shortening deficits in the easternmost part and at least 1000 km in the



Inset



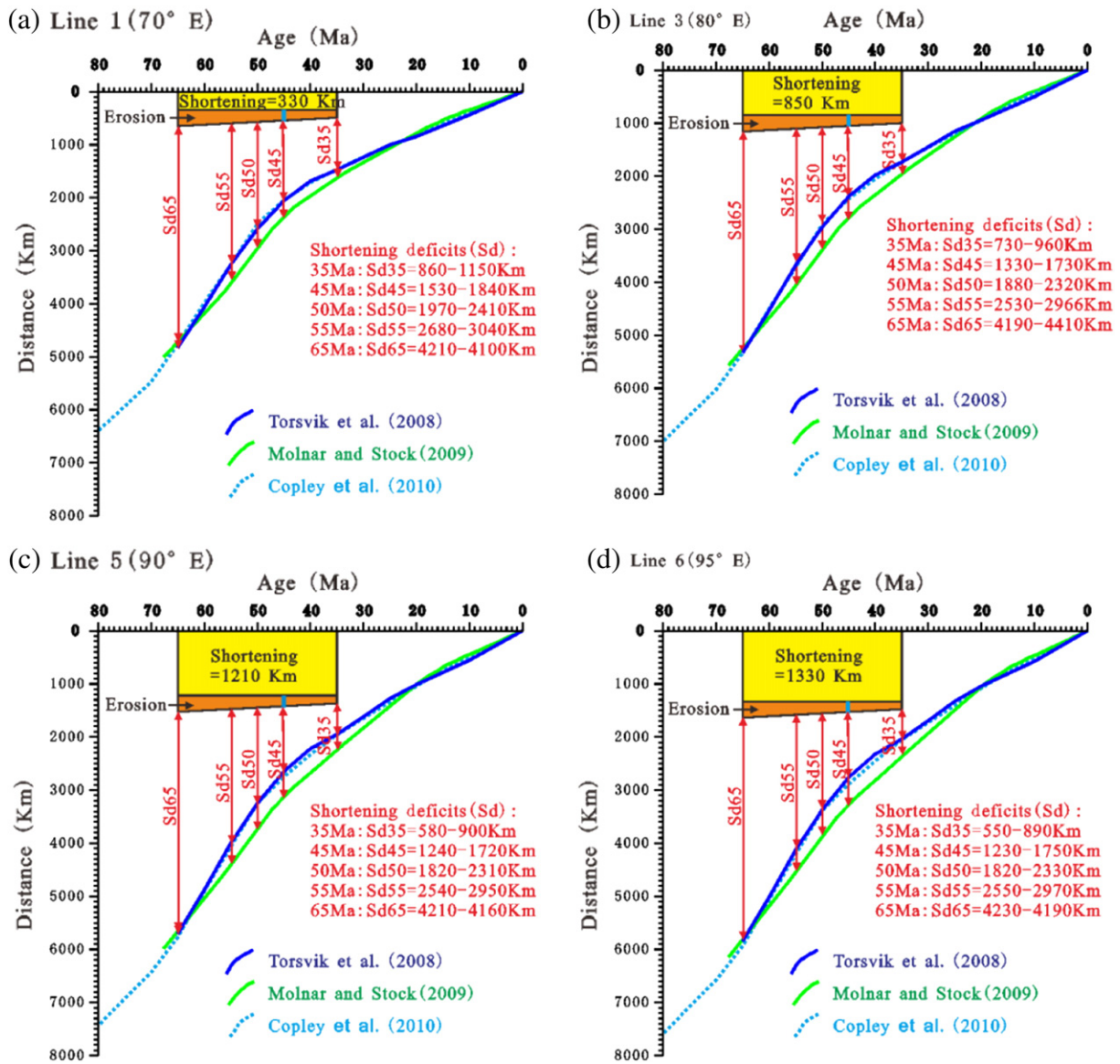


Fig. 19. Shortening deficit estimates along the same four lines as in Fig. 18, with the topography base level hypothesized to be 500 m. The legends are the same as in Fig. 18.

westernmost part are robust although exact shortening deficits cannot be known at the present knowledge’s level. The shortening deficits can simply be attributed to the NNE-NE-ENE-EW movement of east Eurasia and region around the Arctic in step progressively approaching North America. In other words, the “missing” crust indicated by the shortening deficits extruded into the NW Pacific with the Eurasian and NW North American plates undergoing large non-rigid deformation.

4.2. Method of reconstruction of non-rigid deformation of the EUAR

4.2.1. Non-rigid deformation of plates

Geological and geophysical data indicate deformation of both continental and oceanic plates is non-rigid in some cases and some diffuse

plate boundaries in both continents and oceans exceed a length of 1000 km on a side (e.g., Dewey and Burke, 1973; England and McKenzie, 1982; Ratschbacher and Ben-Avraham, 1995; England and Molnar, 1997; Gordon et al., 1998; Hall, 2002; Kronenberg et al., 2002).

Several lines of evidence suggest that the lithosphere of the continents may act like a viscous fluid over geological timescales just as the mantle does (e.g., Oxford University, see <http://www.earth.ox.ac.uk/~geodesy/research.html>). Most of all the numerical modeling of deformation of the LTP is made under the assumption of non-rigidity of continental plates (e.g., England and Houseman, 1986; Royden et al., 1997; Yang and Liu, 2009).

Non-rigid deformation of the oceanic crust of some marginal basins was advocated by several workers (e.g., Mrozowski and Hayes, 1979; Gordon, 1998). We postulate that transform faults within oceanic plates

Fig. 18. Shortening deficit estimates along the four lines, Lines 1, 3, 5 and 6 (see the lower inset (left) for their locations), with the topography base level hypothesized to be zero meters. Yellow areas show the shortenings that are calculated based on the present topography and the topography base level using the method proposed by Le Pichon et al. (1992), with the possible initial collision time widow ranging from 35 to 65 Ma. Orange areas show erosion corrections, which are equal to 200 km at 45 Ma (blue bars. Le Pichon et al. (1992)) and linearly change with time. The predicted convergences or shortenings between India and Eurasia at given reference points (red dots, which are close to the southern ends of the lines, respectively) versus age are calculated according to Torsvik et al. (2008), Molnar and Stock (2009) and Copley et al. (2010). The red arrows denote shortening deficit ranges at the five given initial collision times (65, 55, 50, 45 and 35 Ma) on basis of Torsvik et al. (2008) and Molnar and Stock (2009). The lower insets (left) and (right) show the locations of the four lines among ten lines and the predicted convergences, and the real shortenings along the lines, respectively (after Le Pichon et al. (1992)). The colored topography map in the lower inset (left) is after NASA.

can accommodate mega-scale, non-rigid shearing deformation whose principal shear can be either sub-parallel or sub-perpendicular to the transform faults.

Mechanically, the non-rigid deformation of the upper crust of a plate occurs easier when it is horizontally compressed or sheared than when it is stretched (or spread). If a plate is compared to an ice sheet, it is rigid like a flowing ice sheet when driven by underlying uniformly-flowing water (like mantle convection), and it may be non-rigid like a glacier when driven by gravity (somewhat like compression or collision on the lateral sides). Non-rigid plate deformation in geological history is possibly much more common than previously recognized. It should be noted that diffuse horizontal nearly-simple shears over a wide range of region are not easy to identify because these shears are close to plane strain deformation and can cause minor uplifts or subsidence in topography. Also, the general non-rigid deformation may be accommodated by countless small strike-slip faults and fractures.

It is emphasized that the present rigidity of some plates or blocks (e.g., the Siberia block) indicated by GPS and similar data (e.g., Smith et al., 1990; Larson et al., 1997; Heflin et al., 2004) does not necessarily mean their past rigidity. The present motions of plates as shown by the NUVEL-1A and MORVEL models (e.g., DeMets et al., 1994, 2010) generally represent those of the past 3 to 6 Ma and perhaps even the past 15 Ma, when the marginal basins of NW Pacific basically stopped spreading. Nevertheless, GPS and similar data show that there are not only significant differences between the models and the measurements at most plate boundaries, but also in some cases at considerable distances from the boundary (e.g., Smith and Baltuck, 1993).

Understanding continental and oceanic plates' non-rigidity is of key importance to understanding global tectonic settings of formation of the gigantic linked dextral pull-apart rift system of the NW Pacific.

4.2.2. Method of reconstruction of non-rigid deformation of the EUAR

Reconstruction of rigid plate motion on the sphere is made using the Euler Theorem and all points in a rigid plate rotate about identical poles and in the same angles (e.g., Cox and Hart, 1986). However, its points have different poles and/or different rotation angles when a plate undergoes non-rigid deformation. Usually, exact description of motions of points in a real non-rigid plate is too complicated to solve. Dividing a large non-rigid plate into many small rigid plates could be an approximate method to reconstruct their motions. But clearly this method is not exact enough to describe continuous deformation over wide regions. We suggest that rotational pole and angle functions, where rotational poles and angles vary continuously with positions of points, are used to approximately describe continuous deformation. Clearly, formats of the functions depend on the deformation pattern of a deformed plate.

Deformation of the EUAR (except for the marginal basins) can be divided into two parts: (1) "local" thickening of the LTP that results from the diffuse boundary effect of the collision between the Indian and Eurasian plates, and "local" opening of the Eurasian Basin that results from CW rotation of the North American plate relative to the Eurasian plate; (2) "background" diffuse deformation that results from background (or far-field) effects of the collision. The first part can be treated in ways similar to these in many previous reconstructions (e.g., simply NNE-shortening for the LTP). The far-field effects that were responsible for rifting of the marginal pull-apart basin system of the NW Pacific will be the focus of this study.

The total diffuse deformation (local and background diffuse deformation together) of the EUAR can be assumed to have moved in NNE-NE-ENE-EW complex arcuate circuits, progressively approaching North America (Fig. 16), rather than in great or small circles. This is due to resistance from the Pacific oceanic plate being smaller than resistance from North American continental plate. In other words, points on the South China block moved NNE; points in the arctic region moved in directions more-or-less parallel to the strikes of transform faults in the

Eurasian Basin that was spreading; points in the other regions moved in compatible directions. Magnitudes of motion of points along the line (named as MRLr in Fig. 16) in front of the eastern syntaxis of the collision belt are the largest. The motion magnitudes of other points on the either side of the MRLr decrease both toward the NW and the SE. Hence, the region northwest of the MRLr is sheared CCW relative to the west Europe, Greenland and northern North America. The region southeast of the MRLr is sheared CW relative to the most eastern margin of the plate. If local thickening in the LTP is subtracted from the total diffuse deformation, the residual diffuse deformation is the background, diffuse deformation.

For simplicity of modeling the background, diffuse deformation, it is assumed that points of the largest movements from any given time to present follow a single curve, which goes from about the northern end of the East Vietnam fault through the west of the North China block, to the region north of Okhotsk Sea (Fig. 16). The curve is here termed the Maximum Rotation Line (MRLb). Points of the MRLb could have the same rotational radius, but don't have the same rotational pole, as it is actually not a circle on globe. For its southern segment, the average strike is about NS directed and its average pole should be located to the east of the southern segment of the MRLb. For its northern segment, the average strike is east-west and its average pole should be located to the south of the northern segment. If the western Europe to northeastern North America region undergoes little non-rigid deformation, then rotation angles of points in the region NW of the MRLb progressively decrease from maximum values along the MRLb to zero along the west Europe and northeastern North America regions. The region southeast of the MRLb undergoes dextral trans-deformation, and rotation angles of the points of this region progressively decrease from the maximum along the MRLb to the proto-arcs of the NW Pacific.

To quantitatively describe this deformation model, many different rotation functions have been attempted. The final model presented here makes simple assumptions that: (1) the finite rotational poles of all the points are located along the equator, and the longitudes of these poles was directly proportional to latitudes of all points considered, and (2) finite rotation angles of points NW of the MRLb were inversely propositional to the arc distances from the poles to the points; finite rotation angles of points of the region southeast of the MRLb is propositional to the arc distances from the poles to the points. If the finite-rotation poles, rotation radius and rotation angles of the points along the MRLb are given, we can use this quantitative model easily to reconstruct positions of the Eurasian and North American plates through modifying the traditional rigid plate reconstructions for any given time.

4.3. Plate tectonic reconstructions of the marginal basins

Using the non-rigid plate reconstruction method for the Eurasian and N. American plates (Section 4.2.2), we present plate reconstructions of the marginal basins of the NW Pacific at four key times: 50, 35, 15 and 5 Ma. All these plate reconstructions start from rigid-plate reconstructions in the African hotspot fixed reference frame that are made by Torsvik et al. (2008), and then modify the rigid-plate reconstructions of the EUAR using the above quantitative non-rigid deformation model. The reconstructions of the marginal basins are based on the analysis of their origin as stated in Section 3 and the approximate reconstructions of the LTP are based on the analysis of its shortening history (Section 4.1.3).

4.3.1. Plate reconstruction at 50 Ma

Northward motion of the South China block since 50 Ma has been estimated using three independent aspects as stated above: (1) 10.04° to 11.25° relative to Samba Island of the east Java arc, as is indicated by the pull-apart amount of the South China Sea basin and the JMCS basin system, (2) more than 1000 km by the paleomagnetic data, and (3) more than 1200 km by the shortening deficits in the easternmost

LTP. If the translation distance and rotation radius since 50 Ma along the MRLb (Fig. 16) are assumed to be 11.25° and 70° respectively, the finite rotation angle along the MRLb is about 12° . The pole of rotation of points of the maximum latitude (90° , the North Pole) is assumed to have been located at (140°E , 0°) and the pole of the points at $\text{N}10^\circ$ (latitude) at (180°E , 0°). By using these rotational parameters the positions of the EUAR at 50 Ma are reconstructed (Fig. 20).

An important problem with this reconstruction of the EUAR is whether or not the non-rigid deformation of the EUAR is close to plane strain because the Cenozoic topography indicates that no large convergence or extension resulted from this background diffuse deformation (except the “local” thickening in the LTP as well as in the Stanovoy Range and the transitional zone between the Eurasian and North American plates). To clarify this problem, contours of ratios of areas of strain ellipses to areas of the unit strain circles are compiled (Fig. 21). Fig. 21 shows that all the ratios are close to one, that is, plane strain, though there exists small extensional (ratios less than 1) and compressional (ratios larger than 1) deformation in some regions. The small extensional strain in some regions in Eurasia could have occurred, for example, in the west Siberia Basin to the Canada Basin region. The small extensional deformation in other regions in Eurasia (e.g., in Europe) could not have occurred, but this extension might be compensated by collision of the Arabian plate with east Eurasia. The small extensional deformation along the western North America could not

necessarily have occurred, but could have been demolished by the thickening along the Cordillera, which was caused by convergence between the North American and the paleo-Pacific (Farallon and Kula) plates. Dextral transpressional deformation and minor amount of uplift could have occurred along east Asia. In addition, local small dextral pull-apart basins (e.g., the Bohai Gulf basin) could have overprinted the slightly uplifted eastern Asia.

The Philippine Sea plate at 50 Ma was located about 20° south of its present position as indicated by paleomagnetic data (mentioned above). It is assumed that the finite rotation pole and finite rotation angle of WPB at 50 Ma are at (210°E , 12°N) and 20° , respectively.

Taking the above kinematical analyses into account, the plate reconstruction of the marginal basins of the NW Pacific and the LTP at 50 Ma is presented (Fig. 22). Some related key issues are summarized as follows.

(1) Before 50 Ma.

In the NW Pacific, there were three oceanic plates: North New Guinea, Pacific and Kula plates (e.g., Hilde et al., 1977; Ben-Avraham, 1978; Seno and Maruyama, 1984; Lewis et al., 2002). There was a NW-trending spreading axis between the Pacific and North New Guinea plates, across which NE-striking transform faults developed. To the north, these transform faults linked to NNW-striking transform faults within the western Pacific Plate.

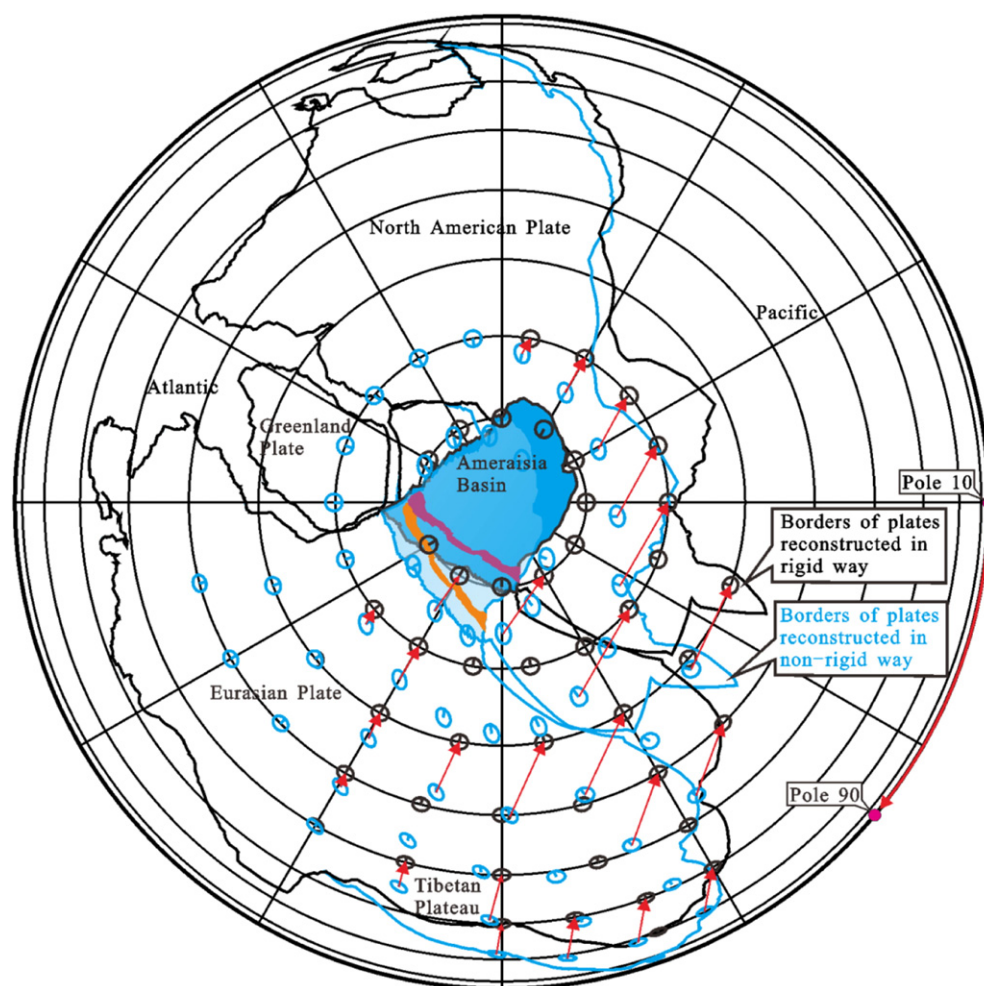


Fig. 20. Reconstruction of the diffuse background deformation of the EUAR at 50 Ma. Black lines represent the positions of plates in rigid plate reconstruction in African Hotspot Fixed Reference Frame (Torsvik et al., 2008). Blue lines are positions of the plates in the reconstruction by this paper. Violet and orange areas are Lomonosov rise reconstructed in rigid and non-rigid ways, respectively. Pole 10 and Pole 90 denote the Euler poles of rotation of points located on 10° and 90° latitudes on the rigid Eurasian and North American plates for the background diffuse deformation reconstruction, respectively. Black small ellipses are unit circles (one degree arc distance radius) on the rigid Eurasian plate and blue ellipses are restored from the unit circles in the non-rigid way. Note that the rigid plate reconstruction in the African Hotspot Fixed Reference Frame doesn't show “local” contractional deformation of the Tibetan Plateau and its adjacent regions. Note that the marginal seas are not included in the EUAR. See the text for details.

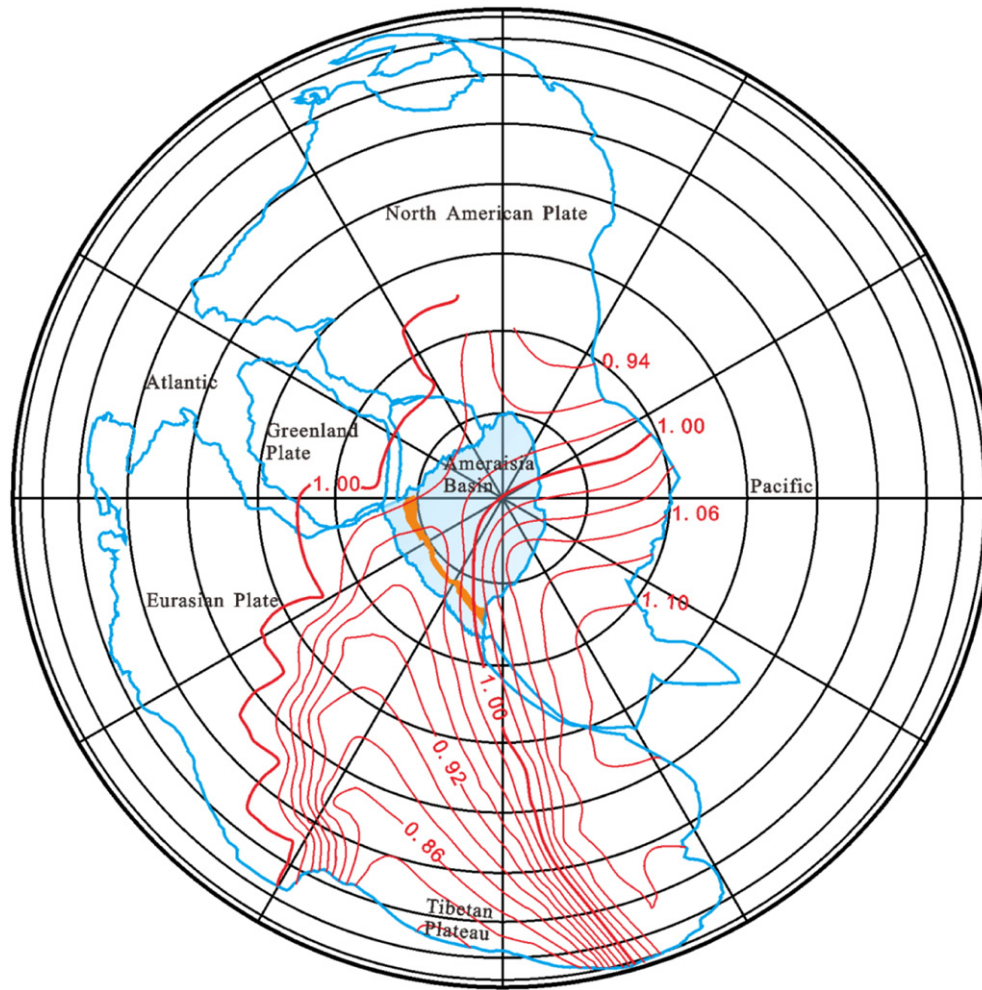


Fig. 21. Contours of area changes in the EUA for the background non-rigid deformation since about 50 Ma. The values labeled on the contours (red lines) are ratios of the restored ellipses' areas to the areas of the unit circles as shown in Fig. 20. The contours clearly show that the non-rigid deformation is close to the plane strain. The regions delimited by the less than one-labeled contours incur slight transensional deformation and those with larger than one-labeled contours exhibit slight transpressional deformation. Orange areas are Lomonosov rise. Note that the marginal seas are not included in the EUA. See the text for details.

Along the continental margin of the NW Pacific, there had possibly already existed right-stepping mega-faults that include the East Vietnam, Manila–East Korea, Tartar–Tanakura and East Okhotsk faults.

The geometry and positions of the basins and blocks in the Banda Sea region are very difficult to determine, because this region has been intensively deformed, and because its geology and geophysics are still poorly known although several evolutionary scenarios have been put forward (e.g., Charlton, 1986; Lee and McCabe, 1986; Hall, 2002, 2012; Hinschberger et al., 2005). Many papers suggest that the micro-continental blocks including the east and south arms of Sulawesi, the Banda Ridge, Buru–Seram and Sula were parts of the Australian continental block (e.g., Lee and Lawver, 1995; Hall, 2002). However, their affinities to and times of rifting away from Gondwanaland are uncertain (e.g., Hartono, 1990; Ali and Hall, 1995; Vroon et al., 1996) and their paleomagnetic data are contradictory (e.g., Johnsma and Barber, 1980; Ali and Hall, 1995). The Banda Sea region might be a mosaic of continental crusts and the Mesozoic and Cenozoic oceanic crust because some ophiolites (e.g., Buton and Seram ophiolites) are Mesozoic (Hall, 2002). We suggest that the Java arc was linked to the NNW-trending proto-Inner Banda arc, and the East Sundaland trench as a paleo-plate boundary was located between Sundaland and the Banda Sea region rather than between Sundaland and Indian Ocean (Fig. 22).

There are two possibilities regarding the position of the south margin of the Lhasa block (Fig. 22): it trended in NW, roughly parallel to

the Sumatra Trench, this means that there is no “coincident” large gulf in the south margin of the Eurasian Plate to “wait for” the coming India block “to fill”; there is a “coincident” large gulf west of the Burma Block, which might have formed by collision of the Lhasa and Qiangtang blocks with Asia during Mesozoic (or other causes). Considering the possible initial collision time and shortening deficits as mentioned above, the second possibility is adopted.

The Tibetan Plateau region possibly had no high average altitude as suggested by Dewey et al. (1988). The continental arc along the south margin of the Eurasian plate might have been thin like the Sumatra and Java arcs at present. Although crust of the Lhasa and Qiangtang blocks could have been thickened in the Mesozoic (e.g., Murphy et al., 1997), crust of the Qiangtang block might have returned to about normal (or moderately abnormal) thickness just before the collision between India and Asia because of erosion. As mentioned above (see Figs. 18 and 19 for details), if the LTP had had high altitude or significantly thickened crust just before the initial collision, there would have been unrealistic shortening deficits in it. The Lhasa block could be as high as the present Sumatra arc.

The overlap and gap between the Eurasian and North American plates in NE Asia are similar to these in the rigid plate reconstruction. This indicates diffuse deformation around the boundary between the two plates after 50 Ma. Some special rotational function for the points in eastern and northeastern Asia could be found to eliminate the overlap



Fig. 22. Plate reconstruction of the NW Pacific margin and the Large Tibetan Plateau at 50 Ma. Pink area north of India block is north part of the Great India that has been subducted under the Tibetan Plateau and accreted to Himalayas (HYM). Black arrows represent motion vectors of their starting points (black dots) from 50 to 35 Ma. Dark blue dashed line is an alternative segment of the boundary between Tethys and Asia. Red dotted lines in oceanic crust of marginal basins are magnetic lineations. Deep yellow and dark blue areas denote overlap and gap between the Eurasian and North American plates, respectively. Note that the local deformation in Stanovoy and the transitional zone between the Eurasian and North American plates are not reconstructed (see Section 3.7 for details). Possible small displacements between the South China, North China, Mongolia and Siberia blocks are not reconstructed (except their background deformation). Marginal basins of the SW Pacific (dark gray area) are not reconstructed. Abbreviations (alphabetically): AST = ancient East Sunda Trench, ALF = Aleutian fault, BHR = Benham Rise (possibly formed at 49.4 Ma), IBMF = Izu–Bonin–Mariana fault, KPF = Kyushu–Palau fault, NGA = New Guinea arc, NNGP = North New Guinea plate. Other abbreviations and legends are same as these in Fig. 16. See the text for details.

and gap, but this is difficult to determine and will not significantly help to understand plate reconstructions of the marginal basins of the NW Pacific.

(1) At 50 Ma and between 50 and 35 Ma.

At about 50 Ma, the Australian continental block collided with the New Guinea arc (e.g., Hall, 2002), the polarity of the subduction zone along the New Guinea arc inverted and the New Guinea Central Orogen began to form. This collision was in about NS direction and formed a sinistral transpressional “pop-up” across the Pacific and North New Guinea plates, entrapping the spreading axis between the two plates and NE- and NNW-striking transform faults. The pop-up structure was the proto-Philippine Sea plate (Fig. 22). According to paleomagnetic data (Section 3.9), the Philippine Sea plate (PHP) was located about 20° south of its present position. The PHP was surrounded by the sinistral transpressional faults: the Negros–Cotabato trans-thrust (the west Philippine fault, WPF) west of Philippines–Halmahera in the west, the North Philippine Sea trans-thrust within the Pacific plate in the north, Izu–Bonin–Mariana trans-thrust (IBMF) (possibly a pair of faults along

the Mariana segment) in the east, Yap thrust (YPF) and Palau thrust (PLF) in the south. The Philippine Trench fault (PTF) was a sinistral transpressional one that was parallel with WPF. Within PHP, linkage of two large NNW-striking transform fault with one large NNE-striking transform fault (a segment of the Sofugan fault) formed the Kyushu–Palau Fault (KPF). KPF and the Sofugan fault divided PHP into three sub-basins: West Philippine Basin (WPB), the proto-Parece Vela Basin (PKB) and proto-Shikoku Basin (SKB). SKB was very narrow and would be completely occupied by later Izu–Bonin Ridge and Kyushu–Palau Ridge. With continuation of compression of the northward-moving Australia block and New Guinea arc, PHP gradually formed into a more mature transpressional “pop-up” structure. The Pacific plate subducted below PHP along IBMF-YPF-PLF and the Izu–Bonin–Mariana–Yap–Palau arcs (IBMR-YPR-PLR) began to form. IBM subduction zone has a steep dip angle at present possibly because it resulted from a transpressional thrust rather than the subducting Pacific plate was older and denser. Igneous rock extruded and intruded along zig-zag KPF, and Kyushu–Palau Ridge (KPR) began to form. KPR could include some island–arc geochemical characteristics because of being

close to the subduction zone. Similarly, the Gagua Ridge began to form along the northern segment of PTF. The NW- and NS- striking conjugate faults developed within PHP, and basaltic magma intruded and extruded along some of these faults. The basaltic rocks along the faults could form the linear sea-floor fabrics and magnetic anomalies. These magnetic anomalies of different orientations did not indicate seafloor spreading in different directions. Up to about 45 Ma, WPB could have fully opened, because the oldest age of basalt samples from Benham Rise which extends in NE-trending direction close to the spreading axis (central Philippine Sea fault, CPF) is 49.4 Ma (see summary of Deschamps and Lallemand, 2002). However, if seafloor spreading in WPB had continued to 33 Ma as some authors suggest (e.g., Hilde and Lee, 1984), this spreading must have occurred within the pop-up structure and the oceanic crust subducted into the Philippine Trench. From 50 to 35 Ma, the eastern ridges of PHP continued to undergo local CW rotation because the northward motion of PHP is much larger than the northward component of the motion of the Pacific plate and dextral shear along IBMR, YPR and PLR took place. In the meantime, the northern segment of IBMT retreated towards the Pacific in small scale and the spreading behind IBMR began.

At about 50 Ma, the Indian continent began to collide with the Eurasian plate and impinged east Asia to move in complex, NNE-NE-ENE-EW arcuate circuits (stated above). This happened at the same time as major marginal basins began to open as dextral transtensional basins. The Aleutian and Komandorsky sub-basins of the Bering Sea basin was trapped as a dextral pull-apart in the Pacific plate (or Kula plate) with the Aleutian Trench fault acting as its eastern and southern boundaries. But the Japan Sea and Okhotsk Sea basins underwent much weaker rifting than the northern margin of the South China Sea basin because direction of the Amurian block moved at a high angle to the main boundary faults of the former two basins. An exception is that Celebes Sea might result mainly from the active spreading although the dextral transtension might trigger start of its spreading. We emphasize that the dextral transtension in the marginal basins within the Eurasian plate could occur while PHP move northward because the subduction zone of the PHP along the Asian continent could be anchored (let alone the probable roll-back of PHP) and the western boundary fault of PHP underwent *pure* sinistral strike-slipping (note that exact direction of motion of the Australia continental block was not NS but NNE).

Geometry of the Indochina–Sumatra block (ISK) and the Borneo–Java Arc region at 50 Ma is reconstructed through 25° of CCW rotation of present ISK in the way that has been explained in Section 3.2.3. From 50 to 35 Ma, ISK continued to rotate CW, pushing against the South China block along the NW segment of RRF. The south shelf of the Andaman Sea basin, west of ISK, began to rift as a dextral pull-apart margin.

The Lhasa block as a continental arc probably had higher elevations than other blocks at 50 Ma. The LTP generally began to uplift since 50 Ma. The uplift was mainly attributed to contraction of crust of the Tibet Plateau itself rather than the underplating of the Indian continent. But the North China block (the Alxa region) might be subducted below the Qilianshan block. By 35 Ma, the Lhasa and Qiangtang blocks had nearly reached its present altitude and the northern Tibetan Plateau might have significantly uplifted.

The India–Asia collision might have triggered the Eurasian Basin's spreading along the Gakkel Ridge if the initial collision time were 55 Ma. However, the initial collision time is possibly 50 Ma and it is difficult to correlate the collision with the beginning of the Eurasian Basin's spreading (at about 56 Ma) (e.g., Rowley and Lottes, 1988). As mentioned above, the 55 Ma initial collision age cannot totally be excluded and the correlation between the collision and the rifting start of the Eurasian Basin could be an unsettled problem. Interestingly, the Gakkel Ridge was probably aligned about parallel with the North Atlantic Ridge at around 50 Ma. The Mesozoic Amerasia basin underwent strike-slip deformation since 56 Ma (e.g., Rowley and Lottes, 1988) and its complex magnetic anomalies might have been attributed to the reworking of the Cenozoic non-rigid, trans-deformation.

4.3.2. Plate reconstruction at 35 Ma

The spreading time of oceanic crust of the South China Sea basin is problematical (mentioned above). The reconstruction that is presented here adopts a “conservative” alternative, that is, its spreading time is about 32 to 15 Ma (Briais et al., 1993). The JMCS transtensional system also fulfilled its rifting during this period. This means that the South China block moved northward by nearly 900 km along the central part of the South China Sea basin and the JMCS system. Therefore, it is assumed that the finite rotation angle along the MRLB is 10° and the rotation radius along the MRLB (Fig. 16) is assumed to be 70°. Like for reconstruction at 50 Ma, the pole of rotation of points of the maximum latitude (N90°, the North Pole) is also assumed to have located at (140°E, 0°) and the pole of the points at N10° (latitude) at (180°E, 0°). PHP is assumed to have moved northward about in step with the northward-moving Australia block from 50 to 35 Ma and the finite rotation pole and finite rotation angle of WPB for 35 Ma are at (210°E, 12°N) and 16°, respectively.

Plate reconstruction of the marginal basins of the NW Pacific and the LTP at 35 Ma is shown in Fig. 23. The main evolutionary characteristics from 35 to 15 Ma are summarized as follows.

The Pacific plate kept moving westward. Spreading occurred in the Caroline Sea west of Pacific from at least 36 to 28 Ma (Hegarty et al., 1983; Hegarty and Weissel, 1988). The Caroline Ridge formed during the same time as this spreading. The Caroline Ridge and sea constituted the Caroline plate. Location of this plate and its relationship with the Pacific plate remain a puzzling problem. Many authors believe the Caroline Sea basin was one of the back-arc basins of the NW Pacific and had been located south or southeast of PHP since its formation (e.g., Hall, 2002; Gaina and Müller, 2007; Seton et al., 2012). There would have been a large convergence (more than 2000 km) between the Pacific and Caroline plates if these authors' ideas are correct. However, the southern segment of the boundary between the two plates is the Lyra Trough, which is now an inactive graben, is very small and there is not any evidence (e.g., ancient arc) to indicate existence of a large convergence along this trough. The northern segment of the boundary cannot be found in topography. The Mussau Trench could be an alternative boundary between the two plates, but this trench is also small, and convergence along it is less than 100 km and occurred during late 1 Ma (Hegarty et al., 1983). So the reconstructed Caroline Ridge (plate) moved in step with the Pacific plate. The Caroline Sea basin might be a major oceanic plate most of which has subducted below PHP and the Australia–SW Pacific marginal basin region.

PHP continued to move northward a little slower than the Australia continental block and limited convergence between PHP and the Australia continental block occurred. PHP further evolved into a mature sinistral pop-up structure. Meanwhile, the great eastward movement of the northern IBMR together with the eastward-moving Japan arc caused fan-like spreading behind the ridge since 35 Ma. At about 30 Ma, the spreading entered the proto-Shikoku Basin and the present Shikoku Basin began to open. The spreading propagated southwards and reworked the proto-Parece Vela basin along about NS-striking faults and the Parece Vela Basin became wider. According to the pattern of magnetic lineations, the spreading occurred in east–west direction from 35 (or 30) to 19 Ma and in NE direction from 19 to 15 Ma (C6 to C5c) in both the Shikoku and Parece Vela basins. Change in direction of the spreading possibly indicated that the interaction between related plates changed. It is postulated that there was more intensive convergence between PHP and the Australian block, and sinistral trans-deformation occurred within the sinistral pop-up structure from 19 to 15 Ma. Superposition of the sinistral trans-deformation on the east–west-spreading resulted in sinistral transtensional spreading in the two sub-basins. PHP as a whole moved northward relative to the Pacific plate and the local dextral strike-slip deformation along its eastern ridges continued from 35 to 15 Ma.

With large NNE-NE-ENE-EW movement of the EUAR in steps progressively approaching North America, the marginal basin system of



Fig. 23. Plate reconstruction of the NW Pacific margin and the Large Tibetan Plateau at 35 Ma. Black arrows represent motion-vectors of their starting points (black dots) from 35 to 15 Ma. Green arcuate lines with arrows on the IBMR, YPR and PLR indicate the local CW rotations (see Fig. 15 for more details). Four NS-trending deep-yellow dotted lines in SE WPB and SW PVB are the selected “reduction-to-the-pole magnetic anomaly” lineations (see Fig. 15 for more details). Note that the local deformation in Stanovoy and the transitional zone between the Eurasian and North American plates are not reconstructed (see Section 3.7 for details). Abbreviations (alphabetically): AST = ancient East Sunda Trench, ALF = Aleutian fault, IBMT = Izu–Bonin–Mariana Trench, LYT = Lyra Trench (Trough), PLT = Palau Trench, YPT = Yapu Trench. Other legends and abbreviations are same as in Figs. 16 and 22. See the text for details.

the NW Pacific entered an intensive rifting period from 35 to 15 Ma. However, differences in rifting intensity or pull-apart amount of these basins existed because of different local plate tectonic settings (Fig. 23). At about 32 Ma, seafloor spreading began in the South China Sea basin and the JMCS basin system. At 34 Ma or later (e.g., 30 Ma or 25 Ma) seafloor spreading started in Japan and Okhotsk seas basins. The northern margin of the South China Sea basin and the Shelf Basin of the East China Sea basin generally entered the weaker rifting stage some like passive continental margins when the seafloor spreading proceeded, but intensive rifting continued in the western continental margin of the South China Sea basin in order to keep kinematic balance with the seafloor spreading in the Central and Southwest sub-basins. The Kormandorsky Basin in the Bering Sea spread for intensive dextral shear along the southwest segment of the Aleutian Trench and sub-basins in the outer Bering Shelf underwent dextral transtension. As emphasized above, the dextral transtension in the marginal basins within the Eurasian plate were able to occur while PHP moved further northward (more exactly, PHP moved northward at different rates and slowed down between 32 and 15 Ma according to the paleomagnetic data (e.g., Haston and Fuller, 1991)).

Geometry of ISK and the Borneo–Java Arc region at 35 Ma are reconstructed through 20° of CCW rotation of ISK from their present

positions. From 35 to 15 Ma, ISK continued to rotate CW with the Indian plate pushing on the Eurasian plate. In the Andaman Sea region, the NS-directed dextral pull-apart continued and the oceanic rifting could be generally unusual seafloor spreading that formed Alcock and Sewell oceanic plateaus. Dextral transform margin-type rifting started in the Mergui basin and the East Basin with the principal fault being the Sumatra fault system, when dextral strike slip took place along this fault system because of oblique subduction of the Indian plate.

Shortening and uplifting rates in the LTP were much lower during this period than the last period. Elevation of the LTP generally remained constant. Only the Himalayas and region around the Tarim basin were uplifted.

4.3.3. Plate reconstruction at 15 Ma

At 15 Ma, the eastern Eurasian plate ceased to move NNE- to ENEward. The Eurasian plate and the region around the Arctic are reconstructed as in the rigid reconstruction (Torsvik et al, 2008). For reconstruction of PHP at 15 Ma, its finite rotation pole and finite rotation angle are at (210°E, 12°N) and 9°, respectively. The plate reconstruction of the marginal basins of the NW Pacific and the LTP at 15 Ma is shown in Fig. 24. The main evolutionary characteristics from 15 to 5 Ma are summarized below.



Fig. 24. Plate reconstruction of the NW Pacific margin and the Large Tibetan Plateau at 15 Ma. Black arrows represent motion-vectors of their starting points (black dots) from 15 to 5 Ma. The legends and abbreviations are same as in Figs. 16, 22 and 23. See the text for details.

PHP continued to move northward. The seafloor-spreading in the Shikoku Basin and the Parece Vela Basin also ceased because the Japan arc together with the IBMR did not significantly migrate eastward. WPB was reworked and the magmatic activity (e.g., 10 Ma basalt along the CBF) occurred in this period. The Caroline Ridge was close to IBMR.

All the major basins basically stopped rifting and began to enter the post-rifting period. Most of them were still be reworked by tectonomagmatism and the basaltic flows often occurred forming the seamounts. Sinistral transpressional inversions developed in some of the marginal basins.

Geometry of the ISK reached its present geometry at 15 Ma because the South China Sea basin no longer stretched in a NS-direction. The Borneo–Java Arc region at 15 Ma could have been reconstructed to its present geometry, but a presumed 5° of CW simple shear along north–south-trending vertical planes is added to its present geometry because of its CCW rotation and convergence with the Dangerous Ground–Reed Bank block in the South China Sea basin after 15 Ma. In the Andaman Sea region, NNW-directed weak transensional rifting on the Alcock and Sewell plateaus and NW-directed weak transform margin-type rifting continued in the Mergui Basin from 15 to 5 Ma.

The more rapid shortening and uplift in the LTP resumed since 15 Ma because the Eurasian plate became basically stable. From the Indian Ocean northward to the region around Tianshan, the intensive compressional deformation rejuvenated. The Himalayas rapidly uplifted. The Lhasa and Qiangtang blocks, however, might not have exhibited large-scale uplift and incurred no significant shortening. Instead, the Hoh Xil–Sangpan–Ganze block and the Altyn and Tianshan regions

began to uplift rapidly. The eastern Tibetan Plateau commenced to thrust over the western South China block along the Longmenshan belt. For the rapid convergence and uplift, most of the NS-trending grabens formed on the Tibetan Plateau, as is a typical indicator of the rapid shortening and uplift. The Karakorum fault rejuvenated as a right-slip fault.

A plate dynamic problem is why the east Eurasian plate ceased to move NNE- to ENE-ward since around 15 Ma while the Indian plate was still colliding with it. Rates of the Indian plate relative to the “fixed” Eurasia and the African hotspot fixed frame did not evidently change (Fig. 17). It is speculated here that there were two causes responsible for this: (1) the main part of North American plate (except the region of the Arctic) had rotated to the eastern front of the eastward-moving EUAR and resisted the EUAR’s further eastward-moving; and (2) the convective state of the upper mantle below the Eurasian and North American plates began to change and this might have reduced the northward movement of both the Indian and the eastern Eurasian plates.

4.3.4. Plate reconstruction at 5 Ma

At 5 Ma, the Eurasian plate and the region around the Arctic is also reconstructed in the same way as in the traditional reconstruction (Torsvik et al, 2008). PHP at 5 Ma is reconstructed with its finite rotation pole and finite rotation angle being at (155.53°E , 32.73°N) and 7.54° , respectively. Plate reconstruction of the marginal basins of the NW Pacific and the LTP at 5 Ma is shown in Fig. 25. The main evolutionary characteristics from 5 to 0 Ma are summarized as follows.



Fig. 25. Plate reconstruction of the NW Pacific margin and the Large Tibetan Plateau at 5 Ma. Black arrows represent motion-vectors of their starting points (black dots) from 5 to 0 Ma. Blue arrow denotes direction of local material flow from the Tibetan Plateau to the most northwestern Indochina-Sumatra block. See the text for details. The legends and abbreviations are same as in Figs. 16, 22 and 23. See the text for details.

The Caroline Ridge collided with the southern segment of IBMR and the Mariana Basin began to open. The West Mariana Ridge continued to move relative to IBMR and seafloor spreading in the Mariana Basin has been occurring. PHP generally moved NW-ward. The northern Philippine arc collided with the South China continent and the Taiwan orogen commenced its formation. The northern Philippine Arc tended to push the Taiwan–Sinzi rise to move NS- to NNW-ward relative to the Ryukyu Arc during Pliocene and Quaternary. This could trigger the local dextral transtensional rifting in the Okinawa Trough.

All the marginal sea basins basically stopped rifting, but a little more intensive, though very weak, rifting episodically occurred in this period (5 to 0 Ma) than the last period (15 to 5 Ma).

ISK kept the same geometry as in the last period. The Borneo–Java Arc region rotated CCW, which continued its further convergence with the Dangerous Grounds–Reed Bank block since 5 Ma. Much more intensive NNW-directed transtensional rifting or seafloor spreading occurred in the Central Andaman Basin since about 5 Ma.

The rapid shortening and uplift in the LTP continued following the last period. The Himalayas continued to grow due to shortening. The Lhasa block might have uplifted due to the underplating of the Indian plate. The NS-trending grabens on the Tibetan Plateau rifted intensively. The Hoh Xil–Sangpan–Ganze block and the Altyn and Tianshan regions also kept rapidly uplifting. The eastern Tibetan Plateau seemed to have more rapidly extruded easterly in this period than in the last period, as is indicated by the sinistral strike-slip motion along the Qinling and Jicheng faults that intensified rifting in the Shanxi Basin.

A problem is why the weak rifting was more extensive and intensive in this period than in the last period (e.g., rifting in the Shanxi and

Central Andaman basins, and more rapid subsidence in some marginal basins and their subbasins in this period). We speculate that the convective state of asthenosphere below the Eurasian and North American plates once again evidently changed and more rapid northward motion of the Indian plate resumed if Copley et al. (2010) is correct (Fig. 17), or (and) PHP changed its motion direction from NS to NW at around 5 Ma.

5. Discussion

As summarized in Section 1, various hypotheses for origin of marginal basins have been proposed within the classical plate tectonics, but at present none of them are widely accepted. The genetic mechanism of back-arc basins (e.g., the Japan Sea, Okhotsk Sea and Philippine Sea basins) is still a matter of debate (e.g., Uyeda and Kanamori, 1979; Nur et al., 1993; Xu and Zhang, 2000c; Mantovani et al., 2001; Heuret and Lallemand, 2005; Lallemand et al., 2005; Sdrolias and Müller, 2006; Schellart, 2011; Faccenna et al., 2012; Long and Wirth, 2013). Most of the authors use three subduction-related models, the “trench rollback”, the “corner flow” or/and the “sea anchor” to explain opening of back-arc basins. But Mantovani et al. (2001) deny any mechanism related to plate subduction based on five lines of evidence. We think that comments of Mantovani et al. (2001) are reasonable and further emphasize that geometry of basins indicate their origin. If subduction-related mechanism had played a key role in opening of back-arc basins, they should have exhibited long trough-like shape parallel with the subduction zones rather than rhombic or Lazy-Z shape.

The South China Sea basin (SCS), a key member among the marginal basins, is not a *back-arc* basin (e.g., Taylor and Hayes, 1983). How and why it opened is related to many important problems regarding the tectonic evolution of this region. Most authors believe that its rifting was attributed to: (1) active (and/or slab-pull) spreading assuming that there existed a wide paleo- (or proto-) South China Sea (PSCS) to give enough space to SCS (e.g., Taylor and Hayes, 1983; Gong et al., 1997; Morley, 2002; Clift et al., 2008; Hall, 2012), or (2) sinistral pull-apart (“collision–extrusion”) hypothesizing the rigid Indochina–Borneo block was extruded SSE- to S-ward in a large scale (1000’s km) due to the collision between the Indian and Eurasian plates (e.g., Tapponnier et al., 1982; Jolivet et al., 1990; Briais et al., 1993). We believe that neither of the two hypotheses can reasonably explain origin of SCS for the following reasons.

Wide PSCS possibly didn’t exist. Taylor and Hayes (1983) suggest that SCS is a small “Atlantic-type” marginal basin bounded by the passive margins to the north and south and a dextral transform margin to the west (the East Vietnam fault) and that PSCS subducted S-ward at the Borneo–Palawan trench. However, the later evidence doesn’t support there was a subduction zone south of Luconia Shoals (e.g., Morley, 2002; Hutchison, 2004, 2010; Mazur et al., 2012), so wide west PSCS didn’t exist. Later workers revise Taylor and Hayes’ model and hypothesize that the wide PSCS was only located east of the NW-trending West Baram Line (WBL) or narrowed westward (e.g., Schluter et al., 1996; Hall, 2002, 2012; Morley, 2002; Hutchison, 2004; Clift et al., 2008). But no convincing geological evidence indicates existence of Oligocene–Early Miocene subduction zone around the N. Borneo (Sabah) to Palawan, wherever exact position of the subduction zone is hypothesized (e.g., Taylor and Hayes, 1983; Hall, 2002; Morley, 2002; Clift et al., 2008; Morley, 2012). As Taylor and Hayes (1983) note, the “convergent terrain” is unusual for its almost complete lack of Paleogene plutonic and volcanic rocks. On the basis of geological field data from the Sabah fold belt, Rangin (1989) and Rangin et al. (1990) believe that no continuous deformation occurred throughout the Paleogene, and argue that the main compression began in Middle Miocene as the Sulu–Celebes block moved NW-ward. Tongkul (1994) also report that continuous unfolded sedimentation lasted from Late Eocene through to Early Miocene in north Sabah, and that intensive compression mainly began in mid-Miocene. Seismic reflection data from the N. Borneo Trough (Hutchison, 2004; Clift et al., 2008) clearly show there was no syn-sedimentary compressional deformation below the Deep Regional Unconformity of about 16 Ma age. Therefore, the southernmost margin of SCS possibly was a passive margin during the rifting period of SCS and the wide PSCS east of WBL possibly didn’t exist either. Secondly, if its rifting was driven by a plume, triple-arm rift would have formed, but such a triple arm rift can never be found in SCS. If the PSCS slab subducting in SE direction had pulled SCS to open, normal faults and magnetic anomalies in SCS would have been preferentially oriented NE–SW, but in fact both of them were (asymmetrically) “Lazy-Z” shaped with the magnetic lineations mainly oriented EW in the wider central SCS (Fig. 6), which indicates general pull-apart direction was about N–S.

Although many authors reject the collision–extrusion hypothesis for the origin of SCS (e.g., Dewey et al., 1988; England and Molnar, 1990; Clift et al., 2008; Hall et al., 2008; Morley, 2012), this model has enjoyed wider acceptance for the last decades (e.g., Royden et al., 2008; Yin, 2009). This is possibly for one main reason: it could provide a plausible explanation of plate tectonic setting for formation of SCS, which could not be related to the *back-arc* extension (Taylor and Hayes, 1983; Tamaki and Honza, 1991). However, it contradicts facts, basic theory and physical modeling. (1) The SE extension of the Red River fault (RRF) within SW SCS, which the original version of this hypothesis (e.g., Tapponnier et al., 1982, 1990) requires, didn’t exist (e.g., Ben-Avraham and Uyeda, 1973; Taylor and Hayes, 1980, 1983; Jolivet et al., 1990; Yao et al., 1994; Lee and Lawver, 1995; Gong et al., 1997; Hall,

2002, 2012; Morley, 2002, 2012; Clift et al., 2008; Mazur et al., 2012) (Fig. 6), and RRF extended along the north side of the Yinggehai basin (Fig. 6), rather than along the south side of this basin as shown in some authors’ small-scale tectonic maps (e.g., Tapponnier et al., 1982, 1990). (2) The revised version of this hypothesis suggests that the Red River fault linked to the East Vietnam fault (EVF) and the linked mega fault had large-scale sinistral strike-slip displacements (e.g., Tapponnier et al., 1986; Jolivet et al., 1989, 1990; Briais et al., 1993; Leloup et al., 1995). However, strain pattern in the western continental margin of SCS doesn’t support this because, if SCS was a sinistral pull-apart basin with NS-striking East Vietnam fault being the principal fault, the maximum principal axes of strain ellipses in the western continental margin should have been oriented NE to ENE, which is a basic fault-mechanics theory and a basic experimental result (e.g., Corti et al., 2005; Waldron, 2005). As mentioned in Section 3.2.2, real strain pattern in this margin was compatible with dextral strike-slip deformation along EVF. The general trend of magnetic lineations in the oceanic crust actually exhibits a Lazy-Z shape (Fig. 6), rather than a Lazy-S shape characteristic of sinistral pull-apart oceanic rifting. (3) In the physical modeling on which the original conclusion–extrusion hypothesis is based (Tapponnier et al., 1982), the modeled SCS is not analogous to SCS in geometry, the modeled Indochina block, though CW-rotated, has little SSE- to S-ward translation relative to the modeled Eurasian plate and there is no analog of sinistral strike-slipping EVF (please inspect Figs. 2 and 3 of Tapponnier et al. (1982) carefully).

Almost all the previous hypothesis for origin of marginal basins of the NW Pacific are proposed under a wrong common premise that the large Eurasian plate including east Asia was rigid and remained basically stable during rifting period of the marginal basins, and so they cannot reasonably explain origin of these basins.

6. Conclusions

1. The Bohai Gulf, South China Sea, East China Sea, Japan Sea, Andaman Sea, Okhotsk Sea and Bering Sea basins have typical geometry of dextral pull-apart. Their boundary faults can be interpreted as Y-, R- and R'-faults as well as X-faults. Each of them can be explained to have originated from dextral pull apart. The Java, Makassar, Celebes and Sulu Seas basins together with grabens in Borneo, similar to the central and southern parts of the Shanxi Basin in geometry, comprise a local dextral, transtensional transform margin-type basin system. The overall configuration of the Philippine Sea resembles a typical, sinistral, transpressional “pop-up” structure in physical analog models.
2. These marginal basins except the Philippine Sea basin generally have similar (or compatible) rifting history although there do be some differences in the rifting history between the major basins or their sub-basins due to local differences in tectonic setting. Their rifting history approximately comprises three first-order stages in the Cenozoic: pre-rifting period (pre-mid Eocene), rifting period (mid-Eocene to the early Miocene) and post-rifting period (the mid-Miocene to present).
3. These marginal basins that generally have similar geometry, compatible rifting history and kinematics constitute a gigantic dextral pull-apart system along the NW Pacific margin. The proto-Philippine Sea basin including the West Philippine Basin and the proto-Parece Vela Basin was originally trapped by sinistral transpression resulting from the collision of the Australia continental block with the New Guinea arc in the mid-Eocene (or somewhat earlier). It was then reworked with widening of the Parece Vela Basin and opening of the Shikoku and Mariana basins.
4. Two lines of direct evidence that include the pull-apart amount of the South China Sea basin and JMCS basin system and the shortening deficits in the Large Tibetan Plateau, and one indirect evidence from paleomagnetic data indicate that there was 1000 to 1200 km

of absolute motion of the South China block and other blocks in east Eurasia and region around the Arctic.

5. The initial collision of the Indian plate with the Eurasian plate was about 50 Ma ago, was asynchronous along the collision belt with full collision occurring between the two continents at about 45 Ma (or some later). The uplift history of the LTP since the initial collision can be divided into two first-order stages: (1) the slower uplift stage from 50 to 15 Ma, which contains both rapid and extremely slow uplift sub-stages, and (2) the more rapid uplift stage from 15 Ma to present.
6. The Eurasian plate and the region around the Arctic underwent large, horizontal, nearly simple-shear, diffuse background deformation with maximum translation of 1200 km, and this background deformation caused the dextral pull-apart rifting of the marginal basins along the NW Pacific.
7. Based on the plate reconstructions at 50, 35, 15 and 5 Ma of the marginal basins of the NW Pacific and the Large Tibetan Plateau, rifting history of the marginal basins is closely correlated with the uplift history of the LTP. The two first-order uplift stages of the LTP correspond to the first-order rift and post-rift stages of the marginal basins, respectively.
8. The Philippine Sea basin was trapped as a sinistral transpressional pop-up structure across the Pacific and North New Guinea plates between a NW-trending spreading axis at a position that was 20° south of its present position. Then, it episodically moved northward. While the Japan arc together with the Izu–Bonin–Mariana arc migrated eastward, seafloor spreading occurred in the Shikoku and Parece Vela basins. The collision of the Caroline Ridge with the West Mariana Ridge resulted in the opening of the Mariana Basin.
9. Almost all the previous hypothesis for origin of marginal basins of the NW Pacific that are proposed within the classical plate tectonics cannot reasonably explain origin of these basins because of a wrong common premise that the Eurasian plate remained rigid and basically stable in Cenozoic.

Acknowledgments

Thanks to all the Earth scientists who study tectonics of Asia–Pacific for their great efforts. Without their basic studies, we could have done nothing in this region. Special thanks to Philip England with University of Oxford and to Bernhard Steinberger with GFZ German Research Centre for Geosciences, Potsdam.

References

- Aitchison, J.C., Ali, J.R., Davis, A.M., 2007. When and where did India and Asia collide? *J. Geophys. Res.* 112, B05423. <http://dx.doi.org/10.1029/2006JB0047>.
- Allen, M.B., MacDonald, D.I.M., Xun, Z., Vincent, S.J., Brouet, M.C., 1998. Transtensional deformation in the evolution of the Bohai Basin, northern China. In: Holdsworth, R.E., Strachan, R.A., Dewey, J.F. (Eds.), *Continental Transpressional and Transtensional Tectonics*. Geological Society, London, Special Publications, 135, pp. 215–229.
- Ali, J.R., Hall, R., 1995. Evolution of the boundary between the Philippine Sea Plate and Australia: palaeomagnetic evidence from eastern Indonesia. *Tectonophysics* 251, 251–275.
- Anderson, D.L., 2004. Simple scaling relations in geodynamics: the role of pressure in mantle convection and plume formation. *China Sci. Bull.* 4, 2017–2021.
- Barckhausen, U., Roeser, H.A., 2004. Seafloor spreading anomalies in the South China Sea revisited. In: Clift, P., Hayes, D.E. (Eds.), *Continent–Ocean Interactions in the East Asian Marginal Seas*. AGU Geophysical Monograph, 149, pp. 23–35.
- Basile, C., Brun, J.P., 1999. Transtensional faulting patterns ranging from pull-apart basins to transform continental margin: an experimental investigation. *J. Struct. Geol.* 21, 23–37.
- Baranov, B.V., Seliverstov, N.I., Murav'ev, A.V., Muzurov, E.L., 1991. The Komandorsky Basin as a product of spreading behind a transform plate boundary. *Tectonophysics* 199, 237–269.
- Baranov, B.V., Werner, R., Hoernle, K.A., Tsoy, I.B., van den Bogaard, P., Tararin, I.A., 2002. Evidence for compressional induced high subsidence rates in the Kurile Basin (Okhotsk Sea). *Tectonophysics* 350, 63–97.
- Bartlett, W.L., Friedman, M., Logan, J.M., 1981. Experimental folding and faulting of rocks under confining pressure. *Tectonophysics* 79, 255–277.
- Ben-Avraham, Z., 1978. The evolution of marginal basins and adjacent shelves in east and SE Asia. *Tectonophysics* 45, 269–288.
- Ben-Avraham, Z., 1989. Multiple opening and closing of the eastern Mediterranean and south China basins. *Tectonics* 8, 351–362.
- Ben-Avraham, Z., Emery, K.O., 1973. Structural framework of Sunda Shelf. *AAPG Bull.* 57, 2323–2366.
- Ben-Avraham, Z., Uyeda, S., 1973. The evolution of the China Basin and the Mesozoic Paleogeography of Borneo. *Earth Planet. Sci. Lett.* 18, 365–376.
- Ben-Avraham, Z., Bowin, C.O., Segawa, J., 1972. An extinct spreading centre in the Philippine Sea. *Nature* 250, 453–455.
- Ben-Avraham, Z., Cooper, A.K., 1981. Early evolution of the Bering Sea by collision of ocean rises and North Pacific subduction zone. *Geol. Soc. Am. Bull.* 91, 486–495.
- Ben-Avraham, Z., Zoback, M.D., 1992. Transform-normal extension and asymmetric basins: an alternative to pull-apart models. *Geology* 20, 423–426.
- Bersenev, I.I., Bezverchny, V.L., Lelikov E.P., Pushchin, I.K., Sedin, V.T., 1988. Geological map of the Japan Sea (1:5, 000, 000). Academy of Sciences of the USSR.
- Besse, J., Courtillot, V., 1991. Revised and synthetic apparent polar wander paths of the African, Eurasian, North American and Indian Plates, and true polar wander since 200 Ma. *J. Geophys. Res.* 96, 4029–4050.
- Besse, J., Courtillot, V., 2002. Apparent and true polar wander and the geometry of the geomagnetic field over the last 200 Myr. *J. Geophys. Res.* 107. <http://dx.doi.org/10.1029/2000JB000050>.
- Blisniuk, P.M., Hacker, B.R., Glodny, J., Ratschbacher, L., Bi, S., Wu, Z., McWilliams, M.O., Calvert, A., 2001. Normal faulting in central Tibet since at least 13.5 Myr ago. *Nature* 412, 628–632.
- Bour, O., 1994. Numerical modeling of abnormal fluid pressure in Naverina Basin, Bering Sea. *Mar. Pet. Geol.* 11, 425–440.
- Briaux, A., Partriat, P., Tapponnier, P., 1993. Updated interpretation of magnetic anomalies and seafloor spreading stages in the South China Sea: implications for the Tertiary tectonics of SE Asia. *J. Geophys. Res.* 98, 6299–6328.
- Burchfiel, B., Steward, H., 1966. "Pull-apart" origin of the central segment of Death Valley, California. *Geol. Soc. Am. Bull.* 77, 439–442.
- Charlton, T.R., 1986. A plate model of the eastern Indonesia collision zone. *Nature* 319, 394–396.
- Chen, J., Huang, B., Sun, L., 2010a. New constraints to the onset of the India–Asia collision: paleomagnetic reconnaissance on the Linzong Group in the Lhasa Block, China. *Tectonophysics* 489, 189–209.
- Chen, J., Gao, D., We, N., Wan, R., 2010b. Characteristics of the geomagnetic fields in the South China Sea. *Prog. Geophys.* 25, 376–388.
- Chung, S., Lo, C.H., Lee, T.Y., Zhang, Y., Xie, Y., Li, X., Wang, K.-L., Wang, P.-L., 1998. Diachronous uplift of the Tibetan plateau starting 40 Myr ago. *Nature* 394, 769–773.
- Clift, P., Lee, G., Duc, D.A., Barckhausen, U., Long, H.A., Zhen, S., 2008. Seismic reflection evidence for a Dangerous Grounds miniplate China: no extrusion origin for the South China Sea. *Tectonics* 27, TC3008. <http://dx.doi.org/10.1029/2007TC002216>.
- Clift, P., Lin, J.F., 2001. Preferential mantle lithospheric extension under the South China margin. *Mar. Pet. Geol.* 18, 929–945.
- Clift, P., Carter, A., Krol, M., Kirby, E., 2002. Constraints on India–Eurasia collision in the Arabian sea region taken from the Indus Group, Ladakh Himalaya, India. In: Clift, P., Kroon, D., Gaedicke, C., Craig, J. (Eds.), *The tectonic and climatic evolution of the Arabian Sea region*. Geological Society, London, Special Publication, 195, pp. 97–116.
- Clyde, W.C., Bowen, G.J., Ting, S., Koch, P.L., Wang, Y., Wang, Y., 2003. Paleomagnetism of the Paleogene Lingcha Formation, Hengyang Basin, Hunan Province (China): Implications for chronostratigraphic correlation and Asian block rotations. Unpublished data, University of New Hampshire.
- Cogne, J.P., Halim, N., Chen, Y., Courtillot, V., 1999. Resolving the problem of the shallow magnetizations of Tertiary age in Asia: insights from paleomagnetic data from the Qiantang, Kunlun, and Qaidam blocks (Tibet, China), and a new hypothesis. *J. Geophys. Res.* 104 (17), 1715–1734.
- Cogne, J.P., Besse, J., Chen, Y., Hankard, F., 2013. A new Late Cretaceous to present APWP for Asia and its implications for paleomagnetic shallow inclinations in Central Asia and Cenozoic Eurasian plate deformation. *Geophys. J. Int.* 192, 1000–1024.
- Coleman, M., Hodges, K., 1995. Evidence for Tibetan Plateau uplift before 14 my ago from a minimum age for east–west extension. *Nature* 374, 48–52.
- Copley, A., Avouac, J.-P., Royer, J.-Y., 2010. India–Asia collision and the Cenozoic slowdown of the Indian plate: Implications for the forces driving plate motions. *J. Geophys. Res.* 115, B03410. <http://dx.doi.org/10.1029/2009JB006634>.
- Cooper, A.K., Scholl, D.W., Marlow, M.S., 1976a. Plate tectonic model for the evolution of the Eastern Bering Sea Basin. *Geol. Soc. Am. Bull.* 87, 1119–1126.
- Cooper, A.K., Marlow, M.S., Scholl, D.W., 1976b. Mesozoic magnetic lineations in the Bering Sea marginal basin. *J. Geophys. Res.* 81, 1916–1943.
- Corti, G., Bonini, M., Conticelli, S., Innocenti, F., Manetti, P., Sokoutis, D., 2003. Analogue modelling of continental extension: a review focused on the relations between the patterns of deformation and the presence of magma. *Earth Sci. Rev.* 63, 169–247.
- Corti, G., Moratti, G., Sani, F., 2005. Relations between surface faulting and granite intrusions in analogue models of strike-slip deformation. *J. Struct. Geol.* 27, 1547–1562.
- Cox, A., Hart, B.R., 1986. Plate tectonics: how it works. Blackwell Science Publication (400 pp.).
- Creager, J.S., Scholl, D.W., Supko, P.R., et al. (Eds.), 1973. Initial Report of the Deep Sea Drilling Project, vol. 19. U.S. Government Printing Office, Washington, D.C.
- Cukur, D., Horozal, S., Kim, D.C., Han, H.C., 2011. Seismic stratigraphy and structural analysis of the northern East China Sea Shelf Basin interpreted from multi-channel seismic reflection data and cross-section restoration. *Mar. Pet. Geol.* 28, 1003–1022.
- Curry, R., 2005. Tectonics and history of the Andaman sea region. *J. Asian Earth Sci.* 25, 187–232.
- Curry, R., Moore, D.G., Lawver, L.A., Emmel, F.J., Raitt, R.W., Henry, M., Kieckhefer, R., 1979. Tectonics of the Andaman Sea and Burma. In: Watkins, J., Montadert, L., Dickerson, P.W. (Eds.), *Geological and Geophysical Investigations of Continental Margins*. AAPG Memoir, 29, pp. 189–198.

- Dai, S., Fang, X., Song, C., Gao, J., Gao, D., Li, J., 2005. Early tectonic uplift of the northern Tibetan Plateau. *Chin. Sci. Bull.* 50, 1642–1652.
- Davis, A.S., Gray, L.B., Clague, D.A., Hein, J.R., 2002. The Line Islands revisited: new $^{40}\text{Ar}/^{39}\text{Ar}$ geochronologic evidence for episodes of volcanism due to lithospheric extension. *Geochem. Geophys. Geosyst.* 3, 1–28.
- DeMets, C., Gordon, R.G., Argus, D.F., Stein, S., 1994. Effect of recent revisions to the geomagnetic reversal time scale on estimates of current plate motions. *Geophys. Res. Lett.* 21, 2191–2194.
- DeMets, C., Gordon, R.G., Argus, D.F., 2010. Geologically current plate motions. *Geophys. J. Int.* 181, 1–80.
- Deschamps, A., Lallemand, S., 2002. The West Philippine Basin: an Eocene to Early Oligocene back-arc basin opened between two opposed subduction zones. *J. Geophys. Res.* 107, 1–24.
- Deschamps, A., Okino, K., Fujioka, K., 2002. Late magmatic extension along the central and eastern segments of the West Philippine Basin fossil spreading axis. *Earth Planet. Sci. Lett.* 203, 277–293.
- Dooley, T., McClay, K.R., 1997. Analog modeling of pull-apart basins. *AAPG Bulletin* 81, 1804–1826.
- Dewey, J.F., 1980. Episodicity, sequence, style at convergent plate boundaries. In: Strangway, D.W. (Ed.), *The continental crust and its mineral deposits*. Geological Association of Canada Special Paper, 20, pp. 552–573.
- Dewey, J.F., Burke, 1973. Tibetan, Variscan and Precambrian basement reactivation: products of continental collision. *J. Geol.* 81, 683–692.
- Dewey, J.F., Shackleton, R.M., Chang, C., Sun, Y., 1988. The tectonic evolution of the Tibetan plateau. *Phil. Trans. Roy. Soc. London A* 327, 379–413.
- Dewey, J.F., Cande, S., Pitman, W.C., 1989. Tectonic evolution of the India/Eurasia collision zone. *Ecolage Geol. Helv.* 82, 717–734.
- Dupont-Nivet, G., Hoom, C., Konert, M., 2008. Tibetan uplift prior to the Eocene–Oligocene climate transition: evidence from pollen analysis of the Xining Basin. *Geology* 36, 987–990.
- Dupont-Nivet, G., van Hinsbergen, D.J.J., Torsvik, T.H., 2010. Persistently low Asian paleolatitudes: implications for the India–Asia collision history. *Tectonics* 29, TC5016. <http://dx.doi.org/10.1029/2008TC002437>.
- England, P., Houseman, G., 1986. Finite strain calculations of continental deformation 2. Comparison with the India–Asia collision zone. *J. Geophys. Res.* 91, 3664–3676.
- England, P.C., McKenzie, D.P., 1982. A thin viscous sheet model for continental deformation. *Geophys. J. R. Astron. Soc.* 70, 295–321.
- England, P., Molnar, P., 1990. Right-lateral shear and rotation as the explanation of strike-slip faulting in eastern Tibet. *Nature* 344, 140–142.
- England, P., Molnar, P., 1997. The field of crustal velocity in Asia calculated from Quaternary slip rates on faults. *Geophys. J. Int.* 130, 551–582.
- England, P., Searle, M., 1986. The Cretaceous–Tertiary deformation of the Lhasa Block and its implications for crust thickening in Tibet. *Tectonics* 5, 1–14.
- Fabri, O., Charvet, J., Fournier, M., 1996. Alternate senses of displacement along the Tsushima fault system during the Neogene based on fracture analyses near the western margin of the Japan Sea. *Tectonophysics* 257, 275–295.
- Faccenna, C., Becker, T.W., Lallemand, S., Steinberger, B., 2012. On the role of slab pull in the Cenozoic motion of the Pacific plate. *Geophys. Res. Lett.* 39, L03305. <http://dx.doi.org/10.1029/2011GL050155>.
- Fang, Y., Zhou, F., 1998. Characteristics of stripped magnetic anomalies in the central sea basin of South China Sea. *Geophys. Geochem. Explor.* 22, 272–278 (in Chinese with English abstracts).
- Favela, J., Anderson, D.L., 1999. Extensional tectonics and global volcanism. In: Boschi, E., Ekstrom, G., Morelli, A. (Eds.), *Problems in Geophysics for the New Millennium*, Conference Proceedings, Erice, Italy, pp. 463–498.
- Fielding, E., 1996. Tibet uplift and erosion. *Tectonophysics* 260, 55–84.
- Filatova, N.I., 2004. Cenozoic extension structures in the continental framework of the Japan Sea. *Geotectonica* 38, 459–477.
- Fisher, M.A., William Jr., W., Holmes, M.L., 1982. Geology of Norton Basin and continental shelf beneath northwestern Bering Sea. *APPG Bull.* 66, 255–285.
- Foulger, R.G., 2007. The “Plate” model for the genesis of melting anomalies. In: Foulger, G.R., Jurdy, D.M. (Eds.), *Plates, Plumes, and Planetary Processes*. Geological Society of America Special Paper, 430, pp. 1–28.
- Foulger, G.R., Jurdy, D.M. (Eds.), 2007. *Plates, Plumes, and Planetary Processes*. Geological Society America, Special Paper, 430 (998 + x pp.).
- Foulger, G.R., Natland, J.H., 2003. Is “hotspot” volcanism a consequence of plate tectonics. *Science* 300, 921–922.
- Fournier, M., Jolivet, L., Davey, P., Thomas, J.-C., 2004. Backarc extension and collision: an experimental approach to the tectonics of Asia. *Geophys. J. Int.* 157, 871–889.
- Fujioka, K., Okino, K., Kanamatsu, T., Ohara, Y., Ishisuka, O., Haraguchi, S., Ishii, T., 1999. Enigmatic extinct spreading center in the West Philippine back-arc basin unveiled. *Geology* 27, 1135–1138.
- Fujita, H., 1987. Mobile belts of Asia (Chinese translation from Japanese). Ocean Bureau Publishing House, Beijing, China (230 pp.).
- Fyhn, M.B.W., Boldreel, L.O., Nielsen, L.H., 2009. Geological development of the Central and South Vietnamese margin: implications for the establishment of the South China Sea, Indochinese escape tectonics and Cenozoic volcanism. *Tectonophysics* 478, 184–214.
- Gaina, C., Müller, D., 2007. Cenozoic tectonic and depth age evolution of the Indonesian gateway and associated back-arc basins. *Earth Sci. Rev.* 83, 177–203.
- Garzanti, E., 2008. Comment on “When and where did India and Asia collide?” by Jonathan C. Aitchison, Jason R. Ali and Aileen M. Davis. *J. Geophys. Res.* 113, B04411. <http://dx.doi.org/10.1029/2007JB005276>.
- Gilder, S.A., Zhao, X., Coe, R.S., Meng, Z., Courtillot, V., Besse, J., 1996. Paleomagnetism and tectonics of the southern Tarim basin of Northwestern China. *J. Geophys. Res.* 101, 22,015–22,031.
- Gnibidenko, H.S., Hilde, T.W.C., Gretskeya, E.V., Andreev, A.A., 1995. Kurile (South Okhotsk) back-arc basin. In: Taylor, B. (Ed.), *Back-Arc Basins: Tectonics and Magmatism*. Plenum, New York, pp. 421–449.
- Glatzmaier, G.A., Schubert, G., Bercovici, D., 1990. Chaotic, subduction-like downflows in a spherical model of convection in the Earth's mantle. *Nature* 47, 274–277.
- Gong, Z.S., Li, S., Xie, T., et al. (Eds.), 1997. *Continental Margin Basin Analysis and Hydrocarbon Accumulation of the northern South China Sea*. Science Press, Beijing, China (Chinese with English abstract, 510 pp.).
- Gordon, R.G., DeMets, C., Royer, J.-Y., 1998. Evidence for long-term diffuse deformation of the lithosphere of the equatorial Indian Ocean. *Nature* 395, 370–374.
- Gordon, R.G., 1998. The plate tectonic approximation: Plate nonrigidity, diffuse plate boundaries, and global plate reconstructions. *Annu. Rev. Earth Planet. Sci.* 26, 615–642.
- Green, O.R., Searle, M.P., Corfield, R.I., Corfield, R.M., 2008. Cretaceous–Tertiary Carbonate Platform Evolution and the Age of the India–Asia Collision along the Ladakh Himalaya (Northwest India). *J. Geol.* 116, 331–353.
- Halim, N., Conge, J.P., Chen, Y., Ataie, R., Courtillot, V., Maroux, J., Zhao, R.L., 1998. New Cretaceous and Early Tertiary paleomagnetic results from Xining–Lanzhou basin, Kunlun and Qiantang blocks China: implications for the geodynamic evolution of Asia. *J. Geophys. Res.* 103, 21,023–21,045.
- Hall, R., 2002. Cenozoic geological and plate tectonic evolution of SE Asia and the SW Pacific: computer-based reconstructions model and animations. *J. Asian Earth Sci.* 20, 354–431.
- Hall, R., 2012. Late Jurassic–Cenozoic reconstructions of the Indonesian region and the Indian Ocean. *Tectonophysics* 570–571, 1–41.
- Hall, R., Fuller, M., Ali, J.R., Anderson, C.D., 1995. The Philippine Sea Plate: magnetism and reconstructions. In: Taylor, B., Natland, J. (Eds.), *Active margins and marginal basins of the western Pacific*. AGU Geophysical Monograph, 88, pp. 371–404.
- Hall, R., van Hattum, M.W.A., Spakman, W., 2008. Impact of India–Asia collision on SE Asia: the record in Borneo. *Tectonophysics* 451, 366–389.
- Handiyani, L., 2004. Seismic tomography constraints on reconstructing the Philippine Sea Plate and its margin. (Ph.D. Assertion) Texas A&M University (133 pp.).
- Hankard, F., Cogné, J.P., Kravchinsky, V., Carporzen, L., Bayasgalan, A., Lkhagvadorj, P., 2007. New Tertiary paleomagnetic poles from Mongolia and Siberia at 40, 30, 20, and 13 Ma: clues on the inclination shallowing problem in central Asia. *J. Geophys. Res.* 112 (B02), 101. <http://dx.doi.org/10.1029/2006JB004488>.
- Harding, T.P., 1985. Seismic characteristics and identification of negative flower structures, positive flower structures and positive inversion. *AAPG Bull.* 69, 582–599.
- Harrison, T.M., Copeland, P., Kidd, W.S.F., Yin, A., 1992. Raising Tibet. *Science* 255, 1663–1670.
- Haston, R.B., Fuller, M., 1991. Paleomagnetic data from the Philippine Sea Plate and their significance. *J. Geophys. Res.* 96, 6073–6098.
- Hartono, H.M.S., 1990. Late Cenozoic tectonic development of the Southeast Asian continental margin of the Banda Sea area. *Tectonophysics* 181, 267–276.
- Hayes, D.E., Nissen, S.S., Buhl, P., Diebol, J., Yao, B., Zeng, W., Chen, Y., 1995. Through going crustal faults along the northern margin of the South China Sea and their role in crustal extension. *J. Geophys. Res.* 100, 22435–22446.
- Hegarty, K.A., Weisell, J.K., Hayes, D.E., 1983. Convergence at the Caroline–Pacific Plate boundary: collision and subduction. In: Hayes, D.E. (Ed.), *The Tectonic and Geologic Evolution of Southeast Asian Seas and Islands (Part 2)*. AUG Geophysical Monograph, 27, pp. 326–348.
- Hegarty, K.A., Weisell, J.K., 1988. Complexities in the development of the Caroline Plate region, western equatorial Pacific. In: Nairn, A.E.M., Stehli, F.G., Uyeda, S. (Eds.), *The Pacific Ocean, The Ocean Basins and Margins*, 7B. Plenum Press, New York, pp. 277–301.
- Heflin, M.B., Bar-Sever, Y.E., Jefferson, D.C., et al., 2004. JPL IGS Analysis Center Report, 2001–2003. International GPS Service Technical Reports.
- Henderson, A.L., Najman, Y., Parrish, R., Mark, D.F., Foster, G.L., 2011. Constraints to the timing of India–Eurasia collision: a re-evaluation of evidence from the Indus Basin sedimentary rocks of the Indus–Tsangpo Suture Zone, Ladakh, India. *Earth Sci. Rev.* 106, 265–292.
- Hetényi, G., Cattin, R., Brunet, F., Bollinger, L., Vergne, B., Nábělek, J.L., Diament, M., 2007. Density distribution of the India plate beneath the Tibetan plateau: geophysical and petrological constraints on the kinetics of lower-crustal eclogitization. *Earth Planet. Sci. Lett.* 264, 226–244.
- Heuret, A., Lallemand, S., 2005. Plate motions, slab dynamics and back-arc deformation. *Phys. Earth Planet. Inter.* 149, 31–51.
- Hilde, T.W.C., Uyeda, S., Kroenke, L., 1977. Evolution of the western Pacific and its margin. *Tectonophysics* 38, 145–165.
- Hilde, T.W.C., Lee, C.S., 1984. Origin and evolution of the West Philippine Basin: a new interpretation. *Tectonophysics* 102, 85–104.
- Hinschberger, F., Malod, J.-A., Rehault, J.-P., Villeneuve, M., Royer, J.-Y., Burhanuddin, S., 2005. Late Cenozoic geodynamic evolution of eastern Indonesia. *Tectonophysics* 404, 91–118.
- Hou, G., Qian, X., 1998. The Origin of the Bohai Bay Basin. *J. Peking Univ.* 34, 503–509 (natural science edition).
- Hsu, S.-K., Sibuet, J.C., Shyu, C.-T., 2001. Magnetic inversion in the East China Sea and Okinawa Trough: tectonic implication. *Tectonophysics* 333, 111–122.
- Hsu, S.-K., Yeh, Y., Doo, W.-B., Tsai, C.-H., 2004. New bathymetry and magnetic lineations identifications in the northernmost South China Sea and their tectonic implications. *Mar. Geophys. Res.* 25, 29–44.
- Hsu, Y., Shibuya, H., Merrill, D.L., 1991. Paleomagnetic study of deep-sea sediments from the Cagayan Ridge in the Sulu Sea: results of Leg 124. In: Silver, E.A., Rangin, C., von Breyman, M.T., et al. (Eds.), *Proceedings of the Ocean Drilling Program*. Scientific Results, 124, pp. 511–518.
- Hu, C.Y., 1982. A new insight of formation and oil distribution of Bohai Gulf Basin. *Oil Exp. Geol.* 4, 161–167 (Chinese with English abstracts).

- Huang, K., Opdyke, N., 1992. Paleomagnetism of Cretaceous to lower Tertiary rocks from Southwestern Sichuan: A revisit. *Earth Planet. Sci. Lett.* 12, 29–40.
- Huang, S.T., Ting, H.H., Chen, R.C., Chi, W.R., Hu, C.C., Shen, H.-C., 1992. Basinal framework and tectonic evolution of offshore northern Taiwan. *Pet. Geol. Taiwan* 27, 47–72.
- Huchon, P., Nguyen, T.N.H., Chamot-Rooke, N., 1998. Finite extension across the South Vietnam basins from 3D gravimetric modeling: relation to South China Sea kinematics. *Mar. Pet. Geol.* 15, 619–634.
- Hutchison, C.S., 1989. Geological evolution of South-East Asia. *Oxf. Monogr. Geol. Geophys.* 13, 367.
- Hutchison, C.S., 1996. The “Rajiang accretionary prism” and “Lupar Line” problem of Borneo. In: Hall, R., Blundell, D.J.B. (Eds.), *Tectonic evolution of SE Asia*. Geological Society, London, Special Publications, 106, pp. 247–262.
- Hutchison, C.S., 2004. Marginal basin evolution the southern South China Sea. *Mar. Pet. Geol.* 21, 1129–1148.
- Hutchison, C.S., 2010. The north-west Borneo trough. *Mar. Geol.* 271, 32–43.
- Irving, E., Baker, J., Wynne, P.J., Hamilton, T.S., Wingate, M.T.D., 2000. Evolution of the Queen Charlotte Basin; further paleomagnetic evidence of Tertiary extension and tilting. *Tectonophysics* 326, 1–22.
- Isezaki, N., 1986. A geomagnetic anomaly map of the Japan Sea. *J. Geomagn. Geoelectr.* 38, 403–410.
- Isezaki, N., Shevaldin, Y.V., Ya, Karp B., 1996. Geomagnetic anomalies and of the Japan Sea. In: Isezaki, N., Bersenev, I.I., Tamaki, K., Lelikov, E.P. (Eds.), *Geology and Geophysics of the Japan Sea*. Terra Scientific Publishing Company, Tokyo, Japan, pp. 41–47.
- Jaeger, J.J., Courtillot, V., Tapponnier, P., 1989. Paleontological view of the age of the Deccan Trap, Cretaceous/Tertiary boundary and the India–Asia collision. *Geology* 17, 316–319.
- Jin, Z., Xu, S., Li, Q., 2004. Development and palaeomagnetism of the seamounts in the sub-basin of South China Sea. *Acta Oceanica Sinica* 26, 83–93.
- Johnson, M.R.W., 2002. Shortening budgets and the role of continental subduction during the India–Asia collision. *Earth Sci. Rev.* 59, 101–123.
- Jolivet, L., Huchon, P., Rangin, C., 1989. Tectonic setting of Western Pacific marginal basins. *Tectonophysics* 160, 23–47.
- Jolivet, L., Davy, P., Cobbold, P., 1990. Right-lateral shear along the NW Pacific margin and the India–Eurasia collision. *Tectonics* 9, 1409–1419.
- Jolivet, L., Huchon, P., Brun, J.P., Chamot-Rooke, N., Le Pichon, X., Thomas, J.C., 1991. Arc deformation and marginal basin opening: Japan Sea as a case study. *J. Geophys. Res.* 96, 4367–4384.
- Jolivet, L., Tamaki, K., Fournier, M., 1994. Japan Sea, opening history and mechanism: a synthesis. *J. Geophys. Res.* 99 (22), 237–22259.
- Kapp, P., Guynn, J.H., 2004. Indian punch rifts Tibet. *Geology* 11, 993–996.
- Kapp, P., Yin, A., Harrison, T.M., Ding, T., 2005. Cretaceous–Tertiary shortening, basin development, and volcanism in central Tibet. *Geol. Soc. Am. Bull.* 117, 865–878.
- Kaneoka, I., Takigami, Y., Takaoka, N., Yamashita, S., Tamaki, K., 1992. ^{40}Ar – ^{39}Ar analysis of volcanic rocks recovered from the Japan Sea floor: onstraints on the age of formation of Japan Sea. In: Tamaki, K., Suyehiro, K., Allan, J., et al. (Eds.), *Proceedings of the Ocean Drilling Program, Scientific Results*, 127/128, pp. 819–836.
- Kaneoka, I., Takaoka, N., Miyashita, S., Tokuyama, H., 1994. ^{40}Ar – ^{39}Ar analyses of volcanic rocks recovered from the Okushiri Ridge in the Japan Sea. *Geochem. J.* 28, 1–9.
- Karig, D.E., 1971. Origin and development of marginal basins in western Pacific. *J. Geophys. Res.* 76, 2542–2561.
- Karig, D.E., Ingle, J.C., Boumar, A.H., et al. (Eds.), 1975. *Initial Report of the Deep Sea Drilling Project*, vol. 31. U.S. Government Printing Office, Washington, D.C. <http://dx.doi.org/10.2973/dsdp.proc.31.1975>.
- Karp, B.Y., Hirata, N., Katao, H., 1996. Crustal structure of the Japan Sea. In: Isezaki, N., Bersenev, I.I., Tamaki, K., Ya, Karp B., Lelikov, E.P. (Eds.), *Geology and Geophysics of the Japan Sea*. Terra Scientific Publishing Company, Tokyo, Japan, pp. 75–90.
- Kirby, E., Reiners, P.W., Krol, M.A., Whipple, K.X., Hodges, K.V., Farley, K.A., Tang, W., Chen, Z., 2002. Late Cenozoic evolution of the eastern margin of the Tibetan Plateau: inferences from $^{40}\text{Ar}/^{39}\text{Ar}$ and (U–Th)/He thermochronology. *Tectonics* 21. <http://dx.doi.org/10.1029/2000TC001246>.
- Khan, P.K., Chakraborty, P.P., 2005. Two-phase opening of Andaman Sea: a new seismotectonic insight. *Earth Planet. Sci. Lett.* 229, 259–271.
- Khan, S.D., Walker, D.J., Hall, S.A., Burke, K.C., Shah, M.T., Stöckli, L., 2009. Did the Kohistan–Ladakh island arc collide with India? *Geol. Soc. Am. Bull.* 121, 366–384.
- Kimura, M., 1985. Back-arc rifting in the Okinawa Trough. *Mar. Pet. Geol.* 2, 222–240.
- Kimura, G., Tamaki, K., 1986. Collision, rotation and back-arc spreading of the Okhotsk and Japan Sea. *Tectonics* 5, 389–401.
- Kirillova, G.L., 1988. Breaks and unconformities in section of the ocean floor of the Philippine Sea and adjoining islands. *Pac. Geol.* 6, 26–35.
- Kirillova, G.L., 1993. Types of Cenozoic sedimentary basins of the East Asia and Pacific Ocean junction area. *Palaeogeogr. Palaeoclimatol. Palaeoecol.* 105, 17–32.
- Kong, F., Lawver, L.A., Lee, T.-Y., 2000. Evolution of the southern Taiwan \pm Sinzi Folded Zone and opening of the southern Okinawa trough. *J. Asian Earth Sci.* 18, 325–341.
- Kosygin, Y.A., Zhuravlev, A.V., Sergeev, K.F., Tuyeov, I.K., Tyutrin, I.I., Khvedchuk, I.I., 1985. Geological structure of the young platform of the Sea of Okhotsk. *Int. Geol. Rev.* 27, 1407–1414.
- Koyama, M., 1991. Tectonic evolution of the Philippine Sea Plate based on paleomagnetic results. *J. Geogr.* 100, 628–641 (in Japanese with English abstracts).
- Kronenberg, A., Brandon, M.T., Fletcher, R., Karlstrom, K., Rushmer, T., Simpson, C., Yin, A., 2002. Beyond plate tectonics: rheology and orogenesis of the continents. in: new departures in structural geology and tectonics. *New Departures in Structural Geology and Tectonics*. Stanford University, pp. 13–21 (<http://www.pangea.stanford.edu/~dpollard/NSF/>).
- Kronenk, L., Scott, R., Balshaw, K., et al., 1978. *Deep sea drilling project initial reports*, vol. 59. U.S. Government Printing Office, Washington, D.C.
- Kulinich, R.G., Obzhairov, A.I., 1985. The structure and modern activity of the Sunda Shelf and South China Sea junction zone. *Pac. Geol.* 3, 102–106.
- Kudrass, H.R., Muller, P., Kreuzer, H., Weiss, W., 1990. Volcanic rocks and tertiary carbonates dredged from the Cagayan Ridge and the SW Sulu Sea, Philippines. In: Rangin, C., Silver, E.A., von Breyman, M.T., et al. (Eds.), 124, 93–100.
- Lallemant, S.A., Heuret, A., Boutelier, D., 2005. On the relationships between slab dip, back-arc stress, upper plate absolute motion, and crustal nature in subduction zones. *Geochem. Geophys. Geosyst.* 6, Q09006. <http://dx.doi.org/10.1029/2005GC000917>.
- Lallemant, S., Jolivet, L., 1985. Japan Sea: a pull-apart basin? *Earth Planet. Sci. Lett.* 76, 375–389.
- Lane, L.S., 1998. Latest Cretaceous–Tertiary tectonic evolution of Northern Yukon and adjacent Arctic Alaska. *AAPG Bull.* 82, 1353–1371.
- Langseth, M.G., Hobart, M.A., Horai, K.-I., 1980. Heat flow in the Bering Sea. *J. Geophys. Res.* 85, 3740–3750.
- Larson, K.M., Mueller, J.F., Philippsen, S., 1997. Global plate velocities from the Global Positioning System. *J. Geophys. Res.* 102, 9961–9981.
- Le Pichon, X., Fournier, M., Jolivet, J., 1992. Kinematics, topography, shortening and extrusion in the India–Asia collision. *Tectonics* 11, 1085–1098.
- Le Pichon, X., Henry, P., Goffé, B., 1997. Uplift of Tibet: from eclogites to granulites. *Tectonophysics* 273, 57–76.
- Lee, C.S., McCabe, R., 1986. The Banda–Celebes–Sulu Basins: a trapped piece of Cretaceous–Eocene oceanic crust? *Nature* 322, 51–54.
- Lee, T.-Y., Lawver, L.A., 1995. Cenozoic plate reconstructions of SE Asia. *Tectonophysics* 251, 85–138.
- Leech, M.L., Singh, T.S., Jain, A.K., Klemperer, S.L., Manickavasagam, R.M., 2005. The onset of India–Asia continental collision: Early, steep subduction required by the timing of UHP metamorphism in the western Himalaya. *Earth Planet. Sci. Lett.* 234, 83–97.
- Leg 127 and Leg 128 shipboard scientific parties, 1990. *Evolution of the Japan Sea*. *Nature* 346, 18–20.
- Leloup, P.H., Lacassin, R., Tapponnier, P., Schärer, U., Zhong, D., Liu, X., Zhang, L., Ji, S., Trihn, P.H., 1995. The Ailao Shan–Red River shear zone (Yunnan, China), Tertiary transform boundary of Indochina. *Tectonophysics* 251, 3–84.
- Letouzey, J., Kimura, M., 1986. The Okinawa Trough: genesis of a back-arc basin developing along a continental margin. *Tectonophysics* 125, 209–230.
- Lewis, S.D., 1991. Geophysical setting of the Sulu and Celebes Seas. In: Silver, E.A., Rangin, C., von Breyman, M.T., et al. (Eds.), *Proceedings of the Ocean Drilling Program, Scientific Results*, 124, pp. 65–73.
- Lewis, S.D., Hayes, D.E., 1980. The structure and evolution of the Central Basin Fault, West Philippine Sea. In: Hayes, D.E. (Ed.), *The Evolution of SE Asia Seas and Islands*. AGU Geophysical Monograph, 23, pp. 77–88.
- Lewis, J.C., Byrne, T.B., Tang, X., 2002. A geologic test of the Kula–Pacific Ridge capture mechanism for the formation of the West Philippine Basin. *Geol. Soc. Am. Bull.* 114, 656–664.
- Li, C.-F., Zhou, Z., Li, J., Hao, H., Geng, J., 2007. Structures of the northeasternmost South China Sea continental margin and ocean basin: geophysical constraints and tectonic implications. *Mar. Geophys. Res.* 28, 59–79.
- Li, D.S., 1980. Structural geological features and oilfield distribution in Bohai Gulf Basin. *Acta Pet. Sin.* 1, 6–16 (Chinese with English abstracts).
- Li, P., Wang, W., Liang, H., Huo, Y., 1988. On the studies of the tectonic evolution of the Zhujiangkou basin and South China Sea. *Reports on Petroleum Geology of the (eastern) Zhujiang Kou Basin*, 2, pp. 652–685 (in Chinese).
- Li, S., Yang, S., Xie, X., 1997a. Tectonic evolution of Tertiary basins in Circum-Pacific belt of China and their geodynamic setting. *J. China Univ. Geosci.* 8, 4–10.
- Li, S., Lin, C., Zhang, Q., Yang, S., Wu, P., 1999. Episodic rifting of continental marginal basins and tectonic events since 10 Ma in the South China Sea. *Chin. Sci. Bull.* 44, 10–23.
- Li, S., Lu, F., Lin, C., 1997b. Evolution of Mesozoic and Cenozoic basins in Eastern China and its environ and their geodynamic background (Chinese). China University of Geosciences Press, Wuhan, China (239 pp.).
- Li, T., 1995. The uplifting process and mechanism of the Qinhai–Tibet Plateau. *Bull. Chin. Acad. Geol. Sci.* 16, 331–335 (Chinese with English abstracts).
- Liu, S.S., Chen, J., Pang, Y., 1990. Approach to origin and evolution of South China Sea. In: Li, J.L. (Ed.), *Studies of Tectonics and Evolution of Lithosphere of Southeast China Continent and Sea Region*. China Science and Technology Press, Beijing (Chinese).
- Li, Z., Qiu, Z., Qin, S., 1991. A study on the forming conditions of basalts in the sea mounts of South China Sea. *Acta Mineral. Sin.* 11 (4), 328–336 (in Chinese with English abstracts).
- Li, S., Yang, J., 1997. Discussion on the background of geodynamics in the formation of South China Sea and its marginal sub-basins. In: Gong, Z., Li, S., Xie, T., et al. (Eds.), *Basin Analysis of the Northern Continental Margin of South China Sea and Its Oil and Gas Accumulation*. Science Press, Beijing, China, pp. 122–126 (Chinese with English abstract).
- Liang, L., Pu, Q., Liang, R., He, J., 1997. Geological frame work and closure structure of the Xihu Sag in the East China Sea. *Offshore Oil* 3, 1–6 (in Chinese with English abstracts).
- Liu, H.L., 1999. On extension–contraction-type dextral strike-slip duplex system in the western Nansha Waters, South China Sea. *Mar. Geol. Quat. Geol.* 19, 11–18 (Chinese with English abstract).
- Liu, G.X., 1982. Tectonic characteristics of Shanxi Graben system. (In Chinese with English abstract) In: China Tectonic Committee (Ed.), *Collection of the Second Symposium of Chinese Tectonics*. Science Publishing House, Beijing, China, pp. 56–65.
- Long, M.D., Wirth, E.A., 2013. Mantle flow in subduction systems: The mantle wedge flow field and implications for wedge processes. *J. Geophys. Res.* 118, 1–24. <http://dx.doi.org/10.1002/jgrb.50063>.
- Longley, I.M., 1997. The tectonostratigraphic evolution of SE Asia. In: Murphy, R.W. (Ed.), *Petroleum Geology of Southeast Asia*. Geological Society, London, Special Publications, 126, pp. 311–333.
- Mandl, G., 1988. *Mechanics of tectonic faulting*. Elsevier, Amsterdam (407 pp.).
- Mann, P., Hempton, R., Bradley, D.C., Burke, K., 1983. Development of pull-apart basins. *J. Geol.* 91, 529–554.

- Mantovani, E., Viti, M., Baaucchi, D., Tamburelli, C., Albarello, D., 2001. Back arc extension: which driving mechanism? *J. Virtual Explor.* 3, 17–45.
- Mazur, S., Green, C., Stewart, M.G., Whittaker, J.M., Williams, S., Bouatmani, R., 2012. Displacement along the Red River Fault constrained by extension estimates and plate reconstructions. *Tectonics* 31, TC5008. <http://dx.doi.org/10.1029/2012TC003174>.
- Mashima, H., 2008. Comments on "Evolution of the eastern margin of Korea: constraints on the opening of the East Sea (Japan Sea)" by Kim H. J. et al. [*Tectonophysics* 436 (2007) 37–55]. *Tectonophysics* 455, 404–405.
- Maung, H., 1987. Transcurrent movement in the Burma–Andaman Sea region. *Geology* 15, 911–912.
- Mat-Zin, I.C., Swarbrick, R.E., 1997. The tectonic evolution and associated sedimentation history of Sarawak Basin, eastern Malaysia; a guide for future hydrocarbon exploration. In: Fraser, A.J., Matthews, S.J., Murphy, R.W. (Eds.), *Petroleum geology of Southeast Asia*. Geological Society, London, Special Publications, 126, pp. 237–245.
- McKenzie, D.P., Priestley, K.F., 2010. The thermal structure of Tibetan crust and upper mantle. *EOS Supply* (92), 2010 AGU Fall Meeting, abstract T31E-03.
- McElhinny, M.W., McFadden, P.L., 2000. *Paleomagnetism: continents and oceans*. Academic Press, San Diego (386 pp.).
- McClay, K., Bonora, M., 2001. Analog models of restraining stepovers in strike-slip fault systems. *AAPG Bull.* 85, 233–260.
- McClay, K.R., Dooley, T., Whitehouse, P., Mills, M., 2002. 4-D evolution of rift systems: insights from scaled physical models. *Bull. Am. Assoc. Pet. Geol.* 86, 935–959.
- Mercier, J.L., Tapponnier, P., Carey-Gailhardis, E., Han, T., 1987. Change from Tertiary compression to Quaternary extension in southern Tibet during the India–Asia collision. *Tectonics* 6, 275–304.
- Miyashiro, A., 1986. Hot regions and the origin of marginal basins in the western Pacific. *Tectonophysics* 122, 195–216.
- Molnar, P., England, P., Martinod, J., 1993. Mantle dynamics, uplift of the Tibetan Plateau and the Indian Monsoon. *Rev. Geophys.* 31, 357–396.
- Molnar, P., England, P., 1990. Late Cenozoic uplift of mountain ranges and global climate changes: chick or egg? *Nature* 346, 29–34.
- Molnar, P., Stock, J.M., 2009. Slowing of India's convergence with Eurasia since 20 Ma and its implications for Tibetan mantle dynamics. *Tectonics* 28, TC3001. <http://dx.doi.org/10.1029/2008TC002271>.
- Molnar, P., Tapponnier, P., 1975. Cenozoic tectonics of Asia: effects of a continental collision. *Science* 189, 419–426.
- Morley, C.K., 2002. A tectonic model for the Tertiary evolution of strike-slip faults and rift basins in SE Asia. *Tectonophysics* 347, 189–215.
- Morley, C.K., 2012. Late Cretaceous–Early Palaeogene tectonic development of SE Asia. *Earth Sci. Rev.* 115, 37–75.
- Mrozowski, C.L., Hayes, D.E., 1979. The tectonic evolution of the Parece Vela Basin, Eastern Philippine Sea. *Earth Planet. Sci. Lett.* 46, 49–67.
- Müller, R.D., Royer, J.-Y., Lawver, L.A., 1993. Revised plate motions relative to the hotspots from combined Atlantic and Indian Ocean hotspot tracks. *Geology* 21, 275–278.
- Müller, R.D., Sdrolias, M., 2008. Age, spreading rates, and spreading asymmetry of the world's ocean crust. *Geochem. Geophys. Geosyst.* 9. <http://dx.doi.org/10.1029/2007GC001743>.
- Murphy, M.A., Yin, A., Harrison, T.M., Durr, S.B., Chen, Z., Ryerson, F.J., Kidd, W.S.F., Wang, X., Zhou, X., 1997. Did the Indo-Asia collision alone create the Tibet plateau? *Geology* 25, 719–722.
- Najman, Y., Appel, E., Boudagher-Fadel, M., et al., 2010. Timing of India–Asia collision: geological, biostratigraphic, and palaeomagnetic constraints. *J. Geophys. Res.* 115 (B12), 416. <http://dx.doi.org/10.1029/2010JB007673>.
- Nohda, S., 2009. Formation of the Japan Sea basin: reassessment from Ar–Ar ages and Nd–Sr isotopic data of basement basalts of the Japan Sea and adjacent regions. *J. Asian Earth Sci.* 34, 599–609.
- Nur, A., Dvorkin, J., Mavko, G., Ben-Avraham, Z., 1993. Speculations on the origins and fate of backarc basins. *Ann. Geofis.* 36, 155–163.
- Okino, K., Kasuga, S., Ohara, Y., 1998. A new scenario of the Parece Vela Basin genesis. *Mar. Geophys. Res.* 20, 21–40.
- Okino, K., Ohara, Y., Kasuga, S., Kato, Y., 1999. The Philippine Sea: new survey results reveal the structure and the history of the marginal basins. *Geophys. Res. Lett.* 26, 2287–2290.
- Okubo, Y., Ishihara, T., Daigo, M., 1997. Magnetic anomalies of east and SE Asia and their linear features. *J. Asian Earth Sci.* 15, 161–163.
- Otofujii, Y., Matsuda, T., Nohda, S., 1985. Opening mode of the Japan Sea inferred from the paleomagnetism of the Japan arc. *Nature* 317, 603–604.
- Otofujii, Y.-I., 1995. Late Cretaceous to early Paleogene paleomagnetic results from Sikhote Alin, far eastern Russia (implications for deformation of East Asia). *Tectonophysics* 130, 95–108.
- Otofujii, Y.-I., 2002. Internal deformation of Sikhote Alin volcanic belt, far eastern Russia: Paleocene paleomagnetic results. *Tectonophysics* 350, 181–192.
- Otsuki, K., 1990. Westward migration of the Izu–Bonin Trench, northward motion of the Philippine Sea Plate, and the relationships to the Cenozoic Japanese island arcs. *Tectonophysics* 180, 351–367.
- Park, J.O., Tokuyama, H., Shinohara, M., Suyehiro, K., Taira, A., 1998. Seismic record of tectonic evolution and back-arc rifting in the southern Ryukyu island arc system. *Tectonophysics* 294, 21–42.
- Patrait, P., Achache, J., 1984. India–Eurasia collision chronology has implications for crust shortening and diving mechanism of plates. *Nature* 311, 621–625.
- Polachan, S., Racey, A., 1994. Stratigraphy of the Mergui basin, Andaman Sea: implications for petroleum exploration. *J. Pet. Geol.* 17, 373–406.
- Powell, C.M., Conaghan, P., 1973. Plate tectonics and the Himalayas. *Earth Planet. Sci. Lett.* 20, 1–12.
- Powell, C.M., 1986. Continental underplating model for the rise Tibetan Plateau. *Earth Planet. Sci. Lett.* 81, 79–84.
- Qiu, Y., 2005. Typical structural styles and their relationships with hydrocarbon accumulation and traps in the Zengmu basin, Nansha sea area (the southern China Sea). *Geol. Bull. China* 24, 16–22 (Chinese with English abstracts).
- Ratschbacher, L., Ben-Avraham, Z., 1995. Kinematics of distributed deformation in plate boundary zones with emphasis on the Mediterranean, Anatolia and Eastern Asia. *Special Issue Tectonophysics*, 243. Elsevier Science Pub, Amsterdam (207 pp.).
- Raju, K.A.K., Ramprasad, T., Rao, P.S., Rao, B.R., Varghese, J., 2004. New insights into the tectonic evolution of the Andaman basin, NE Indian Ocean. *Earth Planet. Sci. Lett.* 221, 145–162.
- Rangin, C., 1989. The Sulu Sea, a back arc basin setting within a Neogene collision zone. *Tectonophysics* 161, 119–141.
- Rangin, C., Bellon, H., Benard, F., Letouzey, J., Muller, C., Sandin, T., 1990. Neogene arc-continent collision in Sabah, Northern Borneo (Malaysia). *Tectonophysics* 183, 305–319.
- Rangin, C., Sliver, E.A., 1991. Neogene tectonic evolution of the Celebes and Sulu Sea basins: new sights from Leg 124 drilling. In: Silver, E.A., Rangin, C., von Breyman, M.T., et al. (Eds.), *Proceedings of the Ocean Drilling Program, Scientific Results*, pp. 51–63.
- Ren, A.S., 1999. Remarks on contacts between the Tertiary sequences from viewpoints of the tectonic movements. *Mult. Oil-Gas Field* 1, 50–53 (Chinese).
- Ren, J., Tamaki, K., Li, S., Zhang, J., 2002. Late Mesozoic and Cenozoic rifting and its dynamic setting in Eastern China and adjacent areas. *Tectonophysics* 344, 175–205.
- Replumaz, A., Tapponnier, P., 2003. Reconstruction of the deformed collision zone between India and Asia by backward motion of lithospheric blocks. *J. Geophys. Res.* 108, 2285. <http://dx.doi.org/10.1029/2001JB000661>.
- Richer, B., Fuller, M., Schimidtke, E., Myint, U.T., Win, U.M., Bunopas, S., 1993. Paleomagnetic results from Thailand and Myanmar: implications for the interpretation of tectonic rotations in Southeast Asia. *J. SE Asian Earth Sci.* 8, 247–255.
- Richer, B., Schimidtke, E., Fuller, M., Harbury, N., Samsudin, A.R., 1999. Paleomagnetism of Peninsular Malaysia. *J. Asian Earth Sci.* 17, 477–519.
- Robert, D., 2000. Pull-apart stepover structures in an asphalted road surface—a geological curiosity. *J. Struct. Geol.* 22, 1469–1472.
- Roeser, H.A., 1991. Age of the crust of the SE Sulu Sea basin based on magnetic anomalies and age determined at Site 768. In: Silver, E.A., Rangin, C., von Breyman, M.T., et al. (Eds.), *Proceedings of the Ocean Drilling Program, Scientific Results*, 124, pp. 339–343.
- Rowley, D.B., 1996. Age of initiation of collision between India and Asia: a review of stratigraphic data. *Earth Planet. Sci. Lett.* 154, 1–13.
- Rowley, D.B., Currie, B.S., 2006. Palaeo-altimetry of the late Eocene to Miocene Lunpola basin, central Tibet. *Nature* 439, 677–681.
- Rowley, D.B., Lottes, A.L., 1988. Plate-kinematic reconstruction of the North Atlantic and Arctic: Late Jurassic to present. *Tectonophysics* 155, 73–120.
- Royden, L., Burchfiel, B., King, R., Wang, E., Chen, Z., Shen, F., Liu, Y., 1997. Surface deformation and lower crustal flow in eastern Tibet. *Science* 276, 788–790.
- Royden, L., Burchfiel, C., van der Hilst, R.D., 2008. The geological evolution of the Tibetan Plateau. *Science* 321, 1054–1058.
- Salisbury, M.H., Shinohara, M., Richter, C., et al., 2002. *Proceedings of the Ocean Drilling Program, Initial Reports*, 195. College Station, TX. <http://dx.doi.org/10.2973/odp.proc.ir.195> (Ocean Drilling Program).
- Sandwell, D.T., Smith, W.H.F., 1997. Marine gravity from Geosat and ERS 1 Satellite Altimetry. *J. Geophys. Res.* 102, 10039–10054.
- Satyana, A.H., Nugroho, D., Surantoko, I., 1999. Tectonic controls on the hydrocarbon habitats of the Barito, Kutei, and Tarakan Basins, Eastern Kalimantan, Indonesia major dissimilarities in adjoining basins. *J. Asian Earth Sci.* 17, 99–122.
- Schellart, W.P., 2011. A subduction zone reference frame based on slab geometry and subduction partitioning of plate motion and trench migration. *Geophys. Res. Lett.* 38, L16317. <http://dx.doi.org/10.1029/2011GL048197>.
- Schluter, H.U., Hinz, K., Block, M., 1996. Tectono-stratigraphic terrane and detachment faulting of the South China Sea and Sulu Sea. *Mar. Geol.* 130, 39–78.
- Scholl, D.W., Buffington, E.C., Marlow, M.S., 1975. Plate tectonics and the structural evolution of the Aleutian–Bering Sea region. *GSA Spec. Pap.* 151, 1–32.
- Schreurs, G., Colletta, B., 1998. Analogue modeling of faulting in zones of continental transpression and transtension. In: Holdsworth, R.E., Strachan, R.A., Dewey, J.F. (Eds.), *Continental Transpressional and Transtensional Tectonics*. Geological Society, London, Special Publications, 135, pp. 59–79.
- Schulte-Pelkum, V., Monsalve, G., Sheehan, A., Pandey, M.R., Sapkota, S., Bilham, R., Wu, F., 2005. Imaging the Indian subcontinent beneath the Himalaya. *Nature* 435, 1222–1225.
- Scott, B.R., Kroenke, L., Zakariadze, G., et al., 1980. Evolution of the south Philippine Sea: deep sea drilling project Leg 59 results. In: Kroenke, L., Scott, B.R., Balshaw, K., et al. (Eds.), *Initial Reports of the Deep Sea Drilling Project 59*. US Government Printing Office, Washington, D. C., pp. 803–815.
- Sdrolias, M., Müller, R.D., 2006. Controls on back-arc basin formation. *Geochem. Geophys. Geosyst.* 7, Q04016. <http://dx.doi.org/10.1029/2005GC001090>.
- Sdrolias, M., Roest, W.R., Müller, R.D., 2004. An expression of Philippine Sea plate rotation: the Parece Vela and Shikoku Basins. *Tectonophysics* 394, 69–86.
- Searle, M.P., Simpson, R.L., Law, R.D., Parrish, R.R., Waters, D.J., 2003. The structural geometry, metamorphic and magmatic evolution of the Everest massif, High Himalaya of Nepal–South Tibet. *J. Geol. Soc. Lond.* 160, 345–366.
- Searle, M.P., Windley, B.F., Coward, M.P., Cooper, D.J.W., Rex, A.J., Rex, D.C., Li, T., Xiao, X., Jan, M.Q., Thakur, V.C., Kumar, S., 1987. The closing of Tethys and the tectonics of the Himalaya. *Geol. Soc. Am. Bull.* 98, 678–701.
- Seno, T., Maruyama, S., 1984. Paleogeographic reconstruction and origin of the Philippine Sea. *Tectonophysics* 102, 53–85.
- Seton, M., Müller, R.D., Zahirovic, S., Gaina, C., Torsvik, T., Shephard, G., Talsma, A., Gurnis, M., Turner, M., Maus, S., Chandler, M., 2012. Global continental and ocean basin reconstructions since 200 Ma. *Earth Sci. Rev.* 113, 212–270.

- Shih, T.-C., 1980. Marine magnetic anomalies from the Western Philippine Sea: implications for the evolution of marginal basins. In: Hayes, D.E. (Ed.), *The Tectonic and Geologic Evolution of SE Asian Seas and Islands*. AGU Geophysical Monograph, 23, pp. 49–76.
- Shinjo, R., 1999. Geochemistry of high Mg andesites and the tectonic evolution of the Okinawa Trough–Ryukyu arc system. *Chem. Geol.* 157, 69–88.
- Shiki, T., Mizuno, A., Kobayashi, K., 1985. Data listing of the bottom material dredged and core from the northern Philippine Sea. In: Shiki, T. (Ed.), *Geology of the northern Philippine Sea: Geological Results of the GDP Cruises of Japan*. Tokai University Press, Tokyo, pp. 23–41.
- Sibuet, J.-C., Benoît, D., Hsu, S.-K., Nicolas, T., Jean-Pierre, L.F., Liu, C.-S., 1998. Okinawa trough back-arc basin: Early tectonic and magmatic evolution. *J. Geophys. Res.* 103, 30245–30267.
- Silver, E.A., Rangin, C., 1991a. Tectonic synthesis. In: Silver, E.A., Rangin, C., von Breyman, M.T., et al. (Eds.), *Proceedings of the Ocean Drilling Program, Scientific Results*, 124, pp. 3–9.
- Silver, E.A., Rangin, C., 1991b. Development of the Celebes Basin in the context of Western Pacific marginal basin history. In: Silver, E.A., Rangin, C., von Breyman, M.T., et al. (Eds.), *Proceedings of the Ocean Drilling Program, Scientific Results*, 124, pp. 39–49.
- Simandjuntak, T.O., Barber, A.J., 1996. Contrasting tectonic styles in the Neogene orogenic belts of Indonesia. In: Hall, R., Blundell, D.J.B. (Eds.), *Tectonic evolution of SE Asia*. Geological Society, London, Special Publications, 106, pp. 185–201.
- Sleep, N., Toksöz, M., 1971. Evolution of marginal basins. *Nature* 33, 548–550.
- Smith, D.E., Kolenkiewicz, M.H., Dunn, P.J., Robbins, J.W., Tprence, M.H., Klosko, S.M., Williamson, R.D., Palvis, E.C., Douglas, N.B., 1990. Tectonic motion and deformation from Satellite Laser Ranging to LAGEOS. *J. Geophys. Res.* 95, 22013–22041.
- Smith, D.E., Baltuck, M., 1993. Introduction. In: Smith, D.E., Turcotte, D.L. (Eds.), *Contributions of Space Geodesy to Geodynamics*. Crustal Dynamics: AGU Geodynamics Series, 23, pp. 1–3.
- Song, X.-Y., Chu, C.-L., Rui, Z.-F., 2010. Structural framework and evolution of Xihu Sag in East China Sea Basin. *Geol. J. China Univ.* 16, 86–93 (Chinese with English abstracts).
- Spicer, R., Harris, N., Widdowson, M., Herman, A., Guo, S., Valdes, P., Wolfe, J., Kelley, S., 2003. Constant elevation of southern Tibet over the past 15 million years. *Nature* 421, 622–624.
- Swanson, M.T., 1990. Extensional duplexing in the York Cliffs strike-slip fault system, southern coastal Marine. *J. Struct. Geol.* 12, 499–512.
- Symons, D.T.A., Harris, M.J., Gabites, J.E., Hart, C.J.R., 2000. Eocene (51 Ma) end to northward translation of the Coast Plutonic Complex: paleomagnetism and K–Ar dating of the White Pass Dikes. *Tectonophysics* 326, 93–109.
- Taira, A., 2001. Tectonic evolution of the Japan Island arc system. *Annu. Rev. Earth Planet. Sci.* 29, 109–134.
- Tamaki, K., Honza, E., 1991. Global tectonics and formation of marginal basins: role of the western Pacific. *Eipsodes* 14, 224–230.
- Tamaki, K., Suyehiro, K., Allan, J., Ingle Jr., J.C., Pisciotto, K.A., 1992. Tectonic synthesis and implications of Japan Sea ODP drilling. In: Tamaki, K., Suyehiro, K., Allan, J., McWilliams, M., et al. (Eds.), *Proceedings of the Ocean Drilling Program, Scientific Results*, 127/128, pp. 1333–1348.
- Tapponnier, P., Lacassin, R., Leloup, P.H., Scharer, U., Zhong, D., Wu, H., Liu, X., Ji, S., Zhang, L., Zhong, J., 1990. The Ailao Shan/Red River metamorphic belt: tertiary left-lateral shear between Indochina and South China. *Nature* 343, 431–437.
- Tapponnier, P., Peltzer, G., Le Dayn, A.Y., Armijo, R., Cobbold, P., 1982. Propagating extrusion tectonics in Asia: new insights from simple experiments with plasticine. *Geology* 10, 611–616.
- Tapponnier, P., Xu, Z., Roger, F., Meyer, B., Arnaud, N., Wittlinger, G., Yang, J., 2001. Oblique stepwise rise and growth of the Tibet. *Science* 294, 1671–1677.
- Tapponnier, P., Peltzer, G., Armijo, R., 1986. On the mechanics of the collision between India and Asia. In: Coward, M.P., Ries, A.C. (Eds.), *Collision Tectonics*. Geological Society, London, Special Publications, 19, pp. 115–157.
- Tatsumi, Y., Otofujii, Y.-H., Matsuda, T., Nohda, S., 1989. Opening of the Sea of Japan back-arc basin by asthenospheric injection. *Tectonophysics* 169, 317–329.
- Taylor, B., 1992. Rifting and the volcanic–tectonic evolution of the Izu–Bonin–Mariana arc. *Proceedings of Ocean Drilling Project, Scientific Results*, 126, pp. 627–651.
- Taylor, B., Hayes, D.E., 1980. Tectonic evolution of the South China Sea Basin. In: Hayes, D.E. (Ed.), *The Tectonic and Geologic Evolution of SE Asian Seas and Islands*. AGU Geophysical Monograph, 23, pp. 89–104.
- Taylor, B., Hayes, D.E., 1983. Origin and history of the South China Sea Basin. In: Hayes, D.E. (Ed.), *AGU Geophys. Monogr.* 27, 23–56.
- Tokuyama, H., 1985. Dredged igneous rocks from the Amami Plateau. In: Shiki, T. (Ed.), *Geology of the northern Philippine Sea: Geological Results of the GDP Cruises of Japan*. Tokai University Press, Tokyo, pp. 50–56.
- Tongkul, F., 1994. The geology of Northern Sabah, Malaysia: its relationship to the opening of the South China Sea Basin. *Tectonophysics* 235, 131–147.
- Tosha, T., Hamano, Y., 1988. Paleomagnetism of Tertiary rocks from the Oga peninsula and rotation of NE Japan. *Tectonics* 7, 653–662.
- Torsvik, T.H., Müller, R.D., Van der Voo, B., Steinberger, B., Gaina, C., 2008. Global plate motion frames: toward a unified model. *Rev. Geophys.* 46, RG3004. <http://dx.doi.org/10.1029/2007RG000227>.
- Ueda, Y., 2004. Paleomagnetism of seamounts in the West Philippine Sea as inferred from correlation analysis of magnetic anomalies. *Earth Planets Space* 56, 967–977.
- Uyeda, S., 1982. *Moving earth: sea floor* (Chinese translation from Japanese). Geological Publishing House, Beijing, China (190 pp.).
- Uyeda, S., 1991. The Japanese island arc and the subduction process. *Episodes* 14, 190–198.
- Uyeda, S., Kanamori, H., 1979. Back-arc opening and mode of subduction. *J. Geophys. Res.* 84, 1049–1061.
- Uyeda, S., Ben-Avraham, Z., 1972. Origin and development of the Philippine Sea. *Nat. Phys. Sci.* 240, 176–178.
- van Hinsbergen, D.J.J., Lippert, P.C., Dupont-Nivet, G., McQuarrie, N., Doubrovina, P.V., Spakmani, W., Torsvik, T.H., 2012. Greater India Basin hypothesis and a two-stage Cenozoic collision between India and Asia. *Proc. Natl. Acad. Sci. U. S. A.* 109, 7659–7664.
- van Hinsbergen, D.J.J., Steinberger, B., Doubrovina, P.V., Gassmüller, R., 2011. Acceleration and deceleration of India–Asia convergence since the Cretaceous: roles of mantle plumes and continental collision. *J. Geophys. Res.* 116, B06101. <http://dx.doi.org/10.1029/2010JB008051>.
- Viallon, C., Huchon, P., Barrier, E., 1986. Opening of the Okinawa basin and collision in Taiwan: a retreat trench model with lateral anchoring. *Earth Planet. Sci. Lett.* 80, 145–155.
- Vroon, P.Z., Van Bergin, M.J., Forde, E.G., 1996. Pb and Nd isotope constraints on the provenance of tectonically dispersed continental fragments in east Indonesia. In: Hall, R., Blundell, D.J.B. (Eds.), *Tectonic evolution of Southeast Asia*. Geological Society, London, Special Publication, 106, pp. 445–454.
- Wang, C.S., Li, X.H., Hu, X.M., Jansa, L.F., 2002. Latest marine horizon north of Qomolangma (Mt Everest): implications for closure of Tethys seaway and collision tectonics. *Terra Nova* 14, 114–120.
- Wang, C., Zhao, X., Liu, F., Lippert, P.C., Graham, S.A., Coe, R.S., Yi, H., Zhu, L., Liu, S., Li, Y., 2008. Constraints on the early uplift history of the Tibetan Plateau. *Proc. Natl. Acad. Sci. U. S. A.* 105, 4987–4992.
- Wang, E., Meng, Q., 2009. Mesozoic and Cenozoic tectonic evolution of the Longmenshan fault belt. *Sci. China Ser. D Earth Sci.* 52, 579–592.
- Wang, Q., Coward, M., 1990. The Chaidam basin (NW China): formation and hydrocarbon potential. *J. Pet. Geol.* 13, 93–112.
- Waldron, J.W.F., 2005. Extensional fault arrays in strike-slip and transtension. *J. Struct. Geol.* 27, 23–34.
- Weaver, R., Robertsa, A.P., Flecker, R., Macdonald, D.I.M., 2004. Tertiary geodynamics of Sakhalin (NW Pacific) from anisotropy of magnetic susceptibility fabrics and paleomagnetic data. *Tectonophysics* 279, 25–42.
- Weerd, A.A., Armin, R.A., 1992. Origin and evolution of the Tertiary hydrocarbon-bearing basins in Borneo (Borneo), Indonesia. *AAPG Bull.* 1778–1803.
- Wegener, A., 1929. The origin of continents and oceans (Die Entstehung der Kontinente und Ozeane). In: Briam, J. (Ed.), Dover, New York (246 pp.).
- Weissel, J.K., 1980. Evidence for Eocene oceanic crust in the Celebes Basin. In: Hayes, D.E. (Ed.), *The Tectonic and Geologic Evolution of SE Asian Seas and Islands*. AGU Geophysical Monograph, 23, pp. 37–47.
- White, L.T., Lister, G.S., 2012. The collision of India with Asia. *J. Geodyn.* 56–57, 7–17.
- Wyllie, P.J., 1971. *The dynamic earth*. John Wiley & Sons (416 pp.).
- Worrall, D.M., Kruglgak, V., Kunst, F., Kuznetsov, V., 1996. Tertiary tectonics of the Sea of Okhotsk, Russia: far-field effects of the India–Eurasia collision. *Tectonics* 15, 813–826.
- Xu, J., 1994. Determination of divergent directions of bilateral blocks of grabens. *Oil Exp. Geol.* 16, 334–338 (Chinese with English abstracts).
- Xu, J., 1996. Similarities between Cenozoic basins of different magnitudes in East Asian continental margins (abstract). 30th International Geological Congress (Beijing), No. of the abstract, p. F3071.
- Xu, J., 1997. Similarities between Cenozoic basins of different magnitudes in East Asian continental margins. *Oil Exp. Geol.* 19, 297–304 (Chinese with English abstracts).
- Xu, J., Kelty, T., Ben-Avraham, Z., 2010. Correlation between development of the marginal basin system of the NW Pacific and uplift of the Tibet Plateau. Oral presentation, AGU Fall Meeting, San Francisco, USA.
- Xu, J., Zhang, L., 1999. Genesis of Cenozoic basins in the east margin of Eurasian plate: dextrally pulling apart. *Oil Gas Geol.* 20, 187–191 (Chinese with English abstracts).
- Xu, J., Zhang, L., 2000a. Genesis of Cenozoic basins in the northwestern Pacific margin (2): linled dextral pull-apart basin system. *Oil Gas Geol.* 21, 185–190 (Chinese with English abstracts).
- Xu, J., Zhang, L., 2000b. Genesis of Cenozoic basins in the northwestern Pacific margin (3): tectonic evolution of the post-rifting period. *Oil Gas Geol.* 21, 287–292 (Chinese with English abstracts).
- Xu, J., Zhang, L., 2000c. Genesis of Cenozoic basins in the northwestern Pacific margin (1): comments on basin forming mechanism. *Oil Gas Geol.* 21, 185–190 (Chinese with English abstracts).
- Xu, J., Yang, W., Zeng, Z., Ben-Avraham, Z., Lee, T.-Y., Li, Z., Basile, C., Zhang, L., 2004. Genesis of the South China Sea: intervening of dextral-pull-apart rifting and sinistral transpression. *Earth Sci. Front.* 11, 193–206 (Chinese with English abstracts).
- Xu, X.W., Ma, X.Y., Deng, Q.D., 1993. Neotectonic activity along the Shanxi rift system, China. *Tectonophysics* 219, 305–325.
- Yamaji, A., 2003. Slab rollback suggested by latest Miocene to Pliocene forearc stress and migration of volcanic front in southern Kyushu, northern Ryukyu Arc. *Tectonophysics* 364, 9–24.
- Yamamoto, H., 1993. Submarine geology and post-opening tectonic movements in the southern region of the Sea of Japan. *Mar. Geol.* 112, 133–150.
- Yang, Y., Liu, M., 2009. Crustal thickening and lateral extrusion during the Indo-Asian collision: a 3D viscous flow model. *Tectonophysics* 465, 128–135.
- Yao, B., Zeng, W., Hayes, D.E., 1994. The geological memoir of South China Sea Surveyed jointly by China and USA. (in Chinese) China University of Geosciences Press, Wuhan, China (206 pp.).
- Yin, A., 2009. Cenozoic tectonic evolution of Asia: a preliminary synthesis. *Tectonophysics* 465, 293–325.
- Yin, A., Harrison, W., 2000. Geologic evolution of the Himalayan–Tibetan orogen. *Annu. Rev. Earth Planet. Sci.* 28, 211–280.
- Yuan, Y., Wang, B., Tang, X., Lai, X., Fan, S., Liu, Z., 1992. Cretaceous–Early Tertiary Paleolatitue migration in Sanshui Basin of South China and the Evolution of South China Sea. *Tropic Oceans* 11, 37–44 (Chinese with English abstracts).

- Yoon, S.H., Chough, S.K., 1995. Regional strike slip in the eastern continental margin of Korea and its tectonic implications for the evolution of Ulleung Basin, East Sea (Sea of Japan). *Geol. Soc. Am. Bull.* 107, 83–97.
- Yu, H.-S., Chow, J., 1997. Cenozoic basins in northern Taiwan and tectonic implications for the development of the eastern Asian continental margin. *Palaeogeogr. Palaeoclimatol. Palaeoecol.* 131, 133–144.
- Yu, Z., Yang, C., Liao, Q., 1999. *Natural Gas Geology of Huanghua Depression, Bohai Gulf Basin* (in Chinese). Petroleum Industry Press, Beijing, China (207 pp.).
- Zeng, W., 1991. Comprehensive study of Guangzhou–Palawan transect. *Geol. Res. South China Sea* 3, 39–64 (Chinese with English abstracts).
- Zhao, J.-H., 2004. The forming factors and evolvement of the Mesozoic and Cenozoic Basin in the East China Sea. *Mar. Pet.* 6, 6–14 (Chinese with English abstracts).
- Zhao, W.L., Morgan, W.J., 1985. Uplift of Tibetan Plateau. *Tectonics* 4, 359–369.
- Zhou, D., Chen, H., Wu, S., Yu, H., 2002. Opening of the South China Sea by dextral splitting of East Asian continental margin. *Acta Geol. Sin.* 76, 181–190 (Chinese with English abstracts).
- Zhou, J., Xu, F., Wang, T., Cao, A., Yin, C., 2006. Cenozoic deformation history of the Qaidam Basin, NW China: results from cross-section restoration and implications for Qinghai–Tibet Plateau tectonics. *Earth Planet. Sci. Lett.* 243, 195–210.
- Zhu, B., Kidd, S.F., Rowley, D.B., Currie, B.S., Shafique, N., 2005. Age of initiation of the India–Asia collision in the east-central Himalayas. *J. Geol.* 113, 265–285.
- Zhu, B., Kidd, S.F., Rowley, D.B., Currie, B.S., Shafique, N., 2006. Age of initiation of the India–Asia collision in the East-Central Himalaya: a reply. *J. Geol.* 114, 641–643.